



UNIVERSIDADE FEDERAL FLUMINENSE
INSTITUTO DE GEOCIÊNCIAS
DEPARTAMENTO DE GEOLOGIA

MICHEL BRAUN JESIONEK

DIVERSIDADE CRÍPTICA DE ALGAS CALCÁRIAS NÃO-GENICULADAS DO
SUDESTE BRASILEIRO

Universidade Federal Fluminense - UFF

TESE

Niterói - RJ
2020

MICHEL BRAUN JESIONEK

DIVERSIDADE CRÍPTICA DE ALGAS CALCÁRIAS NÃO-GENICULADAS DO
SUDESTE BRASILEIRO

Tese submetida ao Programa
de Pós-Graduação em
Dinâmica dos Oceanos e da
Terra da Universidade
Federal Fluminense como
parte dos requisitos
necessários à obtenção do
grau de Doutor. Área de
Concentração: Ecologia
Marinha – Sistemas
Bentônicos

Orientador: Prof. Dr. Alex Cardoso Bastos

Coorientador: Prof. Dr. Ricardo da Gama Bahia

NITERÓI – RJ

2020

MICHEL BRAUN JESIONEK

DIVERSIDADE CRÍPTICA DE ALGAS CALCÁRIAS NÃO-GENICULADAS DO
SUDESTE BRASILEIRO

Tese submetida ao Programa
de Pós-Graduação em
Dinâmica dos Oceanos e da
Terra da Universidade
Federal Fluminense como
parte dos requisitos
necessários à obtenção do
grau de Doutor. Área de
Concentração: Ecologia
Marinha – Sistemas
Bentônicos

Aprovado em: 20 de março de 2020

Banca Examinadora

Dr. Renato Crespo Pereira (UFF)

Dr. Fábio Bettini Pitombo (UFF)

Dr. Leonardo Tavares Salgado (JBRJ)

Dra. Iara Oliveira Costa (UFRB)

Dr. Ricardo da Gama Bahia (JBRJ)

NITERÓI – RJ

2020

FICHA CATALOGRÁFICA

Ficha catalográfica automática - SDC/BIG
Gerada com informações fornecidas pelo autor

J58d Jeshirek, Michel Braun
Diversidade críptica de algas calcárias não-geniculadas
do sudeste brasileiro. / Michel Braun Jeshirek ; Alex Cardoso
Bastos, orientador ; Ricardo da Gama Bahia, coorientador.
Niterói, 2020.
112 f. : il.

Tese (doutorado) -Universidade Federal Fluminense, Niterói,
2020.

DOI: <http://dx.doi.org/10.22409/PPGDOT.2020.d.10386120714>

1. Alga vermelha. 2. Taxonomia. 3. Biologia molecular. 4.
Produção intelectual. I. Bastos, Alex Cardoso, orientador.
II. Bahia, Ricardo da Gama, coorientador. III. Universidade
Federal Fluminense. Instituto de Geociências. IV. Título.

CDD -

Bibliotecário responsável: Sandra Lopes Coelho - CRB7/3389

Agradecimentos.

Dedico esta tese a memória de Gilberto Menezes Amado Filho, meu orientador durante grande parte deste projeto, acreditando neste desafio e não medindo esforços para viabilizar este estudo.

A todos meus colegas de laboratório, que de alguma maneira contribuíram para a elaboração e execução desta dissertação.

Ao Laboratório de Algas e de Biologia Molecular do Instituto de Pesquisas do Jardim Botânico do Rio de Janeiro

A pesquisadora Dra. Mariana Cabral Oliveira do Laboratório de Algas do Instituto de Biociências da Universidade de São Paulo (USP), por me receber e disponibilizar a infraestrutura do laboratório para a maior parte das etapas moleculares deste estudo e toda sua contribuição durante o projeto. Muito obrigado.

A todos que pude conhecer, e dividir o Laboratório de Algas do Instituto de Biologia da USP durante os períodos que trabalhei por lá.

Agradeço imensamente ao meu coorientador e amigo, Dr. Ricardo da Gama Bahia, por poder trabalhar e discutir ideias juntos neste projeto, fundamental para a construção e frutos gerados nesta tese.

Ao Dr. Alex Cardos Bastos, que se prontificou em assumir a responsabilidade da orientação, em sua fase final.

Ao Dr. Fernando Moraes, pelo seu apoio nas coletas e obtenção de imagens no campo.

A Coordenação de Aperfeiçoamento de Pessoal de Nível Superior (CAPES) pela bolsa de doutorado concedida, o que me possibilitou a dedicação às atividades do programa de pós graduação.

ABSTRACT

The taxonomy of non-geniculate coralline algae (NGCA) is considered difficult due to its phenotypic plasticity and the absence of diagnostical features to separate genetically related species. Recent studies have been demonstrated how genetic data is needful to the taxonomy of this group by revealing cryptic diversity, discovering new species, as well as synonymizing species, making old described species to transit among different genera and species over the years. The Southeast Brazil, particularly the Rio de Janeiro state coast, is largely represented by rocky shore habitats where NGCA thrive among the dominant benthic organisms. In addition, there are extensive rhodolith beds reported in Espírito Santo state, demonstrating the great potential of new NGCA records in this region. In this context, the aim of this study was to infer and describe the cryptic diversity of ACNG in these habitats, using molecular and morphoanatomical data. We described three new NGCA taxa occurring in this region, including a new genus, *Tectolithon fluminense* gen. et sp. nov., and two new species, *Crustaphytum atlanticum* sp. nov. from rocky shores along Rio de Janeiro state, and *Sporolithon amadoi* sp. nov. from a rhodolith bed in central Espírito Santo state. The new taxa were evidenced by both molecular and morpho-anatomical analyses, demonstrate the great potential of this South Atlantic region to harbor new records, expanding the knowledge about southeastern Brazilian marine biodiversity, and the ACNG taxonomy. Analyses of the plastid-encoded markers *psbA* and *rbcL* demonstrated that *Tectolithon fluminense* and *Crustaphytum atlanticum* belong to the clade formed by the typically subarctic/arctic *Clathromorphum* complex. The observation of specimens from these taxa with subepithallial initials that are both longer and shorter than their immediate inward derivatives indicates that this morpho-anatomical character should be used with caution for generic delimitation in the Melobesioideae. Based on DNA analysis of type material it was demonstrated that *Sporolithon ptychoides*, previously considered one of the main rhodolith-forming species in Brazil, did not occur in this region and actually corresponds to *Sporolithon amadoi*, a cryptic species described here with similar morpho-anatomical features. The revealed diversity for the Southeast Brazil evidences how alfa taxonomy is important for the NGCA, providing data base for future phylogenetic and phylogeographic studies. The genetic comparison against type material demonstrates to be the only unequivocal way to identify species of NGCA.

Key-words: Morpho-anatomy; Non-geniculate coralline algae; *psbA*; *rbcL*; Taxonomy

RESUMO

A taxonomia de algas calcárias não-geniculadas (ACNG) é dificultada por conta da sua reconhecida plasticidade fenotípica e muitas vezes devido à ausência de caracteres diagnósticos utilizados para separar espécies geneticamente próximas. Estudos recentes vêm mostrando como a informação genética é indispensável à taxonomia do grupo, revelando tanto diversidade críptica, com a descoberta de novas espécies, como sinonimizando espécies e fazendo com que ACNG descritas há muitos anos sejam posicionadas sucessivamente em diferentes gêneros e espécies ao longo do tempo. O sudeste brasileiro, especialmente a costa do estado do Rio de Janeiro, é amplamente representado por habitats rochosos, como costões de praias e ilhas costeiras, onde as ACNG prosperam entre os organismos bentônicos dominantes. Além disso, existe a presença de extensos bancos de rodolitos ocorrendo na plataforma continental do Espírito Santo, demonstrando o grande potencial para novos registros para esta região. Neste contexto, o objetivo deste trabalho foi inferir e descrever a diversidade críptica de ACNG que se desenvolve nestes habitats, utilizando dados moleculares e morfoanatômicos. Três novas espécies para ciência foram descritas: *Tectolithon fluminense* gen. et sp. nov. e *Crustaphytum atlanticum* sp. nov., ocorrendo em habitats rochosos ao longo da costa do estado do Rio de Janeiro e *Sporolithon amadoi* em um banco de rodolitos na costa norte do estado do Espírito Santo. Os novos táxons evidenciados por análises moleculares e morfoanatômicas, demonstram o grande potencial dessa região do Atlântico Sul para abrigar novos registros, expandindo o conhecimento sobre a biodiversidade marinha do sudeste brasileiro e da taxonomia das ACNG. Análises dos marcadores *psbA* e *rbcL* revelaram que *Tectolithon fluminense* e *Crustaphytum atlanticum* pertencem ao clado formado pelo complexo Clathromorphum, tipicamente subártico/árctico. A observação de espécimes desses táxons com iniciais subepiteliais mais longas e mais curtas que suas derivadas internas imediatas indica que essa característica morfoanatômica deve ser utilizada com cautela para delimitação genérica em Melobesioideae. Com base na análise de DNA do material tipo, foi demonstrado que *Sporolithon ptychoides*, anteriormente considerado uma das principais espécies formadoras de rodolitos no Brasil, não ocorre nessa região e, na verdade, corresponde a *Sporolithon amadoi*, uma espécie críptica com características morfoanatômicas similares e descrita no presente estudo. A diversidade revelada o sudeste brasileiro evidencia a importância da taxonomia alfa para as ACNG, fornecendo base de dados para estudos de filogenia e filogeografia do grupo. A comparação genética com material tipo, demonstra ser a única maneira inequívoca de se nomear espécies de ACNG.

Palavras-chave: Morfoanatomia; Algas calcárias não-geniculadas; *psbA*; *rbcL*; Taxonomia.

Sumário

Resumo

Abstract

1. Introdução	14
2. Objetivo Geral	18
3. Metodologia Geral	18
3.1. Área de estudo	18
3.1.1. Rio de Janeiro	18
3.1.2. Espírito Santo	20
3.2. Coleta	20
3.3. Análises morfoanatômicas	21
3.4. Análises Moleculares	22
3.4.1. Extração de DNA	22
3.4.2. Amplificação do DNA (PCR)	23
3.4.3. Marcadores Moleculares	23
4. Referências Bibliográficas	25

Capítulo 1 - Newly discovered coralline algae in Southeast Brazil: <i>Tectolithon fluminense</i> gen. et sp. nov. and <i>Crustaphytum atlanticum</i> sp. nov. (Hapalidiales, Rhodophyta).....	34
Abstract.....	36
Introduction.....	37
Material and Methods.....	39
Results.....	42
Discussion.....	60
Acknowledgements.....	64
Funding.....	64
References.....	65
Supplementary Material.....	74

Capítulo 2 - <i>Sporolithon amadoi</i> sp. nov. (Sporolithales, Rhodophyta), a new rhodolith-forming non-geniculate coralline alga from offshore the northwestern Gulf of Mexico and Brazil.....	81
Abstract.....	82
Introduction.....	83
Material and Methods.....	88
Results.....	89
Discussion.....	93
Acknowledgements.....	104
References.....	104
Conclusões Gerais.....	111

Lista de figuras

Figura 1 (A-D) – Formas de crescimento de algas calcárias não-geniculadas.....	15
Figura 2 – Sítios de coleta ao longo da costa do Estado do Rio de Janeiro.....	18
Figura 3 – Localização do banco de rodolitos no Estado do Espírito Santo (Recifes Esquecidos)	20
Figura 4 – Métodos de coleta utilizados para obtenção de amostras algas calcárias não-geniculadas em região costeira.....	20
Figura 5 – Método de coleta em um banco de rodolitos	21
Figura 6 (A-B) – Imagens obtidas através dos métodos de microscopia utilizados	21
Figura 7 – Uso de microdrill para retirada de tecido para extração de DNA	23

Capítulo 1 - Newly discovered coralline algae in Southeast Brazil: *Tectolithon fluminense* gen. et sp. nov. and *Crustaphytum atlanticum* sp. nov. (Hapalidiales, Rhodophyta)

Figura 1 – Árvore filogenética inferida através de RAxML e análise Bayesiana, do conjunto de dados de <i>psbA</i> (833 pb)	44
Figura 2 - Árvore filogenética inferida através de RAxML e análise Bayesiana, do conjunto de dados de <i>rbcL</i> (1356 pb)	46
Figuras (3-8) – Hábito e anatomia vegetativa de <i>Tectolithon fluminense</i> sp. nov.....	52
Figuras (9-16) – Anatomia de Tetra/Biesporófito de <i>Tectolithon fluminense</i> sp. nov.....	53
Figuras (17-20) – Vista Superficial de MEV dos conceptáculos tetra/biesporangiais de <i>Tectolithon fluminense</i> sp. nov. (RB760361)	54
Figuras (21-28) – Anatomia do gametófito de <i>Tectolithon fluminense</i> sp. nov.....	55
Figuras (29-37) – Hábito, anatomia vegetativa e reprodutiva de <i>Crustaphytum atlanticum</i> sp. nov.	58

Capítulo 2 - *Sporolithon amadoi* sp. nov. (Sporolithales, Rhodophyta), a new rhodolith-forming non-geniculate coralline alga from offshore the northwestern Gulf of Mexico and Brazil.

Figura 1 - Filogenia de Sporolithales com base em análises de Máxima Verossimilhança de sequências concatenadas de <i>psbA</i> e <i>rbcL</i> (2.247 bp).....	90
Figura 2 - Filogenia de Sporolithales com base em análises de Máxima Verossimilhança de sequências de <i>LSU</i> (549 pb).....	93
Figuras (3-10) – Hábito, anatomia vegetativa e reprodutiva do Holótipo de <i>Sporolithon amadoi</i> sp.nov.....	96
Figuras (11-17) – Hábito, anatomia vegetativa e reprodutiva do Isótipo de <i>Sporolithon amadoi</i> sp.nov.....	97
Figuras (18-21) – Anatomia vegetativa de <i>Sporolithon amadoi</i> sp.nov. (LAF 7260)	98
Figuras (22-27) - Anatomia reprodutiva de <i>Sporolithon amadoi</i> sp.nov. (LAF 7260)...	99
Figuras (28-29) - Anatomia vegetativa de <i>Sporolithon amadoi</i> sp.nov. (LAF 7261) ..	100
Figuras (30-37) – Anatomia vegetativa e reprodutiva de <i>Sporolithon amadoi</i> sp.nov. (LAF 7256)	101

Lista de tabelas

Tabela 1 - Localização dos sítios de coleta no estado do Rio de Janeiro.....	5
Capítulo 1 - Newly discovered coralline algae in Southeast Brazil: <i>Tectolithon fluminense</i> gen. et sp. nov. and <i>Crustaphytum atlanticum</i> sp. nov. (Hapalidiales, Rhodophyta)	
Tabela 1 - Características distintivas entre os gêneros do complexo <i>Clathromorphum</i>	59
Tabela S1 - Lista de todas as sequências de <i>psbA</i> e <i>rbcL</i> usadas nas análises filogenéticas.	74
Tabela S2 - Divergência intraespecífica de sequências de <i>psbA</i> em porcentagem e número de nucleotídeos para <i>Tectolithon fluminense</i> analisados neste estudo.....	77
Tabela S3 - Divergência interespecífica da sequência de <i>psbA</i> em porcentagem e número de nucleotídeos para as sequências utilizadas nas análises filogenéticas.....	78
Tabela S4 - Divergência interespecífica da sequência de <i>rbcL</i> em porcentagem e número de nucleotídeos para as sequências utilizadas nas análises filogenéticas.....	80
Capítulo 2 - <i>Sporolithon amadoi</i> sp. nov. (Sporolithales, Rhodophyta), a new rhodolith-forming non-geniculate coralline alga from offshore the northwestern Gulf of Mexico and Brazil.	
Tabela 1 - Lista com números do GenBank e informações de referência para sequências de táxons incluídos nas análises filogenéticas.....	85
Tabela 2 - Divergências de sequência de <i>psbA</i> (850 pb) reportada neste estudo.....	102
Tabela 3 - Divergências de sequência de <i>rbcL</i> (251 pb) reportada neste estudo.....	103

1. INTRODUÇÃO

As algas calcárias não-geniculadas (ACNG), pertencentes à Corallinales, Hapalidiales e Sporolithales, se destacam como um dos principais componentes da flora marinha nos oceanos, exercendo um importante papel ecológico nos costões rochosos e recifes rasos dos ecossistemas marinhos, sendo organismos fundamentais como pioneiros em processos de sucessão ecológica nesses ambientes (Asnaghi *et al.* 2015). A presença de ACNG é altamente importante para alguns organismos bentônicos, tais como algumas espécies de moluscos e corais que tem o assentamento larval e metamorfose ocorrendo preferencialmente ou restritamente na presença de determinadas espécies destas algas (e.g., Morse & Morse 1991; Roberts 2001). Estas algas ocorrem na maioria dos habitats marinhos, tanto nos trópicos como nos polos, em profundidades que variam das zonas entremarés até 274 m (Steneck 1986; Littler & Littler 1994; Le Gall *et al.* 2010). Desenvolvem-se de duas formas principais: crescendo aderidas a um substrato contínuo, formando crostas em costões rochosos (Figura 1A), seixos (Figura 1B), recifes e qualquer outro substrato seja ele natural ou artificial; ou formando nódulos de vida livre conhecidos como rodolitos (Figura 1C). Algumas espécies de ACNG ocorrem tanto formando rodolitos, como fixas a um substrato contínuo como costões rochosos e recifes coralíneos (e.g. *Sporolithon episporum*, Verheij 1993) enquanto outras são conhecidas apenas fixas a substrato contínuo (e.g. gênero *Heydrichia*, Townsend *et al.* 1994) ou exclusivamente formando rodolitos (e.g. *Mesophyllum sphaericum*, Peña *et al.* 2011).

Os rodolitos podem ser formados por uma ou mais espécies de ACNG, além de outros organismos bentônicos como: briozoários, corais, foraminíferos e moluscos. Ocupam áreas do fundo marinho costeiro formando os chamados bancos de rodolitos (Figura 1D). Os bancos de rodolitos são uma aglomeração destes rodolitos vivos ou mortos, que cobrem extensas áreas bentônicas promovendo um habitat tridimensional para as espécies associadas (Nelson 2009; Pereira filho *et al.* 2015), incluindo outras algas e espécies de interesse comercial, fazendo com que os bancos de rodolitos estejam associados a produção de recursos pesqueiros. Outro serviço ecossistêmico importante dos bancos de rodolitos está relacionado com a produção de carbonato de cálcio onde as ACNG também podem contribuir significativamente com os ciclos de cálcio de carbono

nos ecossistemas devido às altas taxas de produção e dissolução de CaCO₃ para (Amado-Filho *et al.* 2012a).

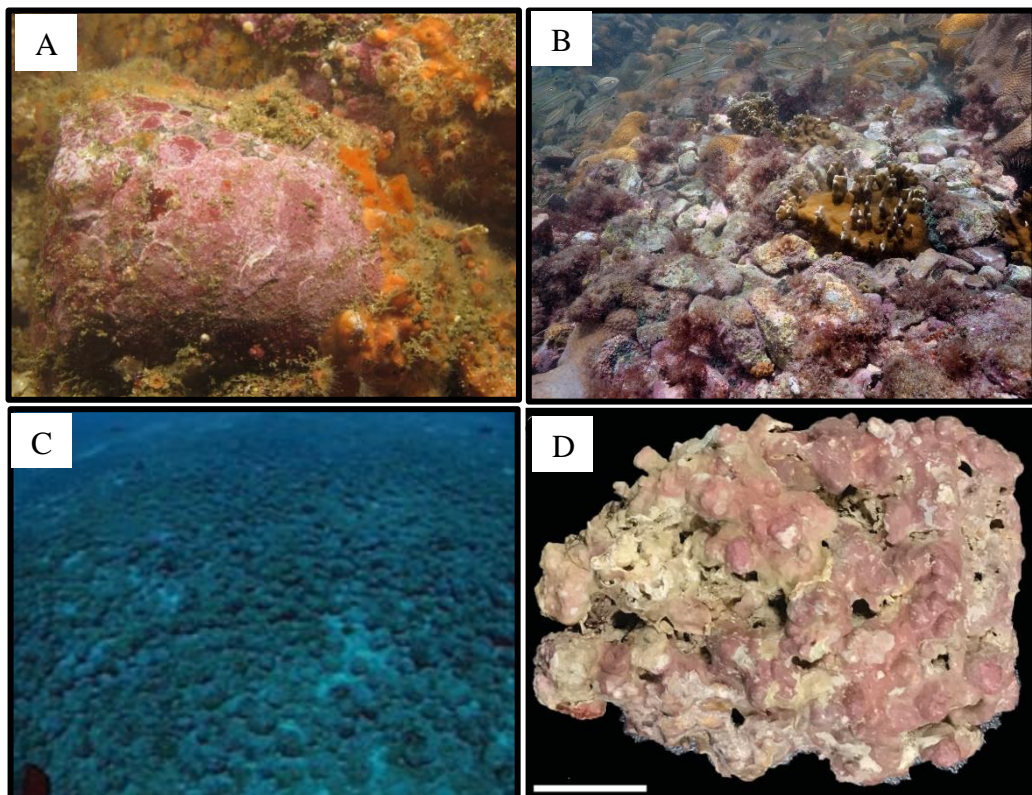


Figura 1 (A-D). Formas de desenvolvimento de ACNG. (A) ACNG crescendo sobre substrato rochoso (Foto: Fernando Moraes). (B) ACNG crescendo sobre seixos rochosos (Foto: Fernando Moraes). (C) Fisionomia típica de um banco de rodolitos (imagem adaptada de Amado-Filho *et al.* 2012). (D) ACNG crescendo na forma de rodolitos (Foto modificada de Richards *et al.* 2019) barra de escala = 1.5cm.

Atualmente, existe um interesse crescente da comunidade científica no estudo das ACNG não apenas pela sua importância ecológica, mas pela particular sensibilidade destes organismos às mudanças climáticas. Apesar de sua reconhecida resiliência (Bosence 1983a ,1983b ,1983c; Steller *et al.* 2003), as ACNG podem ser severamente impactadas pela acidificação dos oceanos e/ou mudanças climáticas prevista para as próximas décadas (Martin & Gatusso 2009; Hall-Spencer *et al.* 2008; Burdett *et al.* 2012; Diaz-Pulido *et al.* 2012; McCoy & Kamenos 2015). Para podermos prever o que pode acontecer com as ACNG frente estas mudanças no futuro, é preciso primeiramente conhecer o presente, com estudos multidisciplinares que envolvam florística através de métodos modernos, filogeografia, genômica, transcriptômica e microbiomas associados, informações ainda muito limitadas (Rindi *et al.* 2019). Devido à sua marcante e contínua presença no registro fóssil desde o Cretáceo Inferior (Aguirre *et al.* 2000), também

despertam interesse pela sua aplicabilidade como indicador paleoambiental e para proxies paleoecológicos (Braga *et al.* 2010; Aguirre *et al.* 2012; Novak *et al.* 2013; McCoy & Kamenos 2015).

As ACNG apresentam uma taxonomia dificultada por conta da sua reconhecida plasticidade fenotípica onde as condições do ambiente podem influenciar na morfologia destes organismos (Steneck & Adey 1976). Muitas vezes, caracteres diagnósticos para separar espécies geneticamente próximas são ausentes (Richards *et al.* 2017; Caragnano *et al.* 2018). Além disso, a taxonomia pioneira baseada apenas em dados morfoanatômicos (e.g. Cabioch, 1972, 1988; Johansen, 1976; Woelkerling, 1988) e ao início relativamente recente de estudos que utilizam dados moleculares, fundamentais para a taxonomia do grupo, têm gerado nas últimas décadas atribuição de nomes de forma incorreta. Desta forma, ainda existe uma carência de informação sobre a real diversidade e distribuição das ACNG nos oceanos.

Com advento da biologia molecular aplicada à taxonomia de algas coralináceas, o conhecimento acerca da diversidade e distribuição deste grupo nos oceanos vem sofrendo mudanças (Hernandez-Kantún 2016; Sissini *et al.* 2016; Gabrielson *et al.* 2018). Este fato pode ser atestado através das recentes e frequentes descobertas de novas espécies (Peña *et al.* 2018; Liu *et al.* 2018; Richards *et al.* 2019; Jeong et al 2019). Este grande avanço pode ser atribuído principalmente ao sucesso em acessar informações genéticas de material histórico, como tipos nomenclaturais depositados em herbários há mais de um século (Hernandez-Kantún *et al.* 2015; Sissini *et al.* 2014; Richards *et al.* 2017; Peña *et al.* 2018; Gabrielson 2018; Gabrielson 2019).

Muitas mudanças taxonômicas vêm ocorrendo no grupo das ACNG em níveis genéricos (Liu *et al.* 2018; Peña *et al.* 2018) específicos (e.g., Gabrielson *et al.* 2019) e inclusive o reconhecimento relativamente recente de novas ordens (Sporolithales e Hapalidiales) outrora agrupadas em Corallinales (Le Gall *et al.* 2010; Nelson *et al.* 2015). Estudos recentes vêm mostrando como a informação genética é indispensável à taxonomia do grupo, revelando tanto diversidade críptica, com a descoberta de novas espécies, como sinonimizando espécies consideradas distintas por inferências baseadas exclusivamente em dados morfoanatômicos (Kato *et al.* 2019; Hernandez Kantun *et al.* 2015; Hind *et al.* 2019) e fazendo com que ACNG descritas há muitos anos sejam posicionadas sucessivamente em diferentes gêneros e espécies ao longo do tempo (e.g.,

Hernandez Kantun 2016; Gabrielson *et al.* 2019). A maior parte dos registros, citados em nível genérico ou em categoria inferior, necessitam de revisão de acordo com os critérios modernos da taxonomia do grupo, incluindo dados morfoanatômicos e moleculares.

O sudeste brasileiro, especialmente a costa do estado do Rio de Janeiro, é amplamente representado por habitats rochosos, como costões de praias e ilhas costeiras, lajes e parcéis, onde as ACNG prosperam entre os organismos bentônicos dominantes, desempenhando um papel fundamental na bioconstrução e ocupação do substrato (Yoneshigue 1985; Tâmega & Figueiredo 2005; Bahia *et al.* 2014; Tâmega *et al.* 2015). Além disso, é documentada a presença de extensos bancos de rodolitos na plataforma continental do estado do Espírito Santo (Amado-Filho *et al.* 2007; Vilas-Boas *et al.* 2009; Amado-Filho *et al.* 2010; Holz *et al.* 2020), além de recifes coralíneos em sua porção norte (Mazzei *et al.* 2016). Entretanto, até o presente, a maioria dos registros de ACNG desta região foram baseados apenas em dados morfoanatômicos, o que demonstra o grande potencial para novos registros para o sudeste brasileiro (Vilas Boas *et al.* 2009, Amado-Filho *et al.* 2010; Henriques *et al.* 2012; Tâmega *et al.* 2015).

O uso da ferramenta molecular para identificação das ACNG pode revelar uma diversidade críptica ao longo da costa do sudeste brasileiro, região conhecida por abrigar a maior diversidade de macroalgas do Brasil (Guimarães 2003, 2006; Amado-Filho *et al.* 2010). Neste contexto, as principais contribuições deste trabalho dizem respeito ao avanço do conhecimento da biodiversidade marinha da região sudeste brasileira, bem como do conhecimento da taxonomia das ACNG tanto em nível morfoanatômico como molecular. Trata-se de informações de base que auxiliarão na correta identificação destas algas, facilitando a pesquisa e direcionando o manejo nas comunidades onde as ACNG estão presentes.

2. OBJETIVO GERAL

Inferir e descrever a diversidade críptica de ACNG que se desenvolve em habitats rochosos e bancos de rodolitos no sudeste do Brasil a partir de dados moleculares associados a dados morfoanatômicos.

3. METODOLOGIA GERAL

3.1 Áreas de Estudo

3.1.1 Rio de Janeiro

Amostras de ACNG foram coletadas em diferentes áreas ao longo da costa do estado do Rio de Janeiro em costões rochosos da costa e ilhas costeiras do mediolitoral até 40m de

profundidade, totalizando 36 sítios amostrais distribuídos em 11 municípios do norte ao sul fluminense, conforme ilustrado na Figura 2. A localização de cada sítio está apresentada na Tabela 1.



Figura 2. Sítios de coleta ao longo da costa do Estado do Rio de Janeiro.

Tabela 1. Localização dos sítios de coleta no estado do Rio de Janeiro.

Sítio de Coleta	Profundidade (m)	Latitude	Longitutde
Arraial do Cabo/Saco do cherne	2-8	22°57'39"S	42°00'18"O
Arraial do Cabo/Cardeiros	2-5	22°57'55"S	41°59'58"O
Arraial do Cabo/Ilha dos porcos	2-6	22°57'55"S	41°59'36"O
Arraial do Cabo/Praia do forno	2-5	22°57'58"S	41°00'28"O
Arraial do Cabo/Ponta do Maramutá	2-5	22°59'27"S	42°00'01"O
Arraial do Cabo/Praia Vermelha	2-6	22°59'13"S	41°59'34"O
Arraial do Cabo/Saco do Inglês	2-26	23°00'24"S	42°00'29"O
Arraial do Cabo/Ilha do Francês	5-11	22°58'56"S	42°02'19"O
Cabo Frio/Capões	5-15	22°51'48"S	41°55'17"O
Cabo Frio/Ilha Comprida (Ponta sul)	2-6	22°52'11"S	41°57'03"O
Cabo Frio/Ilha dos Pargos (Enseada do Pinguim)	5-20	22°51'11"S	41°54'21"O
Cabo Frio/Ilha dos Pargos (Enseada Meia Lua)	5-15	22°51'26"S	41°54'29"O
Cabo Frio/Ilha Comprida(Enseada do Cabrito)	2-11	22°52'20"S	41°57'00"O
Cabo Frio/Ilha dos Papagaios (3ª enseada)	5-15	22°53'52"S	41°58'57"O
Cabo Frio/Ilha dos Papagaios (1ª enseada)	2-15	22°53'38"S	41°59'12"O
Búzios/Ilha de Âncora (Enseada do Badejo)	5-30	22°46'24"S	41°47'29"O
Búzios/ Lage dos Alagados	30-40	22°46'15"S	41°48'39"O
Búzios/ Praia da Tartaruga	1-3	22°45'18"S	41°54'07"O
Búzios/Praia do Forno (lado esquerdo)	1-4	22°45'44"S	41°52'30"O
Búzios/ Praia Rasa	Costão maré baixa	22°44'04"S	41°57'29"O
Ilha de Itacuruça/ Praia Grande	0,5-1	22°57'14"S	43°54'27"O
Ilha Grande/Ilha dos Meros	5-15	23°12'50"S	44°21'32"O
Ilha Grande/Pendão de Dentro	15-30	23°12'12"S	44°22'03"O
Ilha Grande/Ponta da Lagoa Verde	6-7	23°08'16"S	44°19'41"O
Angra dos Reis/ Ponta Leste	2-5	23°03'01"S	44°15'03"O
Angra dos reis/Ilha da Jipóia	5-10	23°02'20"S	44°22'01"O
Angra dos Reis/ Praia da Biscaia	1-3	23°01'45"S	44°14'15"O
Angra dos Reis/Praia do Laboratório - Usina	2-3	23°00'47"S	44°26'42"O
Macaé/Ilha do Francês - Lado Oeste	6-7	22°24'03"S	44°41'48"O
Macaé/Lage da Cruz	2-5	22°24'45"S	44°42'43"O
Macaé/Ponta da Cavala	2-6	22°23'56"S	41°41'15"O
Macaé/Barro Vermelho	2-8	22°24'06"S	41°41'27"O
Macaé/Leste da Ilha de Santana	3-9	22°24'51"S	41°42'04"O
Paraty/Ilha dos Meros Sul	3-10	23°10'55"S	44°34'31"O
Paraty/Ponta da Cajaíba	3-8	23°13'56"S	44°34'35"O
Paraty/Ilha Deserta	2-9	23°13'16"S	44°33'20"O

3.1.2 Espírito Santo

Amostras foram coletadas em um banco de rodolitos adjacente aos recifes coralíneos conhecidos como Recifes Esquecidos, situados a 30 m de profundidade e cerca de 31 km da costa do estado do Espírito Santo.



Figura 3. Localização do banco de rodolitos amostrado no estado do Espírito Santo (ponto vermelho).

3.2 Coleta

As coletas foram realizadas por meio de mergulho autônomo. As ACNG aderidas ao substrato rochoso foram retiradas em fragmentos que variaram de 2-6 cm de comprimento com auxílio de marreta e ponteira (Figura 4A). Também foram coletados, manualmente, fragmentos e seixos cobertos por ACNG diretamente no substrato (Figura 4B), assim como no banco de rodolitos (Figura 5).

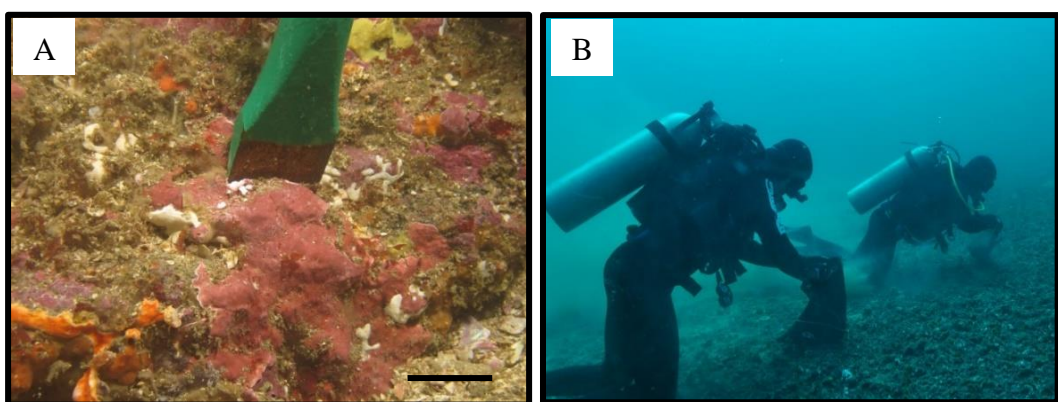


Figura 4 (A-B) Métodos de coleta utilizados para obtenção de amostras de ACNG em região costeira. (A) Detalhe da retirada de crosta de ACNG do substrato rochoso. Barra de escala = 4 cm. (B) Coleta manual de fragmentos e seixos diretamente no substrato (Fotos: Fernando Moraes).

O material coletado foi seco ao ar livre e depois armazenado em sílica gel para manter a integridade do DNA das amostras para as análises moleculares. Os espécimes utilizados no estudo encontram-se depositados no Herbário do Jardim Botânico do Rio de Janeiro (RB).



Figura 5. Método de coleta utilizado no banco de rodolitos (Foto: Fernando Moraes).

3.3 Análises Morfoanatômicas

Duas técnicas foram empregadas para análises morfoanatômicas das ACNG: uma voltada à obtenção de cortes para observação em microscopia óptica (Figura 6A), uma adaptação do protocolo adotado por Maneveldt & Van der Merwe (2012), e outra específica para análises em microscopia eletrônica de varredura (Figura 6B), a mesma adotada por Bahia *et al.* 2010).

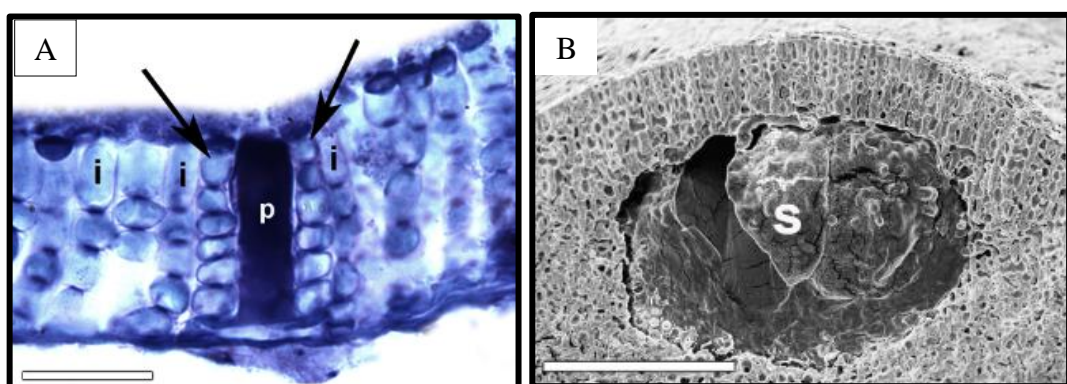


Figura 6 (A-B) Imagens obtidas através dos métodos de microscopia utilizados (Figura modifica de Jesionek *et al.* 2020). (A) Imagem obtida através de microscopia eletrônica de transmissão. Barra de escala = 20 µm. (B) Imagem obtida através de microscopia eletrônica de varredura. Barra de escala = 130 µm.

Para observação em microscopia ótica foram realizadas etapas que consistiram em analisar a amostra em microscópio estereoscópio e selecionar o fragmento com conceptáculos ou soros, seguido de descalcificação do fragmento em ácido nítrico, desidratação do material em série crescente de etanol 70%, 90% e 100%, com pelo menos 1 h de duração em cada concentração, imersão em uma solução do infiltração após a polimerização foram realizados os cortes por meio de uma navalha de aço (Leica fio C) em micrótomo rotatório (Spencer Lens co. 3533) com espessura regulada para 7-10 µm. O material foi corado e colocado em lâminas para seguir com as observações em microscópio ótico de campo claro (Olympus BX43) com câmera digital acoplada e utilizando-se do *software* de processamento de imagens *Scope Image DynamicPro*.

Para análises em microscopia eletrônica de varredura, porções do material foram retirados com alicate de corte para obter cortes da região de interesse do talo e posicionados em um porta-espécime de alumínio (*stub*) com fita adesiva dupla face de carbono. O material passou por processo de metalização, utilizando ouro (cerca de 20 nm de espessura), para observação em microscópio eletrônico de varredura (Zeiss SEM EVO 40) sob uma aceleração de voltagem de 15 kv.

3.4 Análises Moleculares

3.4.1 Extração de DNA

O DNA foi extraído dos exemplares utilizando Qiagen DNeasy Blood and Tissue Kit® (Qiagen, Crawley, UK), seguindo protocolo de Broom *et al.* (2008) com modificações.



Figura 7. Uso de *microdrill* para retirada de tecido para extração de DNA. Seta indicando pó fino gerado durante a maceração.

Para a remoção de amostras de tecido dos espécimes, foram selecionadas áreas livres de epibiontes em microscópio estereoscópico e utilizando um *microdrill* (Dremel® 3000, Breda, Netherlands) com broca de ponta esférica medindo 25 mm. A região selecionada foi desgastada, buscando remover a camada mais superficial da alga, obtendo um pó fino para extração do DNA total, com uma biomassa rica em DNA (Figura 7).

3.4.2 Amplificação do DNA (PCR)

A amplificação dos marcadores de interesse através de PCR (*Polymerase Chain Reaction*) foi realizada utilizando o *kit Illustra PuReTaq Ready-To-Go PCR Beads* (GE Healthcare, Chelfont Amersham, UK). Desta forma, as condições da PCR como temperaturas e tempo de cada etapa variou entre os marcadores. Estas condições estão detalhadas a seguir.

3.4.3 Marcadores Moleculares

Os marcadores utilizados neste estudo foram os cloroplastidiais *psbA* e *rbcL*. O *Photosystem II thylakoid membrane D1* (*psbA*, ~950 pb) é um marcador de natureza altamente variável (Bitner *et al.* 2011), proposto para espécies próximas geneticamente.

É um gene considerado de fácil amplificação. Os *primers* utilizados para amplificação deste marcador foram: *psbAF1* x *psbAR2*. Os ciclos das reações de sequenciamento foram realizadas com *primers* da PCR e mais dois *primers* internos, o *psbA500F* e o *psbA550R* (Yoon *et al.* 2002; Torrano-Silva *et al.* 2014) aumentando a qualidade das sequências consenso.

As etapas da PCR para amplificação do *psbA* consistiram em uma desnaturação inicial à 94°C por 5min; seguido de 35 ciclos com desnaturação à 94°C por 30s, anelamento por 45 s à 52°C, e alongamento à 72°C por 1 min; um ciclo final à 94°C por 30s; e extensão final à 72°C por 7 min. A temperatura de anelamento variou, para algumas amostras, em até 2°C.

O Marcador *Ribulose-1,5-bisphosphate carboxylase large subunit* (*rbcL*, ~1,350 pb) é amplamente utilizado em análises filogenéticas do grupo e estudos de DNA *barcoding* e foi aplicado amplamente a essas algas por Freshwater *et al.* (1994). O uso da extremidade 3' deste gene (*rbcL-3p*) vem sendo utilizado com sucesso em estudos que envolvem material histórico depositado em herbário (Sissini *et al.* 2014), gerando um banco de dados de suma importância.

As etapas da PCR para amplificação do *rbcL* consistiram em uma desnaturação inicial à 94°C por 5 min; seguido de 35 ciclos com desnaturação à 94°C por 30s, anelamento por 45 s à 45°C, e alongamento à 72°C por 1 min; um ciclo final à 94°C por 30s; e extensão final à 72°C por 7 min. A temperatura de anelamento variou, para algumas amostras, em até 2°C.

O material amplificado na PCR foi visualizado em gel de agarose para avaliação do êxito do ensaio e purificado utilizando o *kit Illustra GFX PCR DNA Purification kit* (GE Healthcare, Chelfont Amersham, UK) seguindo o protocolo do fabricante.

Para o sequenciamento de ambos os marcadores, o *kit BigDyeTM Terminator v3.1 Sequencing* (*Applied Biosystems*, Waltham, Massachusetts, EUA) foi utilizado seguindo o protocolo do fabricante. As amostras foram submetidas à 40 ciclos à 96°C por 10s, 50°C por 20s e 60°C por 4min no termociclador DNA ABI 3730 (*Applied Biosystems*). As sequências de consenso foram construídas usando o *software Sequencher®* (v4.1.4, *Gene Codes Corporation*) e cromatogramas foram visualmente verificados quanto a ambiguidades.

4 REFERÊNCIAS BIBLIOGRÁFICAS

- Amado-Filho, G. M., Maneveldt, G., Marins, B. V., Manso, R. C. C., Pacheco, M. R., Guimarães, S. P. B. 2007. Structure of rhodolith beds from a depth gradient of 4 to 55 meters at the south of Espírito Santo coast, Brazil. *Ciencias Marinas*, 32: 34-65.
- Amado-Filho G. M., Maneveldt G. W., Pereira-Filho G. H., Manso R. C. C., Bahia R. G., Barros-Barreto M. B., Guimarães S. M. P. B. 2010. Seaweed diversity associated with a Brazilian tropical rhodoliths bed. *Ciencias Marinas*, 36:3 71–391.
- Amado-Filho G. M., Moura R. L., Bastos A. C., Salgado L. T., Sumida P. Y., Guth A. Z., Francini-Filho R. B., Pereira-Filho G.H, Abrantes D. P., Brasileiro P. S., Bahia R. G., Leal R. N., Kaufman L., Kleypas J. A., Farina M., Thompson F. L. 2012a. Rhodolith beds are major CaCO₃ bio-factories in the tropical south west atlantic. *Plos One*, 7: e35171.
- Aguirre, J., Riding, R., and Braga, J. C. 2000. Diversity of coralline red algae: origination and extinction patterns from the early cretaceous to the pleistocene. *Paleobiology*, 26: 651–667.
- Aguirre, J., Braga, J. C., Martín, J. M., and Betzler, C. (2012). Palaeoenvironmental and stratigraphic significance of Pliocene rhodolith beds and coralline algal bioconstructions from the Carboneras Basin (SE Spain). *Geodiversitas*, 34: 115–136.
- Asnagui, V., Thrush, S.F., Hewitt, J.E., Mangialajo, L., Cattaneo-Vietti, R., Chiantore, M. 2015. Colonisation process and the role of coralline algae in rocky shore community dynamics. *Journal of Sea Research*, 95: 132-138.
- Bahia, R. G., Abrantes, D. P., Brasileiro, P. S. 2010. Rhodolith bed structure along a depth gradient on the northern coast of Bahia, Brazil. *Brazilian Journal of Oceanography*, 58: 323-337.

Bahia R.G., Amado-Filho G.M., Azevedo J. & Maneveldt G.W. 2014. *Porolithon improcerum* (Porolithoideae, Corallinaceae) and *Mesophyllum macroblastum* (Melobesioideae, Hapalidiaceae): new records of crustose coralline red algae for the southwest Atlantic Ocean. *Phytotaxa*, 190: 38–44.

Bittner, L., Payri, C. E., Maneveldt, G. W., Couloux, A., Cruaud, C., de Reviers, B., & Le Gall, L. 2011. Evolutionary history of the Corallinales (Corallinophycidae, Rhodophyta) inferred from nuclear, plastidial and mitochondrial genomes. *Molecular Phylogenetics and Evolution*, 61(3), 697–713.

Bosence DWJ (1983a) Description and classification of rhodoliths (rhodoids, rhodolites). In: Peryt TM (ed) Coated grains. Springer, Berlin, pp 217–224.

Bosence DWJ (1983b) The occurrence and ecology of recent rhodoliths – a review. In: Peryt TM (ed) Coated grains. Springer, Berlin, pp 225–242.

Bosence DWJ (1983c) Coralline algae from the Miocene of Malta. *Palaeontology* 26:147–173.

Braga, J. C., Bassi, D., and Piller, W. (2010). “Palaeoenvironmental significance of Oligocene-Miocene coralline red algae - a review,” in Carbonate Systems During the Oligocene-Miocene Climatic Transition, Vol. 42. eds M. Mutti, W. E. Piller, and C. Betzler (Oxford; Chichester; Hoboken, NJ: IAS Spec. Publ.; Wiley-Blackwell), 165–182.

Broom, J.E.S., Hart, D. R., Farr, T. J., Nelson, W. A., Neill, K. F. Harvey, A. S. Woelkerling, W. J. 2008. Utility of psbA and nSSU for phylogenetic reconstruction in the Corallinales based on New Zealand taxa. *Molecular Phylogenetics and Evolution*, 46: 958–973.

Burdett H. L, Aloisio E, Calosi P. et al. 2012. The effect of chronic and acute low pH on the intracellular DMSP production and epithelial cell morphology of red coralline algae. *Marine Biology Research*, 8:756–763

Cabioch J. 1972. Étude sur les Corallinacées. II. La morphogenèse; conséquences systématiques et phylogénétiques. *Cahiers de Biologie Marine*, 13: 137-288.

Cabioch, J., 1988. Morphogenesis and generic concepts in coralline algae—a reappraisal. *Botanica*, 49:1-98.

Caragnano, A., Foetisch, A., Maneveldt, G. W., Millet, L., Liu, L. C., Lin, S. M. Rodondi, G., Payri, C. E. 2018. Revision of Corallinaceae (Corallinales, Rhodophyta): recognizing *Dawsoniolithon* gen. nov., *Parvicellularium* gen. nov. and Chamberlainoideae subfam. nov. containing *Chamberlainium* gen. nov. and *Pneophyllum*. *Journal of Phycology*, 54: 391-409.

Diaz-Polido, G., Anthony, K. R. N., Kline, D. I., Dove, S., Hoegh-Guldberg, O. Interactions between ocean acidification and warming on the mortality and dissolution of coralline algae. *Journal of Phycology*, 48: 32-39.

Freshwater D.W. & Rueness J. 1994. Phylogenetic relationships of some European *Gelidium* (Gelidiales, Rhodophyta) species based upon *rbcL* sequence analysis. *Phycologia*, 33: 187–194.

Gabrielson P.W., Hughey J.R. & Diaz-Pulido G. 2018. Genomics reveals abundant speciation in the coral reef building alga *Porolithon onkodes* (Corallinales, Rhodophyta). *Journal of Phycology*, 54: 429–434.

Guimarães SMPB. 2003 Uma análise da diversidade da flora marinha bentônica do estado do Espírito Santo, Brasil. *Hoehnea* 30: 11–19.

Guimarães SMPB. 2003 Uma análise da diversidade da flora marinha bentônica do estado do Espírito Santo, Brasil. *Hoehnea* 30: 11–19. Guimarães SMPB. 2006. A revised checklist of benthic marine Rhodophyta from the State of Espírito Santo, Brazil. *Bol. Inst. Bot.* 17: 143–194.

Hall-Spencer, J.M., Rodolfo-Metalpa, R., Martin, S., Ransome, E., Fine, M., Turner, S. M., Rowley, S. J., Tedesco, D., Buia, M.C. 2008. Volcanic carbon dioxide vents show ecosystem effects of ocean acidification. *Nature Research*, 454: 96-99.

Henriques M. C., Villas-Boas A. B., Riosmena-Rodríguez R., Figueiredo M. A. O. 2012. New records of rhodolith-forming species (Corallinales, Rhodophyta) from deep water in Espírito Santo State, Brazil. *Helgoland Marine Reserach*, 66:219–231.

Hernandez Kantun J., Rindi F. & Adey W.H. 2015. Sequencing type material resolves the identity and distribution of the generitype *Lithophyllum incrustans*, and related European species *L. hibernicum* and *L. bathyporum* (Corallinales, Rhodophyta). *Journal of Phycology*, 51: 791–807.

Hernandez-Kantun, J., Gabrielson, P., Hughey, J.R., Pezzolesi, L., Rindi, F., Robinson, N. M., Peña, V., Riosmena-Rodriguez, R., Le Gall, L. & Adey, W. 2016. Reassessment of branched *Lithophyllum* spp. (Corallinales, Rhodophyta) in the Caribbean Sea with global implications. *Phycologia*, 55: 619-639.

Hind, K. R., Starko, S., Burt, J. M., Lemay, M. A., Salomon, A. K., Martone, P. T. 2019. Trophic control of cryptic coralline algal diversity. *Proceedings of the National Academy of Sciences*, 116: 15080-15085.

Holz, V. L., Bahia, R. G., Karez, C. S., Vieira F. V., Moraes, F. C., Vale, N. F., Sudatti, D. B., Salgado, L. T., Moura, R. L., Amado-Filho, G. M., and Bastos A. C. 2020. Structure of Rhodolith Beds and Surrounding Habitats at the Doce River Shelf (Brazil). *Diversity*, 12(2): 75.

Jeong, S. Y., Won, B. Y., and Cho, T. O. 2019: Two new encrusting species from the genus *Phymatolithon* (Hapalidiales, Corallinophycidae, Rhodophyta) from Korea, *Phycologia*, 58: 592-604.

Johansen, H.W., 1976. Current status of generic concepts in coralline algae (Rhodophyta). *Phycologia*, 15: 221-244.

Kato, A., and Baba, M. 2019. Distribution of *Lithophyllum kuroshioense* sp.nov., *Lithophyllum subtile* and *L. kaiseri* (Corallinales, Rhodophyta), but not *L. kotschyanum*, in the northwestern Pacific Ocean, *Phycologia*, 58: 648-660.

Le Gall, L., Payri, C.E., Bittner, L. & Saunders, G.W. 2010. Multigene phylogenetic analyses support recognition of the Sporolithales ord. nov. *Molecular Phylogenetics and Evolution*, 54: 302–305.

Littler, M. M. & Littler, D. S. 1994. Plant life of the deep ocean realm. *Biologie in Unserer*.

Liu L.C., Lin S.M., Caragnano A. & Payri C. 2018. Species diversity and molecular phylogeny of non-geniculate coralline algae (Corallinophycidae, Rhodophyta) from Taoyuan algal reefs in northern Taiwan, including *Crustaphytum* gen. nov. and three new species. *Journal of Applied Phycology*, 30: 3455–3469.

Maneveldt, G.W. & Van der Merwe, E. 2012. *Heydrichia cerasina* sp. nov. (Sporolithales, Corallinophycidae, Rhodophyta) from the southernmost tip of Africa. *Phycologia*, 51: 11– 21.

Martin S. Gattuso J. P. 2009. Response of Mediterranean coralline algae to ocean acidification and elevated temperature. *Global Change Biology* 15(8): 2089–2100.

Mazzei E.F., Bertoncini A.A., Pinheiro H.T., Machado L.F., Vilar C.C., Guabiroba H.C., Costa T.J.F., Bueno L.S., Santos L.N., Francini-Filho R.B., Hostim-Silva M., Joyeux

J.C. 2016. Newly discovered reefs in the southern Abrolhos Bank, Brazil: Anthropogenic impacts and urgent conservation needs *Marine Pollution Bulletin*, 114: 123-133.

McCoy, S. & Kamenos, N. 2015. Coralline algae (Rhodophyta) in a changing world: Integrating ecological, physiological, and geochemical responses to global change. *Journal of Phycology*, 51: 6-24.

Morse, D. E., & Morse, A. N. C. 1991. Enzymatic Characterization of the Morphogen Recognized by *Agaricia humilis* (Scleractinian Coral) Larvae, *The Biological Bulletin*, 181, no. 1: 104-122.

Nelson W (2009) Calcified macroalgae—critical to coastal ecosystems and vulnerable to change: a review. *Mar Freshw Res* 60(8):787–801

Nelson, W. A., Sutherland, J. E., Farr, T. J., Hart, D. R., Neill, K. F., Kim, H. J. & Yoon, H. S. 2015. Multi-gene phylogenetic analyses of New Zealand coralline algae: *Corallinapetra Novaezelandiae* gen. et sp. nov. and recognition of the Hapalidiales ord. nov. *Journal Phycology*, 51: 454-468.

Novak, K., Sánchez, M. A. S., Cufar, K., Raventós, J., and Luis, M. Age, climate and intra-annual density fluctuations in *Pinus halepensis* in Spain. *IAWA Journal*, 34: 459-474.

Paul W. Gabrielson, Sandra C. Lindstrom & Jeffery R. Hughey. 2019: *Neopolyborolithon loculosum* is a junior synonym of *N. arcticum* comb. nov. (Hapalidiales, Rhodophyta), based on sequencing type material, *Phycologia*, 58: 229-233.

Peña, V., Adey, W.H., Riosmena-Rodríguez, R., Jung, M.Y., Afonso-Carrillo, J., Choi, H.G. & Bárbara, I. 2011. *Mesophyllum sphaericum* sp. nov. (Corallinales, Rhodophyta): a new maerl-forming species from the Northeast Atlantic. *Journal of Phycology*, 47: 911–927.

- Peña, Viviana & Gall, Line & Rösler, Anja & Payri, Claude & Braga, Juan. (2018). *Adeylithon bosencei* gen. et sp. nov. (Corallinales, Rhodophyta): a new reef-building genus with anatomical affinities with the fossil Aethesolithon. *Journal of Phycology*, 55: 134-145.
- Pereira-Filho GH, Veras PC, Francini-Filho RB, Moura RL and others (2015) Effects of the sand tilefish *Malacanthus plumieri* on the structure and dynamics of a rhodolith bed in the Fernando de Noronha Archipelago, tropical West Atlantic. *Mar Ecol Prog Ser* 541:65-73.
- Richards J.L., Sauvage T., Schmidt W.E., Frederiq S., Hughey J.R. & Gabrielson P.W. 2017. The coralline genera *Sporolithon* and *Heydrichia* clarified by sequencing type material of their generitypes and other species. *Journal of Phycology* 53: 1044–1059.
- Rindi, F., Braga, J. C., Martin, S., Peña, V., Le Gall, L., Caragnano, A. and Aguirre, J. 2019. Coralline Algae in a Changing Mediterranean Sea: How Can We Predict Their Future, if We Do Not Know Their Present? Front. *Marine Science*, 6: 723.
- Roberts, R. 2001. A review of settlement cues for larval abalone (*Haliotis* spp.). *J. Shellfish Res*, 20: 571-586.
- Steller D., L., Riosmena-Rodriguez R, Foster M. S. Roberts C. A. 2003. Rhodolith bed diversity in the Gulf of California: the importance of rhodolith structure and consequences of disturbance. *Aquat Conserv*, 13: S5–S20.
- Sissini M.N., Oliveira M.C., Gabrielson P.W., Robinson N.M., Okolodkov Y. B., Riosmena-Rodríguez R. & Horta P.A. 2014. *Mesophyllum erubescens* (Corallinales, Rhodophyta)—so many species in one epithet. *Phytotaxa*, 190: 299–319.
- Steneck, R. S. & Adey, W. H. 1976. The role of environment in control of morphology in *Lithophyllum congestum*, a Caribbean algal ridge builder. *Botanica Marina*, 19: 197–215.

Steneck, R. S. 1986. The ecology of coralline algal crusts: convergent patterns and adaptive strategies. *Annual Review of Ecological Systematics*, 17: 273-303.

Tâmega F.T.S. & Figueiredo M.A.O. 2005. Distribuição das algas calcárias incrustantes (corallinales, rhodophyta) em diferentes habitats na praia do forno, Armação dos Búzios, Rio de Janeiro. *Rodriguésia*, 87: 123-132.

Tâmega F.T.S., Riosmena-Rodriguez R., Spotorno-Oliveira P., Mariath R., Khader S. & Figueiredo M.A.O. 2015. Taxonomy and distribution of non-geniculate coralline red algae (Corallinales, Rhodophyta) on rocky reefs from Ilha Grande Bay, Brazil. *Phytotaxa*, 192(4): 267-278.

Torrano-Silva B.N., Riosmena-Rodriguez R. & Oliveira M.C. 2014. Systematic position of Paulsilvella in the Lithophylloideae (Corallinaceae, Rhodophyta) confirmed by molecular data. *Phytotaxa*, 190: 94–111.

Townsend, R.A., Chamberlain, Y.M. & Keats, D.W. 1994. *Heydrichia woelkerlingii* gen. et sp. nov., a newly discovered non-geniculate red alga (Corallinales, Rhodophyta) from Cape Province, South Africa. *Phycologia* 33: 177–186.

Verheij, E. 1993. The genus *Sporolithon* (Sporolithaceae fam. nov., Corallinales, Rhodophyta) from the Spermonde Archipelago, Indonesia. *Phycologia* 32: 184–196.

Villas-Boas, A. B., Riosmena-Rodriguez, R., Amado-Filho, G. M., Maneveldt, G .W., Figueiredo, M. A. O. 2009. Rhodolith-forming species of *Lithophyllum* (Corallinales; Rhodophyta) from Espírito Santo, Brazil, including the description of *L. depressum* sp. nov. *Phycologia*, 48: 237-248.

Yoneshigue Y. 1985. Taxonomie et ecologie des algues marines dans la region de Cabo Frio (Rio de Janeiro, Bresil). PhD thesis. Université d'Aix Marseille, Marseille, France. 466 pp.

Woelkerling, W.J. 1988. The coralline red algae: an analysis of the genera and sub-families of nongeniculate Corallinaceae. British Museum Natural History and Oxford University Press, London.

Capítulo 1

Newly discovered coralline algae in Southeast Brazil: *Tectolithon fluminense* gen. et sp. nov. and *Crustaphytum atlanticum* sp. nov. (Hapalidiales, Rhodophyta).

MICHEL B. JESIONEK, RICARDO G. BAHIA, MANOELA B. LYRA, LUIS A.B. LEÃO,
MARIANA C. OLIVEIRA AND GILBERTO M. AMADO-FILHO

Artigo publicado no periódico *Phycologia* em janeiro de 2020.

Newly discovered coralline algae in Southeast Brazil: *Tectolithon fluminense* gen. et sp. nov. and *Crustaphytum atlanticum* sp. nov. (Hapalidiales, Rhodophyta).

MICHEL B. JESIONEK^{1*}, RICARDO G. BAHIA¹, MANOELA B. LYRA¹, LUIS A.B. LEÃO¹,
MARIANA C. OLIVEIRA² AND GILBERTO M. AMADO-FILHO¹

¹*Instituto de Pesquisas Jardim Botânico do Rio de Janeiro, Diretoria de Pesquisa*

Científica, Rua Pacheco Leão 915, 22460-030, Rio de Janeiro, RJ, Brazil

²*University of São Paulo, Biosciences Institute, Botany Department, Rua do Matão 277,
05508-090, São Paulo, Brazil*

CONTACT

Corresponding author: mbraunbr@gmail.com

RUNNING TITLE

Tectolithon fluminense gen. et sp. nov. and *Crustaphytum atlanticum* sp. nov. from
Brazil.

ABSTRACT

Two new Melobesioideae, *Tectolithon fluminense* gen. et sp. nov. and *Crustaphytum atlanticum* sp. nov., were described based on specimens collected at depths from 2 to 30 m in a tropical to subtropical transitional region of Southeast Brazil. Analyses of the plastid-encoded markers *psbA* and *rbcL* demonstrated that these taxonomic novelties belong to the clade formed by the typically subarctic/arctic *Clathromorphum* complex. *Tectolithon fluminense* has tetra/bisporangial and carposporangial conceptacles that typically become buried in the thallus because of an enveloping process caused by the development of a vegetative rim that grows from the margins of the conceptacle. The rim then fuses and creates a vegetative cover. The development of this vegetative cover is described in detail and its possible convergent evolution in other taxa is discussed. *Crustaphytum atlanticum* differed morpho-anatomically from the generitype, *C. pacificum* (the only other known species in this genus), by thallus thickness, maximum number of epithallial cell layers, relative size of subepithallial initials and tetra/bisporangial conceptacle chamber dimensions. The observation of specimens from *Tectolithon* and *Crustaphytum* with subepithallial initials that are both longer and shorter than their immediate inward derivatives indicates that this morpho-anatomical character should be used with caution for generic delimitation in the Melobesioideae.

KEY WORDS

Corallinophycidae; Melobesioideae; Morpho-anatomy; Non-geniculate coralline algae; *psbA*; *rbcL*; Taxonomy

INTRODUCTION

The Southeast (SE) Brazilian coastline is largely represented by rocky shore habitats where non-geniculate coralline algae (Corallinales, Hapalidiales and Sporolithales; Corallinophycidae, Rhodophyta) thrive among the dominant benthic organisms and are poorly studied (Yoneshigue 1985, Bahia *et al.* 2014, Tâmega *et al.* 2015). This coast lies in a transitional region between tropical and subtropical zones, that is periodically influenced by upwelling, associated with the local wind regime and bathymetry, that is prevalent during spring–summer (Valentin 2001). These upwelling conditions are characterised by high nutrient concentrations and coastal sea surface temperatures below 18 °C, with temperatures occasionally reaching as low as 13 °C (Valentin 1984; Guimaraens & Coutinho 1996). However, during the non-upwelling period, coastal sea surface waters are characterised by lower nutrient concentrations and temperatures above 21 °C. Such variability in environmental conditions may help explain why this region is considered the richest marine area of the southwest Atlantic, supporting typically tropical and subtropical taxa, as well as temperate taxa adapted to colder waters (Yoneshigue-Valentin & Valentin 1992, Guimarães 2003, Brasileiro *et al.* 2009).

Knowledge of coralline algal species composition and distribution worldwide has been greatly improved since the incorporation of DNA sequencing in taxonomic studies, particularly after the development of successful methods for sequencing old type specimens (Gabrielson *et al.* 2011; Hind *et al.* 2014; Sissini *et al.* 2014, Basso *et al.* 2015; Richards *et al.* 2017). Within the family Hapalidiaceae (Hapalidiales), the main advances were related to generic and specific circumscription, as well as to diversity assessments within the subfamily Melobesioideae (Peña *et al.* 2011, 2014,

2015; Carro *et al.* 2014; Hernandez-Kantun *et al.* 2014; Pardo *et al.* 2014; Sissini *et al.* 2014; Adey *et al.* 2015, 2018; Melbourne *et al.* 2017; Liu *et al.* 2018).

By sequencing three genes (SSU, *rbcL* and *psbA*), Adey *et al.* (2015) found that patterns of cell division, cell elongation and calcification, in addition to ecological and distribution data, could be used to distinguish typically subarctic/arctic genera in this subfamily, in what they called the *Clathromorphum* complex (which includes *Clathromorphum* Foslie, *Neopolyborolithon* W.H.Adey & H.W.Johansen, *Leptophytum* W.H.Adey and *Callilithophytum* P.W.Gabrielson, W.H.Adey, G.P.Johnson & Hernández-Kantún). Despite the reports of *Clathromorphum* species in the Southern Hemisphere (Chamberlain *et al.* 1995; Mendoza & Cabioch 1985; Mendoza *et al.* 1996), DNA sequence data are still required to confirm the occurrence of this genus in that region.

Recently, by gathering evidence from the molecular markers SSU and *psbA*, Liu *et al.* (2018) described a new genus, *Crustaphytum* L.-C.Liu & S.-M.Lin, which was shown to belong to the clade formed by the *Clathromorphum* complex. However, unlike the typically cold-water genera from this complex, *Crustaphytum* is currently known only from the tropical to subtropical Western Pacific Ocean in both the Northern (Taiwan) and Southern (New Caledonia) hemispheres. Following their finding, Liu *et al.* (2018) proposed the following suite of morpho-anatomical characters to distinguish genera of the *Clathromorphum* complex: (1) thallus thickness; (2) growth form (e.g. encrusting, warty, foliose); (3) habit (epilithic, epiphytic, or parasitic); (4) hypothallus growth pattern (coaxial, non-coaxial); (5) anatomy of perithallial cells during thallus growth (all cells gradually elongated, only cells in meristematic layer elongated); (6) orientation of calcite crystals in the meristem (only radially, both vertically and

radially); (7) number of epithallial cell layers; (8) sporangia formation (only tetrasporangia, both bisporangia and tetrasporangia); (9) dimensions of tetra/bisporangial conceptacle chambers; (10) structure of tetra/bisporangial conceptacle roof at maturity (flat-topped, protruding, sunken); and 11) nature of spermatangial systems (branched, unbranched).

During the course of investigating non-geniculate coralline algae from SE Brazil, we found several specimens with multiporate conceptacles attributable to the Melobesioideae (*sensu* Harvey *et al.* 2003). Molecular analyses indicated that they belonged to the same clade as the *Clathromorphum* complex (*sensu* Adey *et al.* 2015) and supported two distinct taxonomic novelties: a new genus, *Tectolithon*, and a new species of *Crustaphytum*. This paper describes both species using a molecular-assisted alpha taxonomic approach (Saunders 2005) and discusses the taxonomic implications for the circumscription of taxa within the Melobesioideae.

MATERIAL AND METHODS

Specimen Collection and Preparation

Specimens were collected from 2 to 30 m depths using SCUBA diving and free diving during 2015 and 2016 on rocky shores off the coast of Rio de Janeiro State, Brazil (from 21°18' to 23°22'S). Detailed site and collection information is provided in Table S1. Fragments ranging from approximately 2 to 7 cm were collected from substrates using a hammer and chisel. Samples, including those selected for morpho-anatomical analysis, were brushed to remove epibionts, air dried, and preserved in silica gel,.

Morpho-anatomical Analyses

Samples for light microscopy examination were prepared using the histological methods described by Maneveldt & van der Merwe (2012). Samples for scanning electron microscopy (SEM) were prepared according to Bahia *et al.* (2010). For species descriptions, the growth-form terminology followed Woelkerling *et al.* (1993) and the thallus anatomical terminology followed Adey & Adey (1973). Distance between primary pit connections was determined for cell length measurements. Maximum cell lumen at right angle to the length was measured for cell diameter. Conceptacle measurements followed Adey & Adey (1973). No uniform number of cells and chambers were measured which explains why ranges and not averages with means are provided. For these ranges, the same criteria adopted by Maneveldt *et al.* (2017) were considered. External morphological analyses were performed on all sequenced specimens. From these, eight sequenced specimens of *Tectolithon fluminense* and both sequenced specimens of *Crustaphytum atlanticum* were selected for further anatomical analyses and (Table S1). All specimens were deposited in the Herbarium of the Rio de Janeiro Botanical Garden (RB); herbarium abbreviations followed Thiers (2019, continuously updated).

DNA Sequence and Phylogenetic Analyses

Extraction and amplification of DNA were carried out at the Instituto de Pesquisas Jardim Botânico do Rio de Janeiro, Brazil. DNA extractions were performed using fragments of thalli that were visually clean and free of epibionts. A microdrill (Dremel® 3000, Breda, Netherlands) was used to grind the surface (pinkish) of the thallus, resulting in a powdered material that was used for extraction (*c.* 15 mg). DNA was

extracted using the Qiagen DNeasy Blood and Tissue Kit® (Qiagen, Crawley, UK) following the modified protocol of Broom *et al.* (2008). Two plastid-encoded markers (*psbA* and *rbcL*) were amplified. The *psbA* gene was amplified using the pairs of primers *psbAF* x *psbAR2* (Yoon 2002). Consensus sequence was 833 base pairs. The *rbcL* gene was amplified using two pairs of primers with the combinations F57 x R1150 and F753 x Rrbc-S (Freshwater and Rueness 1994) and the consensus sequence generated was 1356 base pairs.

Molecular markers were PCR-amplified with an Illustra PuReTaq Ready-To-Go PCR Beads kit (GE Healthcare, Chelfont Amersham, UK) following the manufacturer's protocol in a final volume of 25 µl. The PCR steps for both markers were the same except for the annealing temperature. The procedure consisted of an initial denaturation at 94 °C for 5 min; 35 cycles of denaturation at 94 °C for 30 s, annealing for 45 s at 52 °C for *psbA* and at 45 °C for *rbcL*, and elongation at 72 °C for 1 min; one final cycle at 94 °C for 30 s; and a final extension at 72 °C for 7 min. PCR products were visualised and quantified in agarose gels, and purified using an Illustra GFX PCR DNA Purification kit (GE Healthcare, Chelfont Amersham, UK) following the manufacturer's protocol. Sequencing reactions were performed at Universidade de São Paulo, Brazil. Cycle sequence reactions were performed with PCR primers plus the two internal primers *psbA500F* and *psbA550R* (Yoon *et al.* 2002, Torrano-Silva *et al.* 2014). For both markers, the BigDye™ Terminator v3.1 Sequencing Kit (Applied Biosystems, Waltham, Massachusetts, USA) was used following the manufacturer's protocol. Sequences were obtained in an ABI 3730 DNA Analyser (Applied Biosystems). Consensus sequences were built using Sequencher® (v4.1.4, Gene Codes Corporation) and chromatograms were visually checked for ambiguities.

Datasets were built using sequences of the new species generated in this study plus an additional 29 *psbA* and 20 *rbcL* sequences downloaded from GenBank (the *Clathromorphum complex*, and other representative Melobesioideae and *Sporolithon* [outgroup] specimens), including sequences of type specimens when available.

Phylogenetic relationships were analysed through ML with RAxML 8 (Stamatakis 2014) with 1000 bootstrap replicates (Felsenstein 1985) and Mr. Bayes (Huelsenbeck and Ronquist 2001) with four Monte Carlo–Markov chains, which were run for 5 million generations; trees were sampled every 1000 generations. with 1,250,000 trees discarded as burn-in and using the remaining trees to build the 50% majority rule consensus trees. All phylogenetic analyses were performed in Geneious R7. The jModelTest 2.1.4 (Darriba *et al.* 2012) was used to estimate model parameters.

RESULTS

We generated 17 *psbA* sequences from specimens here attributed to *Tectolithon fluminense*, all of which presented intraspecific sequence divergences of 0 – 0.3% (Table S2). Additionally, we generated two identical *psbA* sequences from specimens here attributed to *Crustaphytum atlanticum*, all collected along the coast of the Rio de Janeiro State (Fig. 1, Table S1). The resultant phylogram showed that the Brazilian specimens belonged to the *Clathromorphum* complex (Fig. 1). The analyses resolved two clades within this complex: (A) was represented by sequences of *Crustaphytum pacificum* L.C.Liu & Showe M.Lin, *C. atlanticum*, *Crustaphytum* sp. and *Tectolithon fluminense*; and (B) was represented by sequences of *Clathromorphum compactum* (Kjellman) Foslie, *Clathromorphum circumscripum* (Strömfelt) Foslie, *Clathromorphum nereostratum* Lebednik, *Callilithophytum parcum* (Setchell & Foslie)

P.W.Gabrielson, W.H.Adey, G.P.Johnson & Hernández-Kantún, *Neopolyporolithon arcticum* (Kjellman) P.W.Gabrielson, S.C.Lindstrom & Hughey, and *N. reclinatum* (Foslie) W.H.Adey & H.W.Johansen. The genus *Tectolithon* formed a highly supported clade, diverging from the closely related genus *Crustaphytum* by 6.3% (Fig. 1, Table S3). Within *Crustaphytum*, *C. atlanticum* formed a highly supported clade, diverging from the holotype of *C. pacificum* (generitype) by 1.6% and from the New Caledonia specimen by 1%.

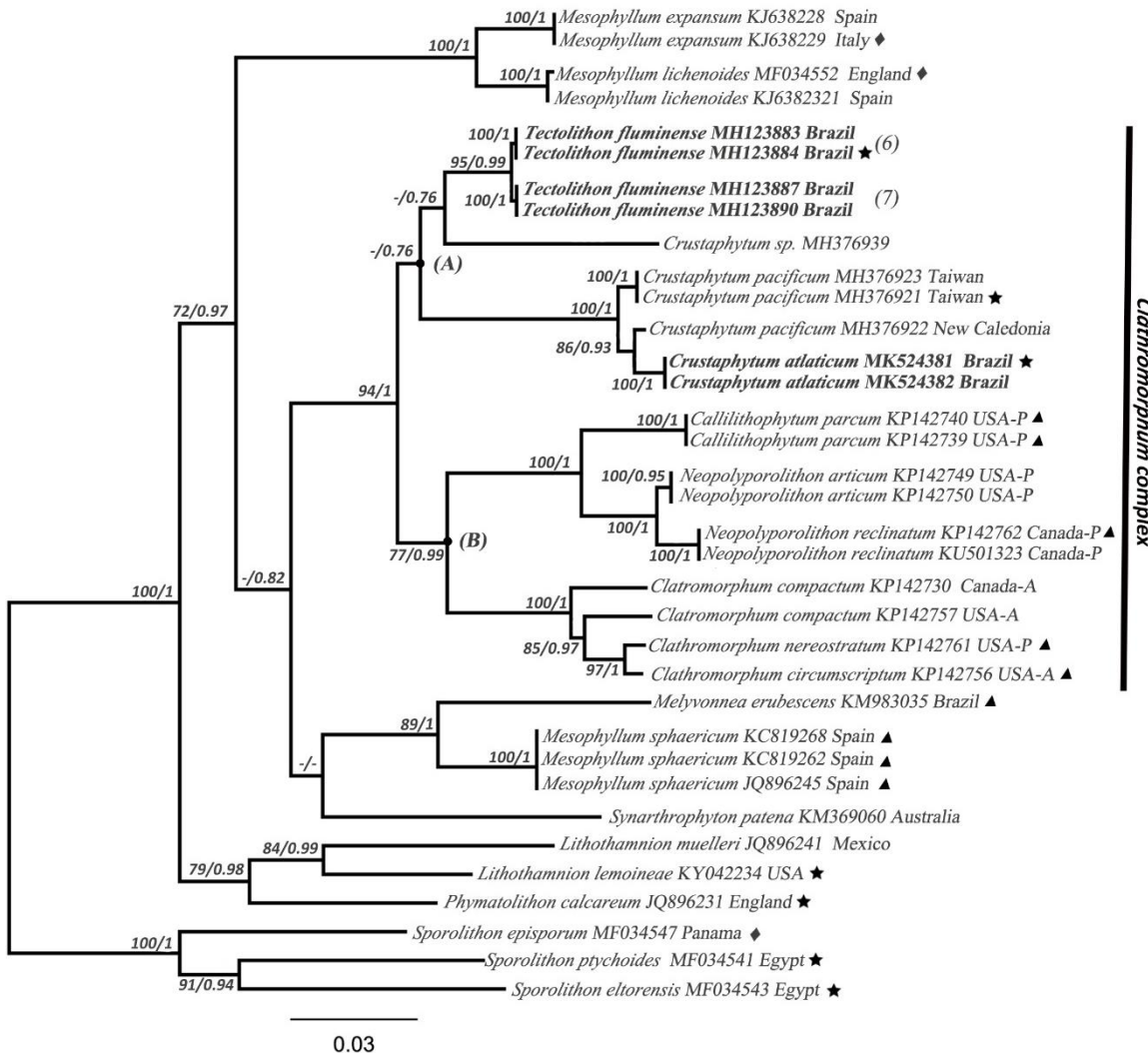


Fig. 1. Phylogenetic tree inferred from RAxML and BI analyses of the *psbA* (833 bp) dataset. Bootstrap support (1000 replicates) and Bayesian posterior probabilities (PP) indicated at nodes. Specimens of *Tectolithon fluminense* and *C. atlanticum* marked in bold. Stars (★) are sequences from type material; triangles (▲) are species whose identification is confirmed by comparison of DNA sequences with type material; diamonds (◆) denote topotypes. Numbers between parentheses represent number of identical sequences beyond the two represented in each clade of *Tectolithon* (see Table S1). The letters P and A next to the localities indicate Pacific and Atlantic Oceans, respectively. Bootstrap values lower than 70% and PP lower than 0.8 are not shown.

In relation to the *rbcL* marker, two sequences were generated, one from a paratype of *T. fluminense* and the other from the isotype of *C. atlanticum*, both due to unsuccessful attempts in obtaining sequences from their respective holotype specimens. Identification of both specimens were confirmed by validation with their respective holotype sequences through comparative *psbA* analyses (99.8% similarity for *T. fluminense* and 100 % similarity for *C. atlanticum*) (Table S3). Analysis of *rbcL* sequences showed that *T. fluminense* differed genetically from currently available sequences from the *Clathromorphum* complex (Fig. 2), differing from its closest neighbour, *Crustaphytum atlanticum*, by 8.5% (Table S4). Two sequences in GenBank (Hapalidiaceae sp., Sissini *et al* 2014) matched exactly the paratype of *T. fluminense*, expanding the occurrence of the species to Santa Catarina State, South Brazil. *Crustaphytum atlanticum* differed by 8.5–12.9% from the other genera of the *Clathromorphum* complex (Table S4). No *rbcL* sequences exist for *C. pacificum* (generitype and currently the only other species in the genus), so a direct comparison with *C. atlanticum* is limited to the *psbA* marker.

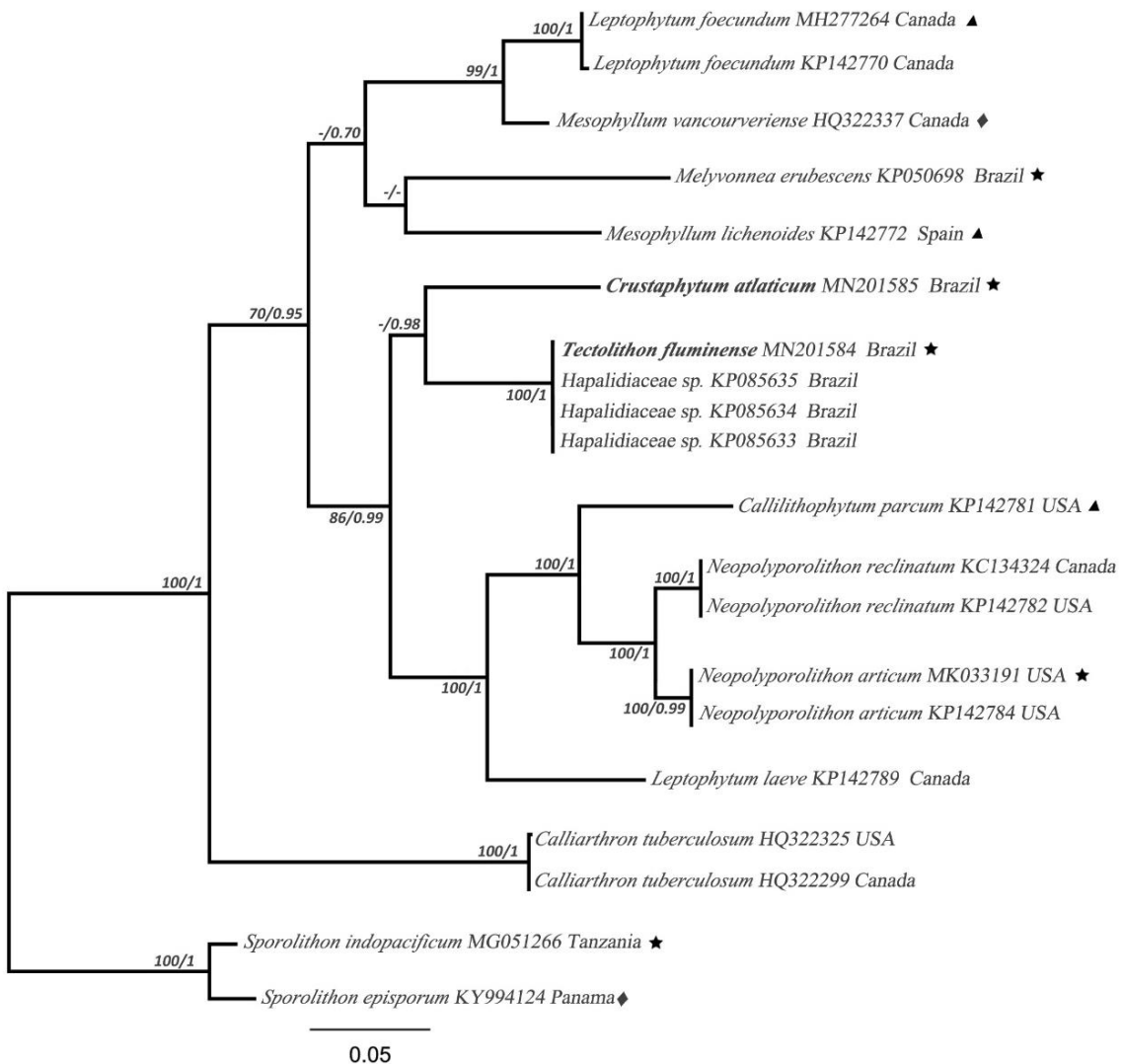


Fig. 2. Phylogenetic tree inferred from RAxML and BI analyses of *rbcL* (1356 bp) dataset. Bootstrap support (1000 replicates) and Bayesian posterior probabilities (PP) indicated at nodes; specimens of *Tectolithon fluminense* and *Crustaphytum atlanticum* marked in bold. Stars (★) are sequences from type material; triangles (▲) are species whose identification is confirmed by comparison of DNA sequences with type material; diamonds (◆) denote topotypes. Numbers in parentheses are the number of sequenced specimens. Bootstrap values lower than 70% and PP lower than 0.8 not shown.

***Tectolithon* Bahia, Jesionek & Amado-Filho gen. nov.**

TYPE SPECIES: *Tectolithon fluminense* Bahia, Jesionek & Amado-Filho sp. nov.

DESCRIPTION: Thallus non-geniculate, epilithic, encrusting to warty. Thallus organisation monomerous and non-coaxial. Epithallial cells with rounded or flattened walls but not flared, formed in a single layer. Subepithallial initials/meristematic cells varying in size and may be the same length, longer or shorter than cells subtending them. Cells of contiguous filaments joined by cell fusions; secondary pit connections

absent. Tetra/bisporangial conceptacles multiporate, protruding above surrounding thallus surface; flat-topped when mature and volcano-like with peripheral rim development when older, producing zonately divided tetra/bisporangia.

Tetra/bisporangial and carposporangial conceptacles becoming buried in thallus as a result of an enveloping process caused by development of vegetative rim that grows from the margins of the conceptacle, fuses and creates a vegetative cover on conceptacle roofs. Gametophytes monoecious or dioecious, producing uniporate conceptacles. Carposporangial conceptacle chambers with a distinctive central pedestal supporting the fertile area. Mature male conceptacles with simple (unbranched) spermatangial systems distributed on the floor, walls and roof of conceptacle chambers.

ETYMOLOGY: The genus prefix ‘*Tecto*’ is derived from the Latin word ‘*tectum*’, meaning ‘roof’, in reference to the development of a vegetative cover on top of the

tetra/bisporangial and carposporangial conceptacle roofs, and suffix ‘*lithon*’ meaning rock (Short & George 2013).

***Tectolithon fluminense* Bahia, Jesionek & Amado-Filho sp. nov.**

Figs 3–28

HOLOTYPE: RB 760367, collected 08 January 2016, leg. MB Jesionek, RG Bahia & GM Amado-Filho, psbA - GenBank MH123884 (Fig. 3).

ISOTYPE: RB 760368, collected 08 January 2016, leg. MB Jesionek, RG Bahia & GM Amado-Filho, psbA - GenBank MH123890.

TYPE LOCALITY: Ilha Comprida, Cabo Frio, Rio de Janeiro State, Brazil (22°52.567'S, 41°56.933'W), subtidal (2–11 m deep), attached to pebble.

ETYMOLOGY: The epithet refers to the holotype locality, Rio de Janeiro State, Brazil; ‘*flumin*’ from the Latin ‘*flumen*’, meaning river (‘*rio*’ in Portuguese), and ‘*ense*’ is from ‘*ensis*’, meaning ‘of’ or ‘from that place’ (Short & George 2013).

ADDITIONAL MATERIAL EXAMINED: See Table S1.

DISTRIBUTION: South Brazil, Santa Catarina State (as unidentified Hapalidiaceae, Sissini *et al.* 2014); Southeast Brazil, Rio de Janeiro State (present study).

Vegetative morphology

Plants were non-geniculate, 100–2000 µm thick, epilithic on primary bedrock, pebbles and boulders in subtidal zone, 2–11 m deep. Thalli were encrusting to warty (Figs 3–5), with internal organisation dorsiventral and a monomerous and plumose hypothallus (non-coaxial; Fig. 6). Hypothallial cells were predominantly elongate, 7–25 µm long and 3–10 µm wide (Fig. 6). Perithallial cells were elongate to rounded, 4–17 µm long and 4–12 µm wide (Figs 7, 8). Subepithallial initials had variable length and were mostly longer than their immediate inward derivatives (Fig. 7), but also as short as, or shorter than their immediate inward derivatives (Fig. 8). Epithallial cells occurred in a single layer, were flattened to rounded, 3–6 µm long and 6–11 µm wide (Figs 7, 8). Cells of contiguous filaments were joined by cell fusions (Fig. 7), and secondary pit connections were not observed. Trichocytes were not observed.

Reproductive morphology

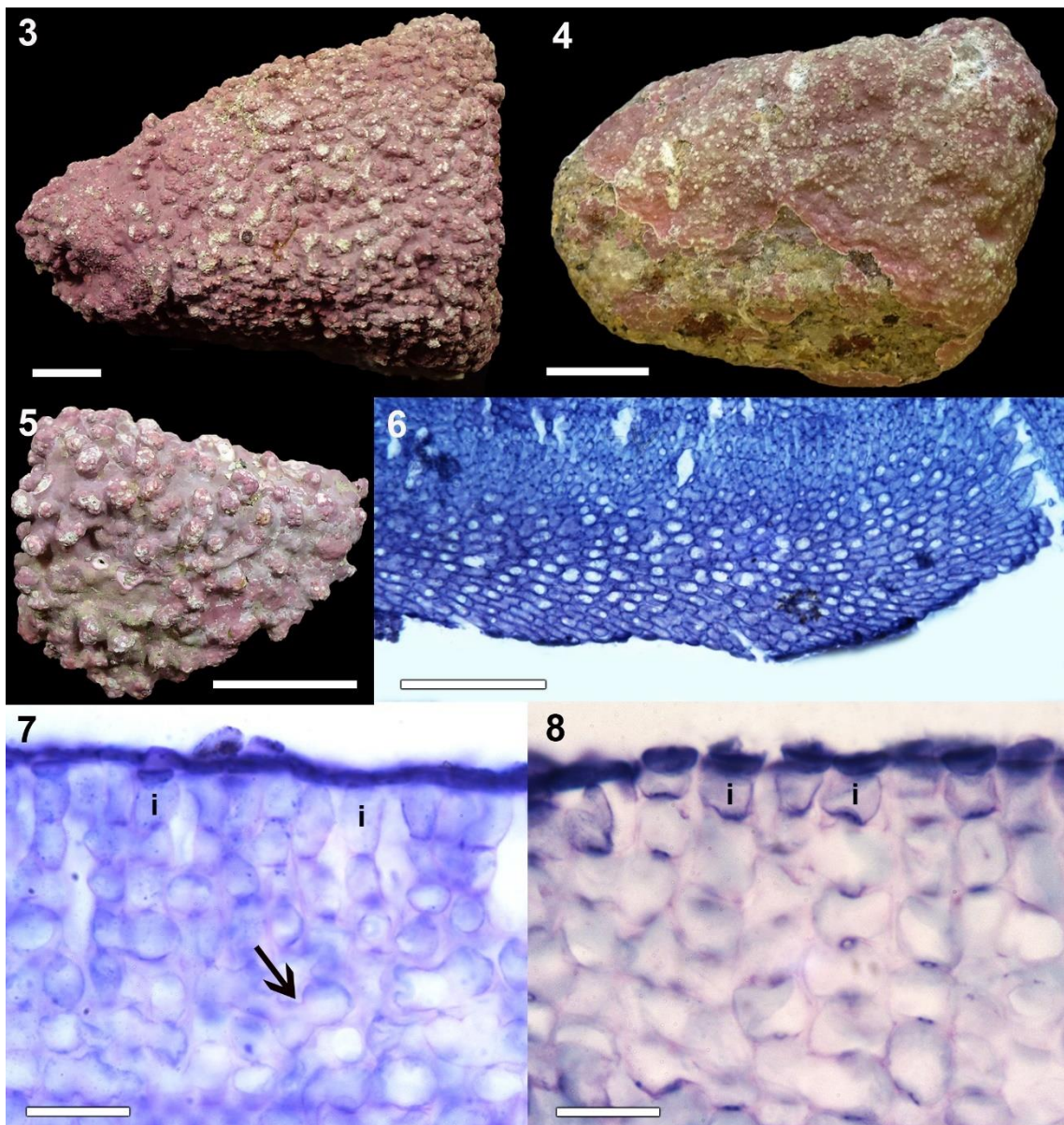
Tetra/bisporangial conceptacles were multiporate (Figs 11–18), protruding above surrounding thallus surface, and flat-topped when mature (Fig. 9) or volcano-like with peripheral rim development when older (Figs 9, 10, 17, 18). Chambers were 80–200 µm high and 200–400 µm wide. The conceptacle floor was 8–16 cells below the surrounding thallus surface. Roof filaments (including epithallial cells) were 4–7 cells long, and filaments lining the conceptacle pore canals were 5–6 cells long (including epithallial cell; Fig. 12). Cells lining pore canals were similar in size and shape to other roof cells (Fig. 12). In surface view, pores were 5–7 µm wide and surrounded by 5–8 rosette cells similar in size or slightly smaller than other roof cells (Figs 19, 20). Tetra/bisporangia scattered across the chamber floor, 120–145 µm in length, 30–55 µm

in diameter; tetra/bisporangial generally the same length as the chamber height. Tetra/biporangial conceptacles were buried in the thallus as a result of an enveloping process caused by the development of a vegetative rim that grows from the margins of the conceptacle pore plate, fuses and creates a vegetative cover (Figs 9, 10, 13–18). This enveloping process, when initiated, gives an impression of a typical volcano-like conceptacle in surface view (Figs 9, 10). Voids, corresponding to the space between the conceptacle pore plate and the vegetative cover, were visible above buried conceptacles (Figs 15, 16). Chambers of buried tetra/bisporangial conceptacles sometimes infilled with vegetative filaments formed by enlarged cells (Fig. 16).

Gametophytes (Figs 21–28) were monoecious or more commonly dioecious. Carpogonial/female conceptacles were uniporate, protruding above surrounding thallus surface (Figs 21, 22). Chambers were 150–200 µm wide and 30–60 µm high. Carpogonia terminated two-celled filaments arising from the floor of the female conceptacle. Carposporangial conceptacles developed after presumed karyogamy. Their chambers were 320–420 µm wide and 90–200 µm high, with a central pedestal across the floor that supported the fertile area (Figs 23, 24). Similarly as in tetra/bisporangial conceptacles, carposporangial conceptacles become buried as a result of an enveloping process caused by the development of a vegetative rim that grows from the margins of the conceptacle (Figs 23, 24). Carposporophytes bore a discontinuous central fusion cell with peripheral gonimoblast filaments and produced terminal carposporangia (Figs 25, 26).

Spermatangial/male conceptacles were uniporate, protruding above the surrounding thallus surface (Fig. 27). Chambers were 140–190 µm wide and 60–110 µm high. Simple (unbranched) spermatangial systems were distributed on the floor, walls,

and roof of the male conceptacle chambers (Figs 27, 28). Older male conceptacles became buried in the perithallium; however, development of a peripheral rim, as seen in tetra/bisporangial and carposporangial conceptacles, was not observed.



Figs 3–8. Habit and vegetative anatomy of *Tectolithon fluminense* sp. Nov

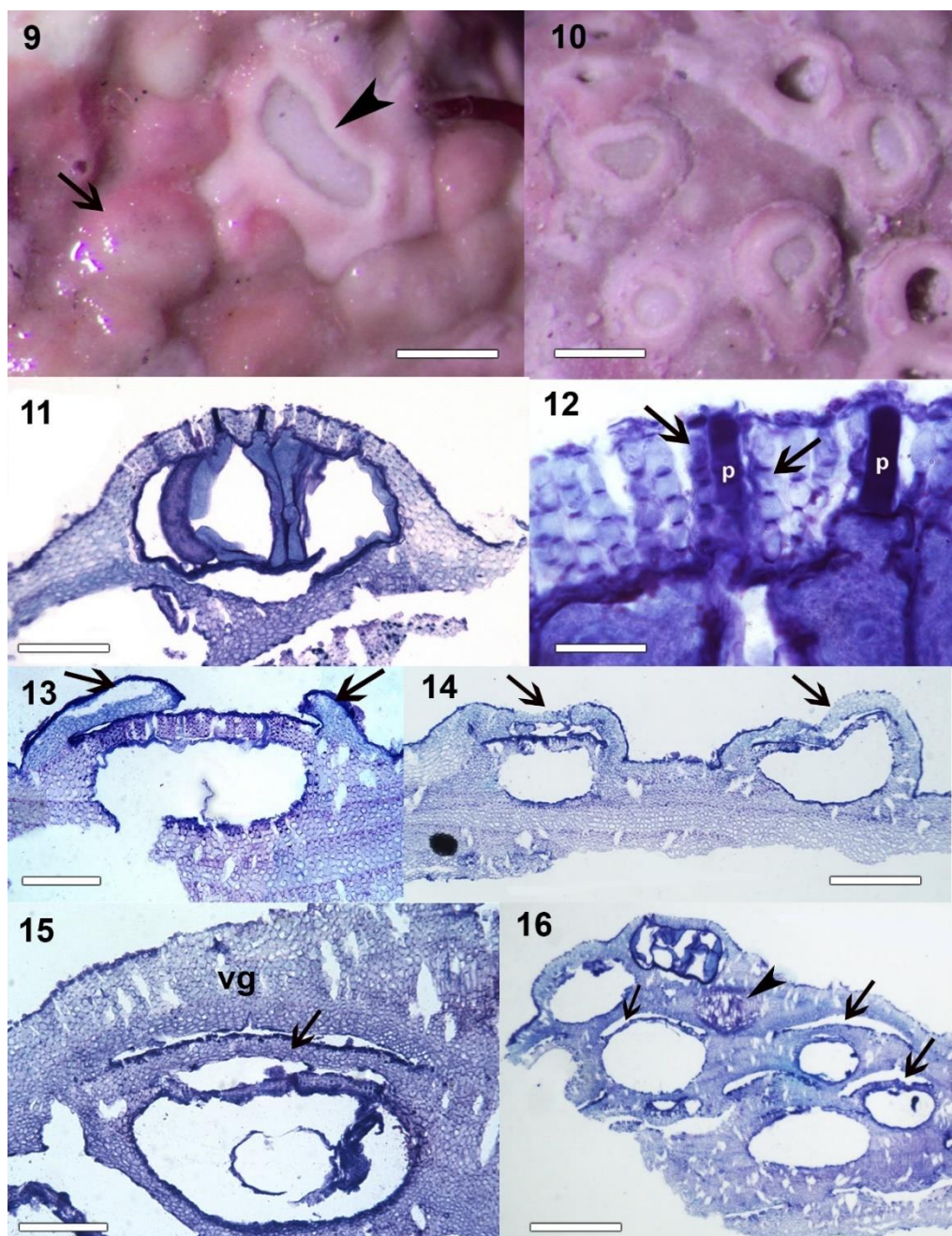
Fig. 3. Warty holotype specimen (RB 760367). Scale bar = 1 cm.

Fig. 4. Encrusting paratype specimen (RB 760361). Scale bar = 1 cm.

Fig. 5. Warty paratype specimen (RB 760353). Scale bar = 1 cm.

Fig. 6. Section through hypothallus showing monomerous, plumose (non-coaxial) construction (RB 760367). Scale bar = 100 µm.

7, 8. ???



Figs 9–16. Tetra/bisporophyte anatomy of *Tectolithon fluminense* sp. nov.

Fig. 9. Surface view showing protruding multiporate tetra/bisporangial conceptacles (RB 760367). Note putative mature conceptacle with domed flat top without any peripheral rim (arrow) and two other, putative older, fused conceptacles with initiated enveloping process caused by rim development (arrow head). Scale bar = 300 µm.

Fig. 10. Surface view showing several multiporate tetra/bisporangial conceptacles with an initiated enveloping process caused by peripheral vegetative rim growth, giving conceptacles a volcano-like appearance (RB 760367). Scale bar = 300 µm.

Fig. 11. Section through mature tetra/bisporangial conceptacle containing remains of tetra or bisporangia (RB 760367). Note absence of vegetative cover. Scale bar = 60 µm.

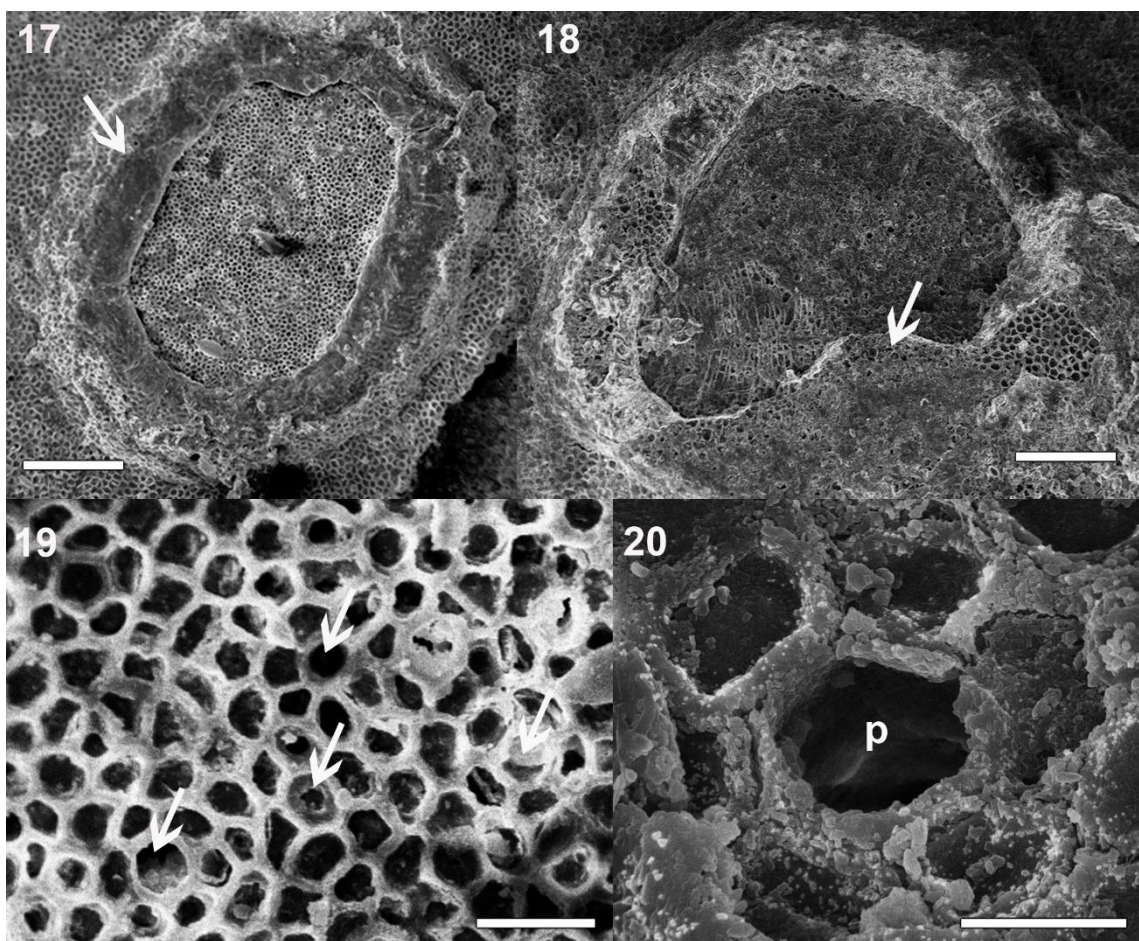
Fig. 12. Section through tetra/bisporangial conceptacle pore plate showing pore canals blocked by a pit plug (p) and bordered by cells similar in size and shape to other roof cells (RB 760367). Scale bar = 20 µm.

Fig. 13. Putative senescent tetra/bisporangial conceptacle with vegetative cover (arrows) caused by enveloping process initiated from margins of conceptacle (RB 760361). Scale bar = 100 µm.

Fig. 14. Section through two senescent tetra/bisporangial conceptacles completely enveloped by vegetative covers (arrows) that first grew from margins of the conceptacle and then became fused (RB 760361). Note space between vegetative covers and conceptacle roofs. Scale bar = 200 µm. RB 760361

Fig. 15. Section through buried tetra/bisporangial conceptacle with conspicuous vegetative cover (arrow) (RB 760361). Note secondary vegetative growth (vg) that has overgrown conceptacle. Scale bar = 100 µm.

Fig. 16. Section of thallus showing mature tetra/bisporangial conceptacles at surface and senescent conceptacles buried in the thallus. Note spaces (arrows) resulting from conceptacle enveloping process and infilled conceptacle with vegetative filaments formed by enlarged cells (arrowhead). Scale bar = 300 µm.



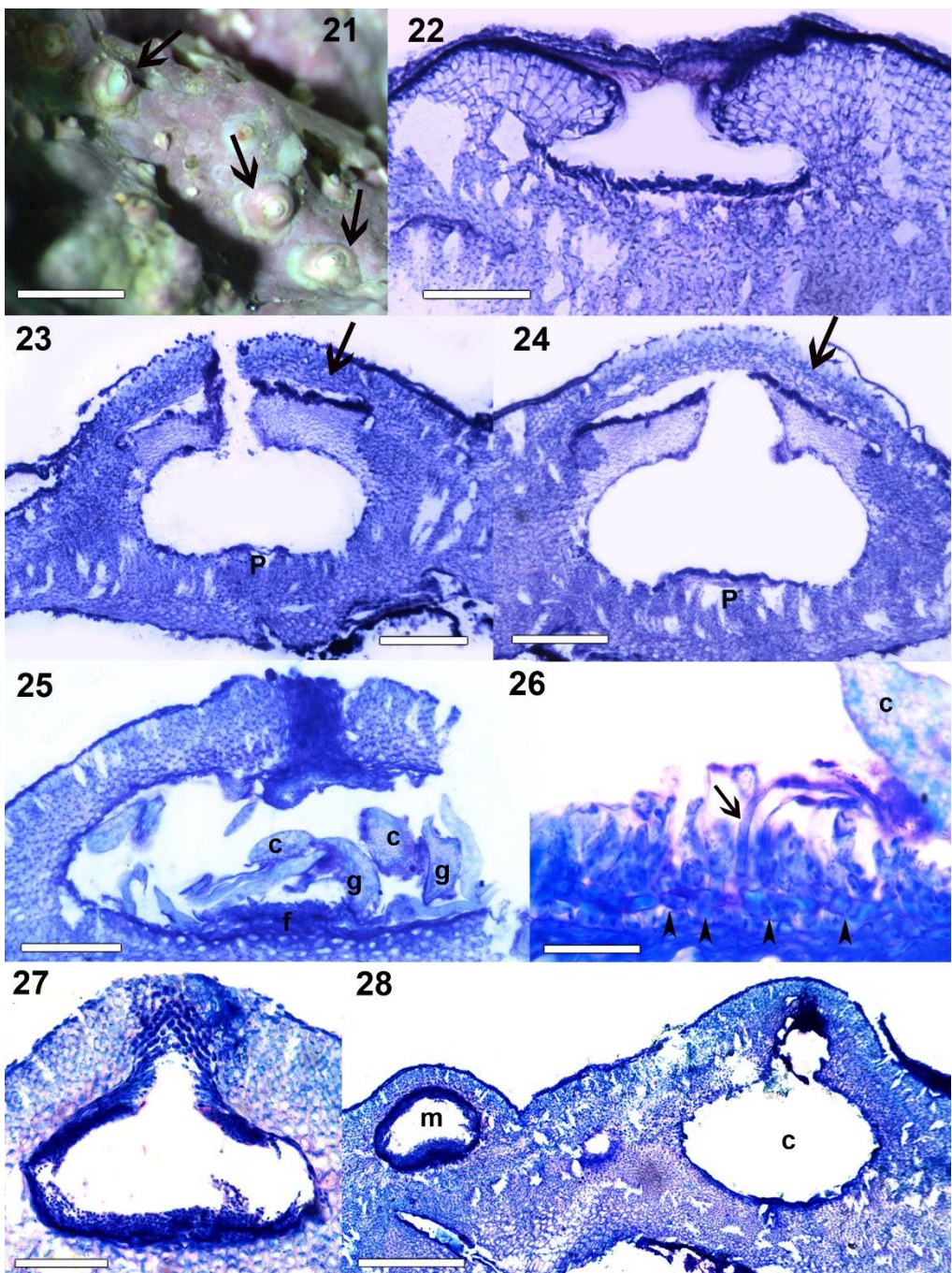
Figs 17–20. SEM surface views of *Tectolithon fluminense* sp. nov. multiporate tetra/bisporangial conceptacles (RB 760361).

Fig. 17. Tetra/bisporangial conceptacle with initiated enveloping process caused by marginal growth of vegetative rim (arrow) giving conceptacle volcano-like appearance. Scale bar = 100 µm.

Fig. 18. Tetra/bisporangial conceptacle in more advanced stage of being enveloped by vegetative rim (arrow). Scale bar = 100 µm.

Fig. 19. Magnified view of pore plate showing pores (arrows) surrounded by 5–8 rosette cells (r) that are similar or slightly smaller than other roof cells. Scale bar = 15 µm.

Fig. 20. Magnified view of pore (p) surrounded by six rosette cells (r). Scale bar = 5 µm.



Figs 21–28 Gametophyte anatomy of *Tectolithon fluminense* sp. nov.

Fig. 21. Carposporangial conceptacles (arrows) in surface view (RB 760371). Note partial envelopment by vegetative cover. Scale bar = 1 mm.

Fig. 22. Female conceptacle primordium containing putative young carpogonial branches distributed across chamber floor (RB 760371). Scale bar = 70 µm.

Fig. 23. Section through empty carposporangial conceptacle with near-complete envelopment by vegetative cover (arrow) initiated from margins of conceptacle (RB 760371). Scale bar = 100 µm.

Fig. 24. Section through carposporangial conceptacle with complete envelopment by vegetative cover (arrow) (RB 760371). Note space between vegetative cover and conceptacle roof and distinctive central pedestal (p) at centre of chamber floor. Scale bar = 100 µm.

Fig. 25. Broken carposporangial conceptacle with central fusion cell (f) and peripheral gonimoblast filaments (g) terminating in carposporangia (c) (RB 760369). Scale bar = 100 µm.

Fig. 26. Magnified view of carposporangial conceptacle chamber with discontinuous central fusion cell (arrowheads), remains of carpogonial branches (arrow), and carposporangium (c) (RB 760369). Scale bar = 25 µm. **Fig. 27.** Mature male conceptacle with spermatangial filaments on floor, walls, and roof of chamber (RB 760369). Scale bar = 60 µm.

Fig. 28. Male (m) and putative carposporangial (c) conceptacles occurring side by side on same thallus (RB 760361). Scale bar = 70 µm. *atlanticum* multiporate tetra/bisporangial conceptacles (RB 760361).

***Crustaphytum atlanticum* Jesionek, Bahia & Amado-Filho sp. nov.**

Figs 29–37

DESCRIPTION:

HOLOTYPE: RB 777607, collected 06 January 2016, *leg. MB Jesionek & RG Bahia*, *psbA* - GenBank MK524381 (Fig. 29).

ISOTYPE: RB 777609, collected 06 January 2016, *leg. MB Jesionek & RG Bahia*, *psbA* - GenBank MK524382.

TYPE LOCALITY: Praia da Biscaia, Angra dos Reis, Rio de Janeiro, Brazil (23°1.750'S, 44°14.217W), subtidal (1–3 m deep), attached to a pebble.

ETYMOLOGY: The specific epithet ‘*atlanticum*’ refers to the Atlantic Ocean, the oceanic basin in which this new species was found.

DISTRIBUTION: Known only known from the type locality.

Vegetative morphology

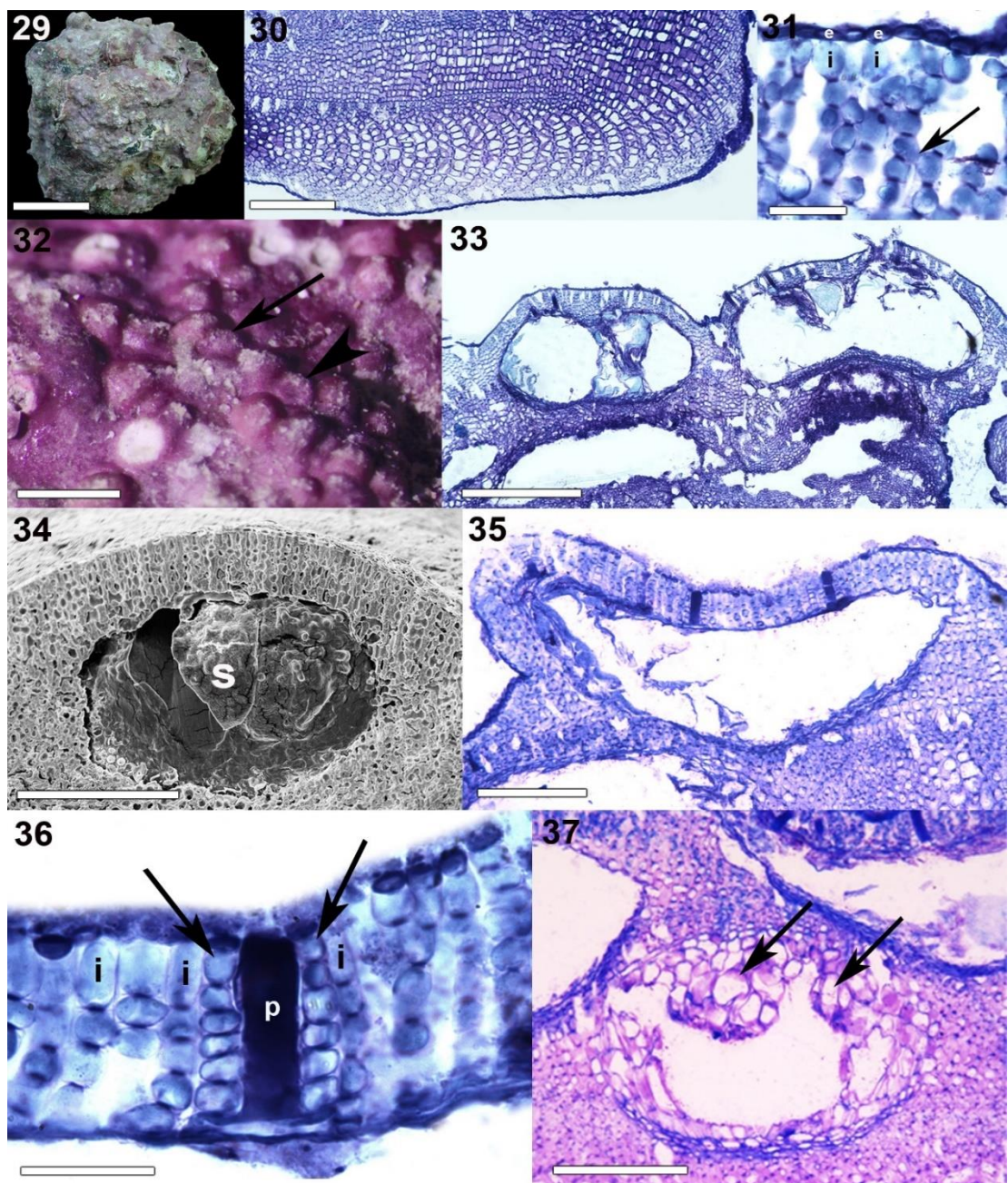
Plants were non-geniculate, 180–600 µm thick, and epilithic on primary bedrock, pebbles, and boulders in the shallow subtidal zone, 1–3 m deep. Thalli were encrusting to warty (Fig. 29), with internal dorsiventral organisation, and the hypothallus

monomerous, predominantly coaxial (Fig. 30). Hypothallial cells were predominantly elongate, 8–25 µm long and 3–10 µm wide (Fig. 30). Perithallial cells were elongate to rounded, 5–22 µm long and 4–12 µm wide (Figs 30, 31). Subepithallial initials were as long as or longer than their immediate inward derivatives (Fig. 31). Epithallial cells occurred in a single layer, were flattened to rounded, 3–5 µm long and 5–9 µm wide (Fig. 31). Cells of contiguous filaments were joined by cell fusions (Fig. 31). Neither secondary pit connections nor trichocytes were observed.

Reproductive morphology

Tetra/bisporangial conceptacles were multiporate (Figs 33, 35) and protruded above the surrounding thallus surface; they were densely crowded and contiguous, either volcano-like (with central sunken pore plate) or domed, with a flat-topped appearance (Figs 32–35). Volcano-like morphology seemed to result from contiguous conceptacle development where one conceptacle deformed another during growth. Chambers were 100–200 µm high and 250–420 µm wide. Conceptacle floors were 13–20 cells below surrounding thallus surface. Filaments lining the pore canals were 6–9 cells long, and similar in size and shape to other roof cells, with the exception of the subepithallial initial, which is shorter than those comprising other roof filaments (Fig. 36). It was not possible to determine the pore diameters or the number of rosette cells.

Tetra/bisporangia were 90–120 µm long and 30–65 µm wide, and scattered across the conceptacle chamber floor. Tetra/bisporangial conceptacles were buried in the thallus, their chambers sometimes infilled with vegetative filaments formed by enlarged cells (Fig. 37).



Figs 29–37. Habit, vegetative and reproductive anatomy of *Crustaphyllum atlanticum* sp. nov..

Fig. 29. Encrusting to warty holotype specimen (RB 777607). Scale bar = 2.5 cm.

Fig. 30. Section through hypothallus showing monomerous, coaxial construction (RB 777609). Scale bar = 300 µm.

Fig. 31. Section through outer thallus with rounded to flattened epithallial cells (e), subepithallial initials (i) that are as long as, or longer than, their immediate inward derivatives, and cell fusion linking adjacent filaments (arrow) (RB 777607). Scale bar = 20 µm.

Fig. 32. Surface view with densely crowded, contiguous multiporate tetra/bisporangial conceptacles (RB 777607). Note occurrence of both domed, flat-topped (arrow) as well as volcano-like conceptacles (with central sunken pore plate; arrowhead). Scale bar = 1 mm.

Fig. 33. Section through two contiguous tetra/bisporangial conceptacles protruding above adjacent vegetative thallus surface (RB 777609). Scale bar = 250 µm.

Fig. 34. SEM fracture through tetra/bisporangial conceptacle containing putative remains of tetra/bisporangia (S) (RB 777607). Scale bar = 130 µm.

Fig. 35. Section through tetra/bisporangial conceptacle with central sunken pore plate (RB 777607). Scale bar = 100 µm.

Fig. 36. Section through tetra/bisporangial conceptacle pore plate showing pit plug (p) and filaments lining pore canal composed of 6–9 cells similar in size and shape to other roof cells. Note that subepithallial initials lining pore canal (arrows) are shorter than subepithallial initials of other roof filaments (i) (RB 777607). Scale bar = 20 µm.

Fig. 37. Section through buried tetra/bisporangial conceptacle partially infilled by enlarged cells (arrows) (RB 777607). Scale bar = 120 µm.

atlanticum multiporate tetra/bisporangial conceptacles (RB 760361).

Table 1. Distinguishing features of genera of the *Clathromorphum* complex. Table modified from Liu *et al.* (2018).

Feature	<i>Clathromorphum</i> ¹	<i>Callilithophytum</i> ¹	<i>Crustaphytum</i> ^{2,3}	<i>Leptophytum</i> ^{1, 4}	<i>Neopolyborolithon</i> ¹	<i>Tectolithon</i> ³
Ocean basin	N Pacific, Arctic, NW Atlantic	NE Pacific	SW Atlantic, NW and SW Pacific	N Pacific, Arctic, N Atlantic	N Pacific	SW Atlantic
Climate zone	Subarctic and Arctic	Temperate and Subarctic	Transition between tropical and subtropical	Subarctic and Arctic	Subarctic	Subtropical and transition between subtropical and tropical
Hypothallus	Non-coaxial	Non-coaxial	Predominantly coaxial	Non-coaxial	Non-coaxial	Non-coaxial
Distinctively elongated subepithallial initials*	Present	Present	Absent	Absent	Present	Absent
Meristem split*	Present	Absent	Absent	Absent	Absent	Absent
Number of epithallial cell layers	3–14	4–5	1–2	1–3	1–7	1
Vegetative cover above tetra/ bisporangial conceptacle roofs	Absent	Absent	Absent	Absent	Absent	Present
Spermatangial systems	Unbranched	Unbranched	Branched	Unbranched	Unbranched	Unbranched

¹Adey *et al.* (2015); ²Liu *et al.* (2018); ³present study; ⁴Athanasiadis & Adey (2006).*See Adey *et al.* (2015) for description.

DISCUSSION

Although southeast Brazil has the highest documented marine floral diversity in the southwest Atlantic Ocean (Guimarães 2003; Brasileiro *et al.* 2009), its non-geniculate coralline algal diversity has been largely ignored. This paper has contributed to our understanding of the local non-geniculate coralline algae diversity in this area by describing a new genus and two new species.

Interspecific *psbA* sequence divergence between genera within the *Clathromorphum* complex ranges from 4.1% to 8.2%. In *psbA*, *T. fluminense* diverges genetically from its closest related genus, *Crustaphytum*, by 6.3%, which is within the divergence range found for *psbA* for genera in the *Clathromorphum* complex. Similarly, interspecific *rbcL* sequence divergence between genera within the *Clathromorphum* complex ranges from 3.8 to 15.7 %. In *rbcL*, *T. fluminense* differs genetically from currently available *Clathromorphum* complex specimens by 8.5%. This is considered a reasonable value for generic separation in this clade. *Tectolithon*, as a new genus, is thus sufficiently distinct in genetic divergence in both markers. Three *rbcL* sequences of unidentified Hapalidiaceae in GenBank (KP085632, KP085633 and KP085634, see Sissini *et al.* 2014) matched exactly our sequence of *T. fluminense*. These sequences extend the distribution range of the species, revealing an occurrence in the subtropics as well as in the subtropical-tropical transition zone.

Tectolithon is morpho-anatomically characterised, amongst other features, by tetra/bisporangial and carposporangial conceptacles becoming buried in the thallus as a result of an enveloping process caused by the development of a vegetative rim that grows from the margins of the conceptacle, this rim then fusing to create a vegetative cover over the conceptacles. The overgrowth of conceptacles by vegetative filaments, as part of their burial within the perithallus, is a feature commonly found in many

coralline algal species (Woelkerling 1988). However, the overgrowth of conceptacles as a result of an enveloping process, and as detailed here for *T. fluminense*, is not widely reported. This process was first described and used as a diagnostic character by Basso (1995) for the description of *Lithothamnion minervae* D.Basso (see also Basso *et al.* 2004, figs 3–5). Other Melobesioideae that present this peculiar process include *Lithothamnion* sp. (Basso *et al.* 2004, fig. 11), *Lithothamnion* sp. 1 (Krayesky-Self *et al.* 2016, fig. 1D), *Mesophyllum conchatum* (Setchell & Foslie) W.H.Adey (Athanasiadis *et al.* 2004, fig. 72), *Mesophyllum engelhartii* (Foslie) W.H.Adey (Chamberlain & Keats 1995, figs 42, 43), and *Mesophyllum macedonis* Athanasiadis (Athanasiadis 1999, fig. 17). As this vegetative cover is visible in buried conceptacles, it is likely useful as an ancillary character for the identification of fossil specimens. The physiological significance of this process is, however, unknown. We hypothesise that growth of a vegetative cover over conceptacles after spore/gamete release may have evolved to prevent the entry of pathogens into otherwise exposed conceptacle chambers, although this does not explain why these species have evolved this particular method instead of the method more commonly reported for other species (see Woelkerling 1988). Co-occurrence of this feature in different lineages of Melobesioideae could have resulted from convergent evolution, which is suggested to explain the high degree of morpho-anatomical similarity in many non-geniculate coralline algae (Van der Merwe *et al.* 2015; Maneveldt *et al.* 2017, 2019). It would be interesting to know how widespread this phenomenon is; additional detailed observations are likely to provide such answers.

Features such as shape of epithallial cells, length of subepithallial initials relative to the perithallial cells immediately subtending them, and presence or absence of a core of coaxial filaments, have been considered useful anatomical characters for distinguishing genera within the Melobesioideae (Harvey *et al.* 2003; Harvey &

Woelkerling 2007). For example, the genus *Phymatolithon* had been morpho-anatomically distinguished from all other genera by cell elongation occurring dorsiventrally in the outer thallus so that the subepithallial initials are as short as, or shorter than, their immediate inward perithallial derivatives (Adey 1964; Wilks & Woelkerling 1994, Adey *et al.* 2018). This feature is no longer morpho-anatomically reliable and diagnostic of *Phymatolithon* as the genus shares this character with several species of *Lithothamnion* (Richards *et al.* (2016), with *C. pacificum* (Liu *et al.* 2018) and now also with *T. fluminense* (this study)

Crustaphytum, *Melyvonnea* and *Mesophyllum* are the only genera of the Melobesioideae in which the thallus contains a core of entirely to predominantly coaxial filaments (Woelkerling 1988, Athanasiadis & Ballantine 2014, Liu *et al.* 2018, this study), although the feature may also be present to a lesser degree in *Synarthrophyton* (May & Woelkerling 1988). *Crustaphytum* and *Mesophyllum* can be morpho-anatomically separated from *Melyvonnea* by the number of cells lining the tetra/bisporangial conceptacle pore canals, which are more than five cells long in *Crustaphytum* and *Mesophyllum*, and only three to five cells long in *Melyvonnea* (Athanasiadis & Ballantine 2014). Additionally, *Crustaphytum* may be morpho-anatomically separated from both *Melyvonnea* and *Mesophyllum* by their spermatangial systems, which are branched in *Crustaphytum* (Liu *et al.* 2018) and unbranched (simple) in *Mesophyllum* and *Melyvonnea* (Woelkerling & Harvey 1993; Athanasiadis & Ballantine 2014). Finally, the shape of the epithallial cells (rounded to flattened, but not flared) is useful for distinguishing *Crustaphytum*, along with all the other genera of Melobesioideae, from *Lithothamnion* in which epithallial cells have flared corners (with trapezoidal-shaped lumen; Woelkerling *et al.* 1988; Liu *et al.* 2018).

Liu *et al.* (2018) provided a morpho-anatomical description of *C. pacificum* (generotype and the only other species of *Crustaphytum*) based on sequenced specimens from Taiwan (holotype locality) and from New Caledonia. *Crustaphytum atlanticum* is more closely related to *C. pacificum* specimens from New Caledonia (1% *psbA* sequence divergence) than to the *C. pacificum* holotype (1.6% *psbA* sequence divergence) from Taiwan. It may well be that the New Caledonia specimens represent another distinct species of *Crustaphytum*. This suggestion will need further investigation. Although the interspecific sequence divergence between *C. atlanticum* and *C. pacificum* is apparently low, these two species are geographically distant, which suggests reproductive isolation and a possible speciation process. Moreover, such a low percentage *psbA* sequence divergence can also be observed in two other genera, namely *Neopolyporolithon* and *Clathromorphum*, in which *N. arcticum* (KP142749 and KP142750) diverges from *N. reclinatum* (KU501323 and KP142762) by 1.3% and *C. nereostratum* (KP142761) diverges from *C. circumscripum* (KP142756) by 0.8% (Table S3). It is worth noting that both *C. atlanticum* and *C. pacificum* occurs in proximal latitude degrees: *C. atlanticum* from Brazil (23°S), *C. pacificum* from Taiwan (25°N) and *C. pacificum* from New Caledonia (22°S).

In our *psbA* analysis, *Crustaphytum* was not monophyletic. One sequence (*Crustaphytum* sp., GenBank MH376939), generated by Liu *et al.* (2018) for an undescribed specimen, was positioned as a sister taxon to *Tectolithon fluminense* but without bootstrap support (Fig. 1). The sequence divergence between this specimen of *Crustaphytum* sp. and both *T. fluminense* and *C. pacificum* was 5.7% and 7.9%, respectively. These sequence divergence values suggest that *Crustaphytum* sp. does not belong in *Crustaphytum* and possibly also not in *Tectolithon*, but possibly represents a new genus.

Although a combination of morpho-anatomical characters was found to be useful for placing *T. fuminense* and *C. atlanticum* in *Tectolithon* and *Crustaphytum*, respectively (Table 1), no diagnostic morpho-anatomical features were observed for them. DNA sequences (*psbA* and *rbcL*) are thus currently the only unequivocal way to assign a name to specimens from these two genera.

ACKNOWLEDGEMENTS

We thank Gavin W. Maneveldt and two anonymous reviewers for their valuable comments that greatly improved the manuscript.

FUNDING

Financial support was provided by the Brazilian governmental agency Carlos Chagas Filho Foundation for Research Support in Rio de Janeiro to RGB and GMAF.

REFERENCES

- Adey W.H. 1964. The genus *Phymatolithon* in the Gulf of Maine. *Hydrobiologia* 24: 377–420. DOI: 10.1007/BF00170412.
- Adey W.H. & Adey P.J. 1973. Studies on the biosystematics and ecology of the epilithic crustose Corallinaceae of the British Isles. *British Phycological Journal* 8: 343–407. DOI: 10.1080/00071617300650381.
- Adey W.H., Hernandez-Kantun J.J., Johnson G. & Gabrielson P.W. 2015. DNA sequencing, anatomy, and calcification patterns support a monophyletic, subarctic, carbonate reef-forming *Clathromorphum* (Hapalidiaceae, Corallinales, Rhodophyta). *Journal of Phycology* 51: 189–203. DOI: 10.1111/jpy.12266.
- Adey W.H., Hernandez-Kantun J.J., Gabrielson P.W., Nash M.C. & Hayek L.A.C. 2018. *Phymatolithon (Melobesioideae, Hapalidiales) in the boreal–subarctic transition zone of the North Atlantic*. Smithsonian Contributions to the Marine Sciences 41, Smithsonian Institution Scholarly Press, Washington, D.C., USA. 90 pp.
- Athanasiadis A., Lebednik P.A. & Adey W.H. 2004. The genus *Mesophyllum* (Melobesioideae, Corallinales, Rhodophyta) on the northern Pacific coast of North America. *Phycologia* 43: 126–165.
- Athanasiadis A. & Ballantine D.L. 2014. The genera *Melyvonnea* gen. nov. and *Mesophyllum* s.s. (Melobesioideae, Corallinales, Rhodophyta) particularly from the central Atlantic Ocean. *Nordic Journal of Botany* 32: 385–436. DOI:10.1111/njb.00265.
- Bahia R.G., Abrantes D.P., Brasileiro P.S., Pereira-Filho G.H. & Amado-Filho G.M. 2010. Rhodolith bed structure along a depth gradient on the northern coast of Bahia

State, Brazil. *Brazilian Journal of Oceanography* 58: 323–337. DOI:

10.1590/S1679-87592010000400007.

Bahia R.G., Amado-Filho G.M., Azevedo J. & Maneveldt G.W. 2014. *Porolithon improcerum* (Porolithoideae, Corallinaceae) and *Mesophyllum macroblastum* (Melobesioideae, Hapalidiaceae): new records of crustose coralline red algae for the southwest Atlantic Ocean. *Phytotaxa* 190: 38–44. DOI: 10.11646/phytotaxa.190.1.5.

Basso D. 1995. Living calcareous algae by a paleontological approach: the genus *Lithothamnion* Heydrich nom. cons. from the soft bottoms of the Tyrrhenian Sea (Mediterranean). *Rivista Italiana di Paleontologia e Stratigrafia* 101: 349–366.

Basso D., Rodondi G. & Mari M. 2004. A comparative study between *Lithothamnion minervae* and the type material of *Millepora fasciculata* (Corallinales, Rhodophyta). *Phycologia* 43: 215–223.

Basso D., Caragnano A., Le Gall L. & Rodondi G. 2015. The genus *Lithophyllum* in the north-western Indian Ocean, with description of *L. yemenense* sp. nov., *L. socotraense* sp. nov., *L. subplicatum* comb. et stat. nov., and the resumed *L. affine*, *L. kaiseri*, and *L. subreduncum* (Rhodophyta, Corallinales). *Phytotaxa* 208: 183–200.

Brasileiro P.S., Yoneshigue-Valentin Y., Bahia R.G., Reis R.P. & Amado-Filho G.M. 2009. Algas marinhas bentônicas da região de Cabo Frio e arredores: síntese do conhecimento. *Rodriguésia* 60: 039–066. DOI: 10.1590/2175-7860200960103.

Broom J.E.S., Hart D.R., Farr T.J., Nelson W.A., Neill K.F., Harvey A.S. & Woelkerling W.J. 2008. Utility of *psbA* and *nSSU* for phylogenetic reconstruction in the Corallinales based on New Zealand taxa. *Molecular Phylogenetics and Evolution* 46: 58–973. DOI: 10.1016/j.ympev.2007.12.016.

Carro B., Lopez L., Peña V., Bárbara I. & Barreiro R. 2014. DNA barcoding allows the accurate assessment of European maerl diversity: a proof-of-concept study.

Phytotaxa 190: 176–189. DOI: 10.11646/phytotaxa.190.1.12

Chamberlain Y.M., Norris R.E., Keats D.W. & Maneveldt G. 1995. *Clathromorphum tubiforme* sp. nov. (Rhodophyta, Corallinaceae) in South Africa with comments on generic characters. *Botanica Marina* 38: 443-454. DOI: 10.1515/botm.1995.38.1-6.443.

Darriba D., Taboada G.L., Doallo R. & Posada D. 2012. jModelTest 2: more models, new heuristics and parallel computing. *Nature Methods* 9: 772–772. DOI: 10.1038/nmeth.2109.

Felsenstein, J. 1985. Confidence limits on phylogenies: an approach using the bootstrap. *Evolution* 39: 783–791. DOI: 10.1111/j.1558-5646.1985.tb00420.x.

Freshwater, D. W. & Rueness, J. 1994. Phylogenetic relationships of some European *Gelidium* (Gelidiales, Rhodophyta) species based upon rbcL sequence analysis. *Phycologia* 33: 187–94. DOI: 10.2216/i0031-8884-33-3-187.1.

Gabrielson P.W., Miller K.A. & Martone P.T. 2011. Morphometric and molecular analyses confirm two species of *Calliarthron* (Corallinales, Rhodophyta), a genus endemic to the northeast Pacific. *Phycologia* 50: 298–316. DOI: 10.2216/10-42.1.

Guimaraens M.A. & Coutinho R. 1996. Spatial and temporal variation of benthic marine algae at the Cabo Frio upwelling region, Rio de Janeiro, Brazil. *Aquatic Botany* 52: 283–299. DOI: 10.1016/0304-3770(95)00511-0.

Guimarães S.M.P.B. 2003. Uma análise da diversidade da flora marinha bentônica do estado do Espírito Santo, Brasil. *Hoehnea* 30: 11–19. DOI: 10.1590/S0104-59702014000300011.

- Harvey A.S. & Woelkerling W.J. 2007. A guide to nongeniculate coralline red algal (Corallinales, Rhodophyta) rhodolith identification. *Ciencias Marinas* 33: 411–426. DOI: 10.7773/cm.v33i4.1210.
- Hind K.R., Gabrielson P.W., Lindstrom S.C. & Martone P.T. 2014. Misleading morphologies and the importance of sequencing type specimens for resolving coralline taxonomy (Corallinales, Rhodophyta): *Pachyarthron cretaceum* is *Corallina officinalis*. *Journal of Phycology* 50: 760–4. DOI: 10.1111/jpy.12205.
- Huelsenbeck J. P. & Ronquist F. 2001. MRBAYES: Bayesian inference of phylogeny. *Bioinformatics* 17: 754–5. DOI: 10.1093/bioinformatics/17.8.754.
- Hernandez Kantun J., Rindi F. & Adey W.H. 2015. Sequencing type material resolves the identity and distribution of the generitype *Lithophyllum incrustans*, and related European species *L. hibernicum* and *L. bathyporum* (Corallinales, Rhodophyta). *Journal of Phycology* 51: 791–807. DOI: 10.1111/jpy.12319.
- Krayeky-Self S., Richards J.L., Rahmatian M. & Fredericq S. 2016. Aragonite infill in overgrown conceptacles of coralline *Lithothamnion* spp. (Hapalidiaceae, Hapalidiales, Rhodophyta): new insights in biomineralization and phylomineralogy. *Journal of Phycology* 52: 161–73. DOI: 10.1111/jpy.12392.
- Liu L.C., Lin S.M., Caragnano A. & Payri C. 2018. Species diversity and molecular phylogeny of non-geniculate coralline algae (Corallinophycidae, Rhodophyta) from Taoyuan algal reefs in northern Taiwan, including *Crustaphytum* gen. nov. and three new species. *Journal of Applied Phycology* 30: 3455–3469. DOI: 10.1007/s10811-018-1620-1.

- Maneveldt G.W. & Van der Merwe E. 2012. *Heydrichia cerasina* sp. nov. (Sporolithales, Corallinophycidae, Rhodophyta) from the southernmost tip of Africa. *Phycologia* 51: 11–21. DOI: 10.2216/11-05.1.
- Maneveldt G.W., Gabrielson P.W. & Kangwe J. 2017. *Sporolithon indopacificum* sp. nov. (Sporolithales, Rhodophyta) from tropical western Indian and western Pacific oceans: first report, confirmed by DNA sequence data, of a widely distributed species of *Sporolithon*. *Phytotaxa* 326: 115–128. DOI: 10.11646/phytotaxa.326.2.3
- Maneveldt G.W., Gabrielson P.W., Townsend R.A. & Kangwe J. 2019. *Lithophyllum longense* (Corallinales, Rhodophyta): a species with a widespread Indian Ocean distribution. *Phytotaxa* 419: 149–168. DOI: 10.11646/phytotaxa.419.2.2
- Mendoza M.L. & Cabioch J. 1985. Critique et comparaison morphogénétique des genres *Clathromorphum* et *Antarcticophyllum* (Rhodophyta, Corallinaceae). Conséquences biogéographiques et systématiques. *Cahiers de Biologie Marine* 26: 251–266.
- May D.I. & Woelkerling W.J. 1988. Studies on the genus *Synarthrophyton* (Corallinaceae, Rhodophyta) and its type species, *S. patena* (J.D. Hooker et W.H. Harvey) Townsend. *Phycologia* 26: 50–71. DOI: 10.2216/i0031-8884-27-1-50.1
- Peña V., Adey W.H., Riosmena-Rodríguez R., Jung M.Y., Afonso-Carrillo J., Choi H.G. & Bárbara I. 2011. *Mesophyllum sphaericum* sp. nov. (Corallinales, Rhodophyta): a new maerl-forming species from the northeast Atlantic. *Journal of Phycology* 47: 911–927. DOI: 10.1111/j.1529-8817.2011.01015.x.
- Peña V., Rousseau F., Reviers B. & Le Gall L. 2014. First assessment of the diversity of coralline species forming maerl and rhodoliths in Guadeloupe, Caribbean using an integrative systematic approach. *Phytotaxa* 190: 190–215. DOI: 10.11646/phytotaxa.190.1.13.

- Peña V., De Clerck O., Afonso-Carrillo J., Ballesteros E., Bárbara I., Barreiro R. & Le Gall L. 2015. An integrative systematic approach to species diversity and distribution in the genus *Mesophyllum* (Corallinales, Rhodophyta) in Atlantic and Mediterranean Europe. *European Journal of Phycology* 50: 20–36. DOI: 10.1080/09670262.2014.981294.
- Richards J.L., Vieira-Pinto T., Schmidt W.E., Sauvage T., Gabrielson P.W., Oliveira M.C. & Fredericq S. 2016. Molecular and morphological diversity of *Lithothamnion* spp. (Hapalidiales, Rhodophyta) from deepwater rhodolith beds in the northwestern Gulf of Mexico. *Phytotaxa* 278: 81-114. DOI: 10.11646/phytotaxa.278.2.1
- Richards J.L., Sauvage T., Schmidt W.E., Fredericq S., Hughey J.R. & Gabrielson P.W. 2017. The coralline genera *Sporolithon* and *Heydrichia* clarified by sequencing type material of their generitypes and other species. *Journal of Phycology* 53: 1044–1059. DOI: 10.1080/09670262.2014.981294.
- Richards, J., L., Bahia, R., G., Jesionek, M. B., And Fredericq, S. 2019. *Sporolithon amadoi* sp. nov. (Sporolithales, Rhodophyta), a new rhodolith-forming non-geniculate coralline alga from offshore the northwestern Gulf of Mexico and Brazil. *Phytotaxa*. 423: 49-67.
- Stamatakis A. 2014. RAxML version 8: a tool for phylogenetic analysis and post-analysis of large phylogenies. *Bioinformatics* 30: 1312-1313. DOI: 10.1093/bioinformatics/btu033
- Steneck R.S. & Adey W.H. 1976. The role of environment in control of morphology in *Lithophyllum congestum*, a Caribbean algal ridge builder. *Botanica Marina* 19: 197–215. DOI: 10.1515/botm.1976.19.4.197

- Saunders G.W. 2005. Applying DNA barcoding to red macroalgae: a preliminary appraisal holds promise for future applications. *Philosophical Transactions of the Royal Society of London* 360(1462): 1879–1888. DOI: 10.1098/rstb.2005.1719.
- Short E. & George A. 2013. *A primer of botanical Latin with vocabulary*. Cambridge University Press, New York, USA. 339 pp.
- Sissini M.N., Oliveira M.C., Gabrielson P.W., Robinson N.M., Okolodkov Y.B., Riosmena-Rodríguez R. & Horta P.A. 2014. *Mesophyllum erubescens* (Corallinales, Rhodophyta)—so many species in one epithet. *Phytotaxa* 190: 299–319. DOI: 10.11646/phytotaxa.190.1.18.
- Tamura, K., Stecher, G., Peterson, D., Filipski, A., & Kumar, S. 2013. MEGA6: molecular evolutionary genetics analysis version 6.0. *Molecular Biology and Evolution* 30: 2725–2729. DOI: 10.1093/molbev/mst197
- Thiers, B. 2019 (continuously updated). Index Herbariorum: a global directory of public herbaria and associated staff. New York Botanical Garden's Virtual Herbarium. <http://sweetgum.nybg.org/ih/>; searched on 17 September 2019.
- Torrano-Silva B.N., Riosmena-Rodriguez R. & Oliveira M.C. 2014. Systematic position of *Paulsilvella* in the Lithophylloideae (Corallinaceae, Rhodophyta) confirmed by molecular data. *Phytotaxa* 190: 94–111. DOI: 10.11646/phytotaxa.190.1.8
- Valentin J.L. 1984. Analyse des paramètres hidrobiologiques dans remontée de Cabo Frio, Brésil. *Marine Biology* 82: 259–276.
- Valentin J.L. 2001. The Cabo Frio upwelling system, Brazil. In: *Coastal marine ecosystems of Latin America* (Ed. by U. Seeliger & B. Kjerfve), pp. 97–105. Springer, Heidelberg, Germany.
- Van der Merwe E., Miklasz K., Channing A., Maneveldt G.W. & Gabrielson P.W. 2015. DNA sequencing resolves species of *Spongites* (Corallinales, Rhodophyta) in

the northeast Pacific and South Africa, including *S. agulhensis* sp. nov. *Phycologia* 54: 471–490. DOI: 10.2216/15-38.1

Wilks K.M. & Woelkerling W.J. 1994. An account of southern Australian species of *Phymatolithon* (Corallinaceae, Rhodophyta) with comments on *Leptophytum*. *Australian Systematic Botany* 7: 183–223. DOI: 10.1071/SB9940183

Woelkerling W.J. & Irvine L.M. 1986. The neotypification and status of *Mesophyllum* (Corallinaceae, Rhodophyta). *Phycologia* 25: 379–396. DOI: 10.2216/i0031-8884-25-3-379

Woelkerling W.J. & Harvey A. 1992. *Mesophyllum incisum* (Corallinaceae, Rhodophyta) in Southern Australia: implications for generic and specific delimitation in the Melobesioideae. *British Phycological Journal* 27: 381–399. DOI: 10.1080/0007161920065032

Woelkerling W.J. & Harvey A. 1993. An account of southern Australian species of *Mesophyllum* (Corallinaceae, Rhodophyta). *Australian Systematic Botany* 6: 571–637. DOI: 10.1071/SB9930571

Woelkerling W.J., Irvine L.M. & Harvey A. 1993. Growth-forms in non-geniculate coralline red algae (Corallinales, Rhodophyta). *Australian Systematic Botany* 6: 277–93. DOI: 10.1071/SB9930277

Yoneshigue Y. 1985. Taxonomie et ecologie des algues marines dans la region de Cabo Frio (Rio de Janeiro, Bresil). PhD thesis, Université d'Aix Marseille, Marseille. 466 pp.

Yoneshigue Y. & Valentin J.L. 1992. Macroalgae of the Cabo Frio, upwelling region, Brazil: ordination of communities. In: *Coastal plant communities of Latin America* (Ed. by U. Seeliger), pp. 31–50. Academic Press, San Diego, USA.

Yoon H.S., Hackett J. & Bhattacharya D. 2002. A single origin of the peridinin- and fucoxanthin-containing plastids in dinoflagellates through tertiary endosymbiosis.

Proceedings of the National Academy of Sciences of the United States of America

99: 11724–11729. DOI: 10.1073/pnas.172234799.

SUPPLEMENTARY MATERIAL

Table S1. List of *Tectolithon fluminensis* type collection and the dataset of *psbA* and *rbcL* sequences used in analysis.

Species	Location	Collector	Date collected	Specimen voucher	GenBank accession numbers	
					<i>psbA</i>	<i>rbcL</i>
<i>Neopolyphorolithon loculosum</i>	USA, Alaska	P. Lebednik	01-Jun-1969	AM-SM-I	KP142750	-
<i>Mesophyllum sphaericum</i>	Spain, Galicia	-	23-Jun-2011	CPVP 1130	KC819268	-
<i>Mesophyllum sphaericum</i>	Spain, Galicia	-	14-Oct-2008	CPVP 776	KC819262	-
<i>Melyvonnea erubescens</i>	Brazil, Fernando de Noronha	H.N. Ridley, T.S. Lea & G.A. Ramage	Aug-1873	FLOR 14896	KM983035	-
Hapalidiaceae sp	Brazil: Santa Catarina	M. Sissini & L. Ferreira	28-Nov-2012	FLOR 14928	-	KP085633
Hapalidiaceae sp	Brazil: Santa Catarina	M. Sissini & L. Ferreira	28-Nov-2012	FLOR 14929	-	KP085634
<i>Mesophyllum sphaericum</i>	Spain, Galicia	I. Barbara and V. Pena	22-Apr-2010	GALW 15776	JQ896245	-
<i>Neopolyphorolithon reclinatum</i>	Canada: British Columbia, Ridley Island	GWS, B. Clarkston, D. McDevit & K. Roy	08-Jun-2007	GWS 008332	KU501323	KC134324
<i>Mastophoropsis canaliculata</i>	Australia, Tasmania	G.T. Kraft & L. Kraft	22-Jan-2010	GWS 015547	KU501331	-
<i>Sporolithon indopacificum</i>	Tanzania: Zanzibar Island	J. Kangwe, J. Nene & K. Mohammed	06-Jun-2016	L:3964509	-	MG051266
<i>Mesophyllum expansum</i>	Italy, Sicily	Viviana Pena	26-Apr-2011	LLG 4061	KJ638229	-
<i>Synarthrophyton patena</i>	Australia, Kitty Millar Bay	-	16-Oct-1999	LTB 17962	KM369060	-
<i>Crustaphytum pacificum</i>	New Caledonia, Cote Blanote	L.-C. Liu	18-Jun-2014	NC0 14-028	MH376922	-
<i>Mesophyllum vancouverense</i>	Canada: British Columbia	P. W. Gabrielson	10-Aug-2007	NCU 588185	-	HQ322337
<i>Callilithophytum parcum</i>	USA, Washington	P.W. Gabrielson	14-Jun-2017	NCU 588636	KP142740	-
<i>Mesophyllum lichenoides</i>	England, South Devon	J.Brodie	22-Jul-2009	NCU 590286	MF034552	-
<i>Sporolithon episporum</i>	Panama, Bocas del Toro	K.Miklasz	13-Jul-2008	NCU 598843	MF034547	-
<i>Clathromorphum compactum</i>	USA, Maine	J. Halfar	03-Sep-2007	NCU 601308	KP142757	-
<i>Clathromorphum circumscriptum</i>	USA, Maine	S.M.E Gabrielson	13-Oct-2012	NCU 601330	KP142756	-
<i>Sporolithon eltorensis</i>	Egypt, El Tor	T.Sauvage_W.E.Schmidt_D.Gabriel	08-May-2012	NCU 606659	MF034543	-
<i>Clathromorphum nereostratum</i>	USA, Alaska	J. Halfar	07-Jun-2008	NCU 627110	KP142761	-
<i>Sporolithon ptychoides</i>	Egypt, El Tor	T.Sauvage_W.E.Schmidt_D.Gabriel	08-May-2012	NCU606660	MF034541	-
<i>Crustaphytum pacificum</i>	Taiwan, Shimen	S.-M. Lin & L.-C. Liu	25-Jun-2015	NTOU 001357	MH376923	-
<i>Crustaphytum pacificum</i>	Taiwan, Xinwu	S.-M. Lin & L.-C. Liu	15-Jan-2015	NTOU 001359	MH376921	-
<i>Crustaphytum sp.</i>	Taiwan, Xinwu	S.-M. Lin & L.-C. Liu	25-Jan-2015	NTOU 001442	MH376939	-
<i>Sporolithon episporum</i>	Panama: Point Toro	M.A.Howe	07-Jan-1910	NY 900041	-	KY994125

<i>Sporolithon dimotum</i>	Puerto Rico: Lemon Bay	M.A.Howe	27-Jun-1903	NY 900043	-	KY994131
<i>Neopolyporolithon arcticum</i>	USA, Alaska	P. Lebednik	01-Jun-1969	PL2Ar	KP142749	-
<i>Tectolithon fluminensis</i>	Brazil, Rio de Janeiro, Cabo Frio, Ilha dos Papagaios (22°56'38"S, 41°59'12"W, 2-15 m)	Jesionek, M.B & Bahia R.G	08-Jan-2016	RB 760353 (paratype)	MH123888	-
<i>Tectolithon fluminensis</i>	Brazil, Rio de Janeiro, Cabo Frio, Ilha dos Pargos (22°51'11"S; 41°54'21"W, 5-20 m)	Jesionek, M.B & Bahia R.G	07-Jan-2016	RB 760354 (paratype)	MH123876	-
<i>Tectolithon fluminensis</i>	Brazil, Rio de Janeiro, Arraial do Cabo, Saco do Inglês (23°00'24"S, 42°00'29"W, 2-26 m)	Jesionek, M.B & Bahia R.G	06-Jan-2016	RB 760355 (paratype)	MH123886	-
<i>Tectolithon fluminensis</i>	Brazil, Rio de Janeiro, Arraial do Cabo, Saco do Inglês (23°00'24"S, 42°00'29"W, 2-16 m)	Jesionek, M.B & Bahia R.G	06-Jan-2016	RB 760356 (paratype)	MH123889	-
<i>Tectolithon fluminensis</i>	Brazil, Rio de Janeiro, Arraial do Cabo, Saco do Inglês (23°00'24"S, 42°00'29"W, 2-26 m)	Jesionek, M.B & Bahia R.G	06-Jan-2016	RB 760357 (paratype)	MH123885	-
<i>Tectolithon fluminensis</i>	Brazil, Rio de Janeiro, Armação dos Búzios, Ilha da Âncora (22°46'34"S, 41°47'24"W, 5-30m)	Jesionek, M.B & Bahia R.G	09-Jan-2016	RB 760358 (paratype)	MH123882	-
<i>Tectolithon fluminensis</i>	Brazil, Rio de Janeiro, Armação dos Búzios, Ilha da Âncora (22°46'34"S, 41°47'24"W, 5-30 m)	Jesionek, M.B & Bahia R.G	09-Jan-2016	RB 760359 (paratype)	MH123881	-
<i>Tectolithon fluminensis</i>	Brazil, Rio de Janeiro, Rio de Janeiro, Ilhas Tijucas (23°03'27"S, 43°30'52"W, 5-10 m)	Bahia R.G & Lyra M.B	22-Oct-2015	RB 760360 (paratype)	-	-
<i>Tectolithon fluminensis</i>	Brazil, Rio de Janeiro, Rio de Janeiro, Ilhas Tijucas (23°03'27"S, 43°30'52"W, 5-10 m)	Bahia R.G & Lyra M.B	22-Oct-2015	RB 760361 (paratype)	MH123891	-
<i>Tectolithon fluminensis</i>	Brazil, Rio de Janeiro, Armação dos Búzios, Praia do Forno (22°45'43"S, 41°52'30"W, 1-4 m)	Jesionek, M.B & Bahia R.G	10-Jan-2016	RB 760362 (paratype)	MH123879	-
<i>Tectolithon fluminensis</i>	Brazil, Rio de Janeiro, Armação dos Búzios, Praia do Forno (22°45'43"S, 41°52'30"W, 1-4 m)	Jesionek, M.B & Bahia R.G	10-Jan-2016	RB 760363 (paratype)	MH123880	-
<i>Tectolithon fluminensis</i>	Brazil, Rio de Janeiro, Armação dos Búzios, Praia do Forno (22°45'43"S, 41°52'30"W, 1-4 m)	Jesionek, M.B & Bahia R.G	10-Jan-2016	RB 760364 (paratype)	MH123887	MN201584
<i>Tectolithon fluminensis</i>	Brazil, Rio de Janeiro, Itacuruçá, Praia Grande (22°57'03"S, 43°54'35"W, 0.5-1 m)	Jesionek, M.B & Bahia R.G	20-Jan-2016	RB 760365 (paratype)	MH123878	-
<i>Tectolithon fluminensis</i>	Brazil, Rio de Janeiro, Angra dos Reis, Ilha dos Meros (22°12'43"S, 44°21'39"W, 5-15 m)	Jesionek, M.B & Bahia R.G	21-Jan-2016	RB 760366 (paratype)	MH123877	-

<i>Tectolithon fluminensis</i> *	Brazil, Rio de Janeiro, Cabo Frio, Ilha Comprida (22°52'34"S; 41°56'56"W, 2-11 m)	Jesioneck, M.B & Bahia R.G	08-Jan-2016	RB 760367 (holotype)	MH123884	-
<i>Tectolithon fluminensis</i>	Brazil, Rio de Janeiro, Cabo Frio, Ilha Comprida (22°52'34"S, 41°56'56"W, 2-11 m)	Jesioneck, M.B & Bahia R.G	08-Jan-2016	RB 760368 (isotype)	MH123890	-
<i>Tectolithon fluminensis</i>	Brazil, Rio de Janeiro, Cabo Frio, Ilha dos Papagaios (22°53'52"S, 41°58'57"W, 2-15 m)	Jesioneck, M.B & Bahia R.G	08-Jan-2016	RB 760369 (paratype)	MH123892	-
<i>Tectolithon fluminensis</i>	Brazil, Rio de Janeiro, Cabo Frio, Ilha dos Papagaios (22°53'52"S, 41°58'57"W, 2-15 m)	Jesioneck, M.B & Bahia R.G	08-Jan-2016	RB 760370 (paratype)	MH123883	-
<i>Tectolithon fluminensis</i>	Brazil, Rio de Janeiro, Cabo Frio, Ilha dos Papagaios (22°53'52"S, 41°58'57"W, 2-15 m)	Jesioneck, M.B & Bahia R.G	08-Jan-2016	RB 760371 (paratype)	-	-
<i>Crustaphytum atlanticum</i> *	Brazil, Rio de Janeiro, Angra dos Reis, Praia da Biscaia (23°01'45"S, 44°14'15"W, 1-3m)	Jesioneck, M.B & Bahia R.G	20-Jun-2016	RB 777607 (holotype)	MK524381	-
<i>Crustaphytum atlanticum</i>	Brazil, Rio de Janeiro, Angra dos Reis, Praia da Biscaia (23°01'45"S, 44°14'15"W, 1-3m)	Jesioneck, M.B & Bahia R.G	20-Jun-2016	RB 777609 (isotype)	MK524382	MN201585
<i>Calliarthron tuberculosum</i>	USA: California	R. E. Gibbs & W. A. Setchell	08-Jan-1899	TRH B17-2582	-	KP142791
<i>Callilithophytum parcum</i>	USA: California, Monterey Co., Pacific Grove	R. E. Gibbs & W. A. Setchell	08-Jan-1899	TRH B17-2582	-	KP142793
<i>Clathromorphum reclinatum</i>	Canada: British Columbia, Vancouver Island	K. Yendo	Jul-1901	TRH B17-2590	-	KP142803
<i>Melyvonnea erubescens</i>	Brazil: Fernando de Noronha	H.N. Ridley, T.S. Lea & G.A. Ramage	Aug-1873	TRH C15-3212	-	KP050698
<i>Callilithophytum parcum</i>	USA, Washington	P.W. Gabrielson	14-Jun-2017	UC 1918246	KP142740	-
<i>Callilithophytum parcum</i>	USA: California	R. E. Gibbs & W. A. Setchell	08-Jan-1899	UC 745690	-	KP142794
<i>Neopolyporolithon arcticum</i>	Russia: Commander Islands, Bering Island	F. R. Kjellman	19-Aug-1879	UPS A000295	-	KP142807
<i>Neopolyporolithon arcticum</i>	-	-	-	UPS A003730	-	MK033191
<i>Leptophytum foecundum</i>	Canada: Labrador	W.H Adey	04-Aug-1964	US 169189	-	KP142770
<i>Leptophytum laeve</i>	Canada: Newfoundland	W.H Adey	08-Sep-1964	US 170538	-	KP142779
<i>Clathromorphum compactum</i>	Canada, Labrador	W. H. Adey	21-Jul-2011	US 170929	KP142730	-
<i>Leptophytum foecundum</i>	Canada: Labrador	W.H Adey	22-Jul-2013	US 170932	-	KP142790
<i>Leptophytum foecundum</i>	USA: Isle of Shoals	W.H Adey	24-Jul-1961	US 170933	-	KP142771
<i>Leptophytum laeve</i>	Canada: Labrador	W.H Adey	Nov-2013	US 170934	-	KP142789
<i>Lithothamnion tophiforme</i>	Canada: Labrador	W.H Adey	12-Jul-2010	US 170938	-	KP142765
<i>Mesophyllum lichenoides</i>	Spain: Ria de Camarinas	W.H Adey	01-Jul-1968	US 170940	-	KP142772

<i>Mesophyllum expansum</i>	Italy, Sicily	Viviana Pena	01-Aug-2010	VPF 00121	KJ638228	-
<i>Mesophyllum lichenoides</i>	Spain, Galicia	Viviana Pena	19-Jan-2011	VPF 00344	KJ638232	-

Table S2. Intra-specific *psbA* sequence divergence in percentage (lower half) and number of nucleotides (upper half) for *Tectolithon fluminense* analyzed in this study. Stars (★) represent sequences from type material.

	GenBank acession No.	1	2	3	4	5	6	7	8	9	10	11	12	13	14	15	16	17
1	MH123892		1	1	1	1	1	1	1	3	3	3	3	3	3	3	3	3
2	MH123891	0.1		0	0	0	0	0	0	2	2	2	2	2	2	2	2	2
3	MH123890★	0.1	0		0	0	0	0	0	2	2	2	2	2	2	2	2	2
4	MH123889	0.1	0	0		0	0	0	0	2	2	2	2	2	2	2	2	2
5	MH123888	0.1	0	0	0		0	0	0	2	2	2	2	2	2	2	2	2
6	MH123887	0.1	0	0	0	0		0	0	2	2	2	2	2	2	2	2	2
7	MH123886	0.1	0	0	0	0	0		0	2	2	2	2	2	2	2	2	2
8	MH123885	0.1	0	0	0	0	0	0		2	2	2	2	2	2	2	2	2
9	MH123884★	0.3	0.2	0.2	0.2	0.2	0.2	0.2	0.2		0	0	0	0	0	0	0	0
10	MH123883	0.3	0.2	0.2	0.2	0.2	0.2	0.2	0.2	0		0	0	0	0	0	0	0
11	MH123882	0.3	0.2	0.2	0.2	0.2	0.2	0.2	0.2	0		0	0	0	0	0	0	0
12	MH123881	0.3	0.2	0.2	0.2	0.2	0.2	0.2	0.2	0		0	0	0	0	0	0	0
13	MH123880	0.3	0.2	0.2	0.2	0.2	0.2	0.2	0.2	0		0	0	0	0	0	0	0
14	MH123879	0.3	0.2	0.2	0.2	0.2	0.2	0.2	0.2	0		0	0	0	0	0	0	0
15	MH123878	0.3	0.2	0.2	0.2	0.2	0.2	0.2	0.2	0		0	0	0	0	0	0	0
16	MH123877	0.3	0.2	0.2	0.2	0.2	0.2	0.2	0.2	0		0	0	0	0	0	0	0
17	MH123876	0.3	0.2	0.2	0.2	0.2	0.2	0.2	0.2	0		0	0	0	0	0	0	0

Table S3. Interspecific *psbA* sequence divergence in percentage (lower half) and number of nucleotides (upper half) for the sequences used in the phylogenetic analyses. *T. fluminense* (*Tectolithon fluminensis*), *Crust. pacificum* (*Crustaphytum pacificum*), *Mes. lichenoides* (*Mesophyllum lichenoides*), *S. episporum* (*Sporolithon episporum*), *S. eltorensis* (*Sporolithon eltorensis*), *S. ptychoides* (*Sporolithon ptychoides*), *L. lemoineae* (*Lithothamnion lemoinea*), *N. reclinatum* (*Neoplyporolithon reclinatum*), *N. arcticum* (*Neoplyporolithon arcticum*), *C. nereostratum* (*Clathromorphum nereostratum*), *C. compactum* (*Clathromorphum compactum*), *Cal. Parcum* (*Callilithophytum parcum*), *M. erubescens* (*Melyvonnea erubescens*), *Syn. Patena* (*Synarthrophyton patena*), *Mes. expansum* (*Mesophyllum expansum*), *Mes. sphaericum* (*Mesophyllum exphaericum*), *L. muelleri* (*Lithothamnion muelleri*), *P. calcareum* (*Phymatolithon calcareum*), *Cruts. atlanticum* (*Crustaphytum atlanticum*). Stars (★) represent sequences from type material; triangles (▲) represent species whose identification is confirmed by comparison of DNA sequences with type material; diamonds (◆) denote topotypes.

	Specimens	1	2	3	4	5	6	7	8	9	10	11	12	13	14	15	16	17	18	19	20	21	22	23	24	25	26	27	28	29	30	31	32	33	34	35
1	MH123886_ <i>T. fluminense</i>	2	0	2	47	50	52	50	77	98	109	103	75	58	58	52	50	54	56	56	63	63	59	67	68	77	80	79	67	67	67	80	74	52	52	
2	MH123883_ <i>T. fluminense</i>	0.2	2	0	45	50	52	50	77	99	110	104	75	58	58	52	50	54	56	56	63	63	59	65	68	77	80	79	65	65	2	0	45	50	52	
3	MH123890_ <i>T. fluminense</i>	0	0.2	2	47	50	52	50	77	98	109	103	75	58	58	52	50	54	56	56	63	63	59	67	68	77	80	79	67	67	67	80	74	52	52	
4	MH123884_ <i>T. fluminense</i> ★	0.2	0	0.2	45	50	52	50	77	99	110	104	75	58	58	52	50	54	56	56	63	63	59	65	68	77	80	79	65	65	65	80	74	52	52	
5	MH376939_ <i>Crustaphyllum</i> sp.	5.7	5.4	5.7	5.4		66	65	66	82	100	113	104	74	71	71	70	69	72	71	71	76	76	72	68	76	84	82	81	71	71	91	77	65	65	
6	MH376923_ <i>Crust. pacificum</i>	6	6	6	6	8.1		8	0	81	105	116	103	87	67	67	70	69	72	67	66	66	70	73	85	82	86	85	77	77	77	83	86	13	13	
7	MH376922_ <i>Crust. pacificum</i>	6.3	6.3	6.3	6.3	7.8	1		8	84	104	118	104	87	67	67	70	69	72	67	67	67	70	76	84	85	89	88	78	78	78	83	89	8	8	
8	MH376921_ <i>Crust. pacificum</i> ★	6	6	6	6	7.9	0	1		81	105	116	103	87	67	67	70	69	72	67	66	66	70	73	85	82	86	85	77	77	77	83	86	13	13	
9	MF034552_ <i>Mes. lichenoides</i> ◆	9.4	9.4	9.4	9.4	10	9.9	10.3	9.9		101	113	103	79	79	79	80	79	79	79	80	80	82	77	84	0	27	26	76	76	76	86	79	83	83	
10	MF034547_ <i>S. episporum</i> ◆	11.8	11.9	11.8	11.9	12	12.6	12.5	12.6	12.3		75	76	98	98	98	119	116	120	101	101	101	119	91	100	103	105	104	106	106	106	107	93	101	101	
11	MF034543_ <i>S. eltorensis</i> ★	13.1	13.2	13.1	13.2	13.6	14	14.2	14	14.2	91		71	105	121	121	117	111	116	119	119	117	117	114	104	103	116	119	118	122	122	122	103	98	114	114
12	MF034541_ <i>S. ptychoides</i> ★	12.4	12.5	12.4	12.5	12.5	12.4	12.5	12.4	12.6	9.1	8.5		105	108	108	106	106	107	106	106	102	102	107	95	101	106	108	107	107	107	114	96	102	102	
13	KY042234_ <i>L. lemoineae</i> ★	9.2	9.2	9.2	9.2	9.1	10.7	10.7	10.7	10.3	12	12.8	12.8		80	80	87	81	86	76	76	82	87	77	82	79	82	81	73	73	73	57	62	91	91	
14	KU501323_ <i>N. reclinatum</i>	7	7	7	7	8.5	8.1	8.1	8.1	10.3	11.8	14.5	13	10.2	0	69	64	68	11	11	37	37	70	87	83	83	86	85	81	81	96	90	69	69		
15	KP142762_ <i>N. reclinatum</i> ▲	7	7	7	7	8.5	8.1	8.1	8.1	10.3	11.8	14.5	13	10.2	0	69	64	68	11	11	37	37	70	87	83	83	86	85	81	81	96	90	69	69		
16	KP142761_ <i>C. nereostratum</i> ▲	7.8	7.8	7.8	7.8	8.4	8.4	8.4	8.4	10.3	14.3	14	12.7	11.4	8.3	8.3	23	7	65	65	65	65	24	78	86	81	84	83	80	80	96	92	72	72		
17	KP142757_ <i>C. compactum</i>	6	6	6	6	8.3	8.3	8.3	8.3	10.2	13.9	14.7	12.7	9.9	8.3	8.3	97.2		21	60	60	64	64	29	76	82	83	82	76	76	76	92	89	71	71	
18	KP142756_ <i>C. circumscriptum</i> ▲	7.5	7.5	7.5	7.5	8.7	8.7	8.7	8.7	10.3	14.4	13.9	12.8	11.5	8.2	8.2	1.2	97.5		64	64	65	65	26	81	89	81	86	85	79	79	79	97	94	74	74
19	KP142750_ <i>N. arcticum</i> ▲	7.3	7.3	7.3	7.3	8.5	8.1	8.1	8.1	10.3	12.1	14.3	12.7	10.7	1.3	1.3	8.2	8.8	8.3	0	34	34	66	83	77	83	86	85	79	79	92	88	69	69		
20	KP142749_ <i>N. arcticum</i> ▲	7.3	7.3	7.3	7.3	8.5	8.1	8.1	8.1	10.3	12.1	14.3	12.7	10.7	1.3	1.3	8.2	8.8	8.3	0	34	34	66	83	77	83	86	85	79	79	92	88	69	69		
21	KP142740_ <i>Cal. parcum</i> ▲	7.6	7.6	7.6	7.6	9.1	8.1	8.1	8.1	10.2	12.1	14	12.2	10	4.4	4.4	8.2	8.3	8.2	4.1	4.1	0	65	87	81	82	81	78	78	78	99	92	70	70		
22	KP142739_ <i>Cal. parcum</i> ▲	7.6	7.6	7.6	7.6	9.1	8.1	8.1	8.1	10.2	12.1	14	12.2	10	4.4	4.4	8.2	8.3	8.2	4.1	4.1	0	65	87	81	82	81	78	78	78	99	92	70	65		
23	KP142730_ <i>C. compactum</i>	7.1	7.1	7.1	7.1	8.7	8.4	8.4	8.4	10	14.3	14.3	12.8	11.4	8.4	8.4	2.9	3.5	3.1	8.1	8.1	8.2	8.2	80	90	82	87	86	82	82	94	94	72	72		
24	KM983035_ <i>M. erubescens</i> ▲	9.1	8.9	9.1	8.9	10.7	10	11.6	10	11.5	12.4	14.2	13	11.5	11.9	11.9	11.4	11.6	12.9	12.7	12.7	11.9	11.9	11.1	72	77	76	76	46	46	46	81	69	77	77	
25	KM369060_ <i>Syn. patena</i>	8.2	8.2	8.2	8.2	9.1	11.8	11.9	11.8	10.3	12	12.4	12.1	10	10	10	10.3	10.2	10.7	9.2	9.2	10.3	10.3	11.2	10.2	87	87	86	66	66	66	90	70	82	82	
26	KJ638232_ <i>Mes. lichenoides</i> .	9.2	9.2	9.2	9.2	11.9	9.9	11.8	9.9	0	12.4	13.9	12.7	10.3	10	10	10.3	10.2	10.3	10	10	10.2	10.2	11.5	11.6	28	27	78	78	78	88	81	84	84		
27	KJ638229_ <i>Mes. expansum</i> ◆	9.6	9.6	9.6	9.6	9.9	10.3	10.7	10.3	3.3	12.6	14.3	13	10	10.3	10.3	11.9	10	10.3	10.3	10.3	10.2	11.6	11.6	11.6	3.4	1	81	81	81	90	82	88	88		
28	KJ638228_ <i>Mes. expansum</i>	9.5	9.5	9.5	9.5	10.3	11.8	11.4	11.8	3.2	12.5	14.2	12.8	9.9	11.8	11.8	10	10.2	11.8	11.8	11.8	10.3	10.3	11.6	3.2	1.9	81	81	81	89	81	87	87			
29	KC819268_ <i>Mes. sphaericum</i> ▲	8.1	8.2	8.1	8.2	8.6	10.7	9.4	10.7	10.7	12.7	4.7	13.1	8.9	10.3	10.3	9.6	9.1	9.5	9.5	9.5	9.4	9.4	9.9	6.3	8.1	9.4	10.3	10.3	0	0	92	84	78	78	
30	KC819262_ <i>Mes. sphaericum</i> ▲	8	8.2	8	8.2	8.5	10.7	9.4	10.7	10.7	12.7	4.6	12.8	8.9	10.3	10.3	9.6	9.1	9.5	9.5	9.5	9.4	9.4	10.2	6.3	8.1	9.4	10.3	10.3	0	0	92	84	78	78	
31	JQ896245_ <i>Mes. sphaericum</i> ▲	8	8.2	8	8.2	8.5	10.7	9.4	10.7	10.7	12.7	4.6	12.8	8.9	10.3	10.3	9.6	9.1	9.5	9.5	9.5	9.4	9.4	10.2	6.3	8.1	9.4	10.3	10.3	0	0	92	84	78	78	
32	JQ896241_ <i>L. muelleri</i>	9.6	9.6	9.6	9.6	11	10	10	10	11.5	12.8	12.4	14.3	7	12.5	12.5	12.5	11	12.4	11	11	11.9	11.9	12.7	12.9	11.2	11.4	11.2	10.7	12.9	11	11	71	87	87	
33	JQ896231_ <i>P. calcareum</i> ★	8.9	8.9	8.9	8.9	10.7	10.3	10.3	10.3	11.2	11.8	12.5	7.6	11.2	11.2	11	10.7	12.7	11.4	11.4	11	11	12.7	9.4	8.4	10.3	10.3	11.9	11.9	8.5	87	87				
34	MK524381_ <i>Crust. atlanticum</i> ★	7.8	7.8	7.8	7.8	8.2	1.6	1	1.6	11.9	12.1	14.3	12.2	12.9	8.3	8.3	8.6	8.5	8.9	8.3	8.4	8.4	8.6	11.5	10.2	11.9	11.4	11.6	9.4	9.4	11.6	11.6	0	0		
35	MK524382_ <i>Crust. atlanticum</i>	7.8	7.8	7.8	7.8	8.2	1.6	1	1.6	11.9	12.1	14.3	12.2	12.9	8.3	8.3	8.6	8.5	8.9	8.3	8.4	8.4	8.6	11.5	10.2	11.9	11.4	11.6	9.4	9.4	11.6	11.6	0	0		

Table S4. Interspecific *rbcL* sequence divergence in percentage (lower half) and number of nucleotides (upper half) for sequences used in the phylogenetic analyses. Short length sequences (MK033191 *Neopolyporolithon arcticum*, KP085633 Hapalidiaceae sp., KP085634 Hapalidiaceae sp., KP085634 Hapalidiaceae sp., KP050698 *Melyvonnea erubescens*) were not included. Stars (★) represent sequences from type material; triangles (▲) represent specimens whose identification was confirmed by comparison of DNA sequences with type material; diamonds (◆) denote topotypes.

		1	2	3	4	5	6	7	8	9	10	11	12	13	14	15
1	MH277264_Leptophytum_faecundum		211	218	266	177	189	220	154	3	189	58	197	196	212	173
2	MG051266_Sporolithon_indopacificum ★	15.9		37	309	232	241	281	227	213	236	198	222	222	250	207
3	KY994124_Sporolithon_episporum ◆	16.4	2.7		309	236	244	280	235	220	239	204	223	223	249	215
4	KP142789_Leptophytum_laeve	18.3	21.1	21.1		225	223	206	280	268	222	268	304	303	255	247
5	KP142784_Neopolyporolithon_articum ★	13.3	17.1	17.4	14.9		42	154	195	179	40	181	215	214	199	173
6	KP142782_Neopolyporolithon_reclinatum	14.2	17.8	82	14.7	3.1		156	195	192	0	193	219	218	205	176
7	KP142781_Callilithophytum_parcum	15.6	19.9	19.8	16.3	10.4	10.6		241	225	155	225	259	260	240	213
8	KP142772_Mesophyllum_lichenoide	11.6	16.7	17.3	19	14.4	14.4	16.8		157	193	149	215	214	203	163
9	KP142770_Leptophytum_faecundum	0.2	15.7	16.2	18.1	13.2	14.2	15.7	11.6		189	60	201	200	216	177
10	KC134324_Neopolyporolithon_reclinatum	14.2	17.7	18	14.9	97	0	10.7	14.5	14.2		189	216	215	201	171
11	HQ322337_Mesophyllum_vancouverense ◆	4.4	14.6	15	18.1	13.3	14.2	15.7	89	4.4	14.2		179	178	212	168
12	HQ322325_Calliarthron_tubulosum	14.8	16.4	16.4	20.7	15.9	16.2	18.2	15.9	14.8	16.2	13.2		1	236	204
13	HQ322299_Calliarthron_tubulosum	14.7	16.4	16.4	20.7	15.8	16.1	18.2	15.8	14.7	16.2	13.1	0.1		235	203
14	MN201585_Crustaphytum_atlanticum ★	15.5	18	17.9	16.7	14.2	14.6	16.3	14.5	15.4	14.6	15.2	16.9	16.9		148
15	MN201584_Tectolithon_fluminense ▲	0.87	15.3	15.9	16.5	12.8	13	14.8	12	13.1	12.9	12.4	15	15		10.4

Capítulo 2

***Sporolithon amadoi* sp. nov. (Sporolithales, Rhodophyta), a new rhodolith-forming non-geniculate coralline alga from offshore the northwestern Gulf of Mexico and Brazil.**

JOSEPH L. RICHARDS^{1,*}, RICARDO G. BAHIA², MICHEL B. JESIONEK², & SUZANNE FREDERICQ¹

Artigo publicado no periódico *Phytotaxa* em novembro de 2019.

***Sporolithon amadoi* sp. nov. (Sporolithales, Rhodophyta), a new rhodolith-forming non-geniculate coralline alga from offshore the northwestern Gulf of Mexico and Brazil.**

JOSEPH L. RICHARDS^{1,*}, RICARDO G. BAHIA², MICHEL B. JESIONEK², & SUZANNE FREDERICQ¹

¹*University of Louisiana at Lafayette, Biology Department, Lafayette, LA 70504-3602, U.S.A.*

²*Instituto de Pesquisas Jardim Botânico do Rio de Janeiro, Diretoria de Pesquisa Científica, Rua Pacheco Leão 915, Rio de Janeiro, RJ 22460-030, Brazil*

*Corresponding author (Joer207@gmail.com)

This article is dedicated in loving memory to Dr. Gilberto M. Amado-Filho (October 6, 1959 – March 15, 2019).

Abstract

DNA sequence analysis of plastid-encoded *psbA* and *rbcL* loci, and nuclear-encoded LSU rDNA of rhodolith-forming specimens of Sporolithales from Brazil and the northwestern Gulf of Mexico reveal that they belong to an unnamed species of *Sporolithon* (Sporolithaceae).

Sporolithon amadoi sp. nov. is morpho-anatomically characterized by a vegetative thallus reaching more than 20 cell layers, a tetrasporophyte with tetrasporangial sori slightly raised above the thallus surface that become overgrown and buried after spore release, and by cruciately divided tetrasporangia with pores surrounded by 9–13 rosette cells. Since these morpho-anatomical features are shared with some other *Sporolithon* species, identification of this species can only be confirmed by DNA sequences.

Key words: Abrolhos bank, biogeography, CCA, coralline algae, marine algae, marine biodiversity, mesophotic, reefs, rhodoliths, seaweeds

Abbreviations: CCA = crustose coralline algae; GB = GenBank; ML = Maximum Likelihood; NWGMx = northwestern Gulf of Mexico; SEGMr = southeastern Gulf of Mexico; SEM = Scanning Electron Microscope

Running title: *Sporolithon amadoi* sp. nov.

Introduction

The name *Sporolithon ptychoides* Heydrich has previously been assigned to crustose (non-geniculate) coralline algal (CCA) specimens from Brazil exhibiting the following features: 1) raised tetrasporangial sori, 2) a layer of elongate cells at the base of tetrasporangia, 3) tetrasporangial compartments that are not sloughed off after spore release, 4) paraphyses between tetrasporangial compartments comprised of 3-5 cells (Bahia *et al.* 2011, Bahia *et al.* 2015), and 5) 8-11 rosette cells surrounding the pores of tetrasporangial compartments. Recent studies, however, have shown that performing comparative analyses of DNA sequences based on sequences of type specimens is the only way to unequivocally identify non-geniculate coralline algae and that morpho-anatomical characters alone can be misleading (Hind *et al.* 2015, Gabrielson *et al.* 2018, Richards *et al.* 2017, Richards *et al.* 2018a). Richards *et al.* (2017) showed that DNA sequences (*psbA* and *rbcL*) of Brazilian specimens identified as *Sporolithon ptychoides* based on morpho-anatomy did not form a clade with sequences of the type and topotype specimens of *S. ptychoides* from El Tor, Egypt. Other species that do not slough off their tetrasporangial sori, i.e. *S. molle* (Heydrich) Heydrich (type locality: El Tor, Egypt), *S. dimotum* (Foslie & M. Howe) Yamaguishi-Tomita ex M.J. Wynne (type locality: Lemon Bay, near Guánica, Puerto Rico), and *S. yoneshigueae* Bahia, Amado-Filho, Maneveldt & W.H.Adey

(type locality: Bahia, Brazil), were also shown to be different species than the Brazilian specimens identified previously as *S. ptychoides* (Richards *et al.* 2017, Bahia *et al.* 2015). Additionally, the sequences from the Brazilian specimens were identical to the taxon referred to as *Sporolithon* sp. nov. (LAF 7260) from the northwestern Gulf of Mexico (Fredericq *et al.* 2019). Herein, we describe this taxon as a new species of *Sporolithon* from Brazil and the Gulf of Mexico.

TABLE 1. List of GenBank numbers and reference information for sequences of taxa included in phylogenetic analyses. Sequences in concatenated tree (Fig. 1) shown in italics. Type specimens and specimens of species whose identifications are confirmed by comparison to type or topotype material are shown in bold. *Not analyzed in present study.

Taxa	Id. No. & type designation where applicable.	Locality	Reference	GenBank Accession No.		
				psbA	rbcL	LSU
<i>Clathromorphum compactum</i>	US 170929	Labrador, Canada	Adey <i>et al.</i> 2015	<i>KP142730</i>	<i>KP142774</i>	-
<i>Heydrichia cerasina</i>	NCU 617165 isotype	Western Cape Province, South Africa	Richards <i>et al.</i> 2017	<i>MF034551</i>	<i>KY994128</i>	<i>KY980439</i>
<i>Heydrichia homalopasta</i>	NZC0748	New Zealand	Broom <i>et al.</i> 2008	<i>DQ167931</i>	-	-
<i>Heydrichia woelkerlingii</i>	NCU 597127 topotype	South Africa	Mateo-Cid <i>et al.</i> 2014, Adey <i>et al.</i> 2015	<i>JQ917415</i>	<i>KP142788</i>	-
<i>Lithophyllum incrustans</i>	GALW 15746 (E137) [species identity confirmed by comparison of rbcL to holotype]	France	Hernández-Kantun <i>et al.</i> 2015	<i>JQ896238</i>	<i>KR708543</i>	-
<i>Lithophyllum neocongestum</i>	US 223011 holotype	Caribbean Panama	Hernández-Kantún <i>et al.</i> 2016	<i>KX020466</i>	<i>KX020484</i>	-
<i>Membranoptera platyphylla</i>	UC 1856248	Washington, U.S.A.	Hughey <i>et al.</i> 2017	<i>KT266849</i>	<i>KT266849</i>	-
<i>Membranoptera tenuis</i>	UC 266439 neotype	Washington, U.S.A.	Hughey <i>et al.</i> 2017	<i>KP675983</i>	<i>KP675983</i>	-
<i>Membranoptera weeksiae</i>	UC 264804 holotype	California, U.S.A.	Hughey <i>et al.</i> 2017	<i>KJ513670</i>	<i>KJ513670</i>	-
<i>Mesophyllum lichenoides</i>	LBC0031	France	Bittner <i>et al.</i> 2011	*GQ917439	-	<i>GQ917312</i>
<i>Neopolyoporolithon reclinatum</i>	UBC A88609	British Columbia, Canada	Adey <i>et al.</i> 2015	<i>KP142762</i>	<i>KP142806</i>	-
<i>Phymatolithon calcareum</i>	LBC0001 [psbA and COI is identical to neotype of this species]	France	Bittner <i>et al.</i> 2011	*GQ917436	-	<i>GQ917309</i>
<i>Renouxia</i> sp.	LAF 6170	Egypt	Lee <i>et al.</i> 2018	<i>MH281629</i>	<i>MH281629</i>	<i>MK091141</i>
<i>Rhodogorgon carriebowensis</i>	WELT TBA	Panama, Caribbean Sea	Nelson <i>et al.</i> 2015	<i>KM369059</i>	<i>KM369119</i>	-
<i>Rhodogorgon</i> sp.	N.A.	N.A.	Harper & Saunders 2001	-	-	<i>AF419142</i>
<i>Rhodogorgon</i> sp.	SGAD1304047	Indonesia	Lee <i>et al.</i> 2018	*MH281630	*MH281630	<i>MK091143</i>
Sporolithales sp. A (as <i>H. woelkerlingii</i>)	NZC2014	New Zealand	Nelson <i>et al.</i> 2015	<i>FJ361382</i>	<i>KM369120</i>	-
<i>Sporolithon amadoi</i> (as <i>Sporolithon ptychoides</i>)	RB 621750	Abrolhos Archipelago, Brazil	Jesioneck <i>et al.</i> 2016	<i>KY485313</i>	-	-
<i>Sporolithon amadoi</i>	RB 779739 paratype	Amazon Reefs, Itaubal, Amapá, Brazil (01°19'08" N; 46°50'09" W), 55 m deep, leg. GM Amado-Filho, 17.vii.2017	Present study	<i>MN434067</i>	-	-

<i>Sporolithon amadoi</i>	RB 779740 paratype	Amazon Reefs, Itaubal, Amapá, Brazil (01°19'08" N; 46°50'09" W), 55 m deep, <i>leg.</i> GM Amado-Filho, 17.vii.2017	Present study	MN434068	-	-
<i>Sporolithon amadoi</i>	RB 779736 holotype	Recifes Esquecidos, São Mateus (São Mateus 18°52'32" S; 39°26'13" W), Espírito Santo, Brazil, 30 m deep, <i>leg.</i> RG Bahia, 14.iii.2018	Present study	MN434069	-	-
<i>Sporolithon amadoi</i>	RB 779737 isotype	Recifes Esquecidos, São Mateus (18°52'32" S; 39°26'13" W), Espírito Santo, Brazil, 30 m deep, <i>leg.</i> RG Bahia, 14.iii.2018	Present study	MN434070	-	-
<i>Sporolithon amadoi</i>	RB 779738 isotype	Recifes Esquecidos, São Mateus (18°52'32" S; 39°26'13" W), Espírito Santo, Brazil, 30 m deep, <i>leg.</i> RG Bahia, 14.iii.2018	Present study	MN434071	-	-
<i>Sporolithon amadoi</i> (as <i>Sporolithon ptychoides</i>)	Amado-Filho Brazil 8	Fernando de Noronha Archipelago, Brazil	Bahia <i>et al.</i> 2014	KC870926	-	-
<i>Sporolithon amadoi</i> (as <i>Sporolithon ptychoides</i>)	Amado-Filho Brazil 7	Fernando de Noronha Archipelago, Brazil	Bahia <i>et al.</i> 2014	KC870927	-	-
<i>Sporolithon amadoi</i> (as <i>Sporolithon cf. ptychoides</i>)	GM AF6	Fernando de Noronha Archipelago, Brazil	Adey <i>et al.</i> 2015	KP142753	KP142787	-
<i>Sporolithon amadoi</i>	LAF 7256 (5-4-18-4-2) paratype	Ewing Bank (28° 05.937' N; 91°; 01.349' W), NWGMx, offshore Louisiana, U.S.A., 70 meters deep, <i>leg.</i> J. Richards & S. Fredericq, 4.v.2018	Present Study	MN266235	MN258542	MN266234
<i>Sporolithon amadoi</i>	LAF 7260 (5-7-18-3-4) paratype	Bright Bank (27° 53.353' N; 93°; 17.964' W), NWGMx, offshore Louisiana-Texas border, U.S.A., 50-58 meters deep, <i>leg.</i> J. Richards & S. Fredericq, 7.v.2018	Present Study	MN266236	-	-
<i>Sporolithon amadoi</i>	LAF 7261 (5-7-18-3-4) paratype	Bright Bank (27° 53.353' N; 93°; 17.964' W), NWGMx, offshore Louisiana-Texas Border, U.S.A., 50-58 meters deep, <i>leg.</i> J. Richards & S. Fredericq, 7.v.2018	Present Study	MN266237	-	-
<i>Sporolithon dimotum</i>	NY 900043 (Howe 2667) holotype	Lemon Bay, near Guanica, Puerto Rico	Richards <i>et al.</i> 2017	-	KY994131	-
<i>Sporolithon durum</i>	NZC2375	New Zealand	Nelson <i>et al.</i> 2015	FJ361583	KM369122	-
<i>Sporolithon durum</i>	Aus	Australia	Nelson <i>et al.</i> 2015	DQ168023	KM369121	-
<i>Sporolithon eltoensis</i>	NCU 606659 (LAF 5850) holotype	El Tor, Egypt, Gulf of Suez	Richards <i>et al.</i> 2017	MF034543	MG051269	KY980433
<i>Sporolithon eltoensis</i>	LAF 5767 (NCU 649164)	Dahab, Egypt, Gulf of Aqaba	Richards <i>et al.</i> 2017	MF034544	-	KY980434
<i>Sporolithon episporum</i>	NCU 598843 (PHYKOS 5467) [<i>rbcL</i> is identical to holotype of this species]	Bocas del Toro, Panama, Caribbean Sea	Richards <i>et al.</i> 2017	MF034547	KY994124	-
<i>Sporolithon indopacificum</i>	L 3964509 holotype	Tanzania	Maneveldt <i>et al.</i> 2017	MG051270	MG051266	-

<i>Sporolithon mesophoticum</i>	NCU 658543 (BDA 2048) holotype	Plantagenet (Argus) Bank, SSW of Bermuda	Richards <i>et al.</i> 2018b	<i>MK159180</i>	<i>MK159181</i>	-
<i>Sporolithon molle</i>	NCU 606657 (LAF 5848) topotype [<i>rbcL</i> is identical to isolectotype of this species]	El Tor, Egypt, Gulf of Suez	Maneveldt <i>et al.</i> 2017, Richards <i>et al.</i> 2017	<i>MG051272</i>	<i>KY994120</i>	<i>KY980432</i>
<i>Sporolithon ptychoides</i>	NCU 606660 (LAF 5875) topotype [<i>rbcL</i> is identical to lectotype of this species]	El Tor, Egypt, Gulf of Suez	Richards <i>et al.</i> 2017	<i>MF034541</i>	<i>KY994117</i>	<i>KY980430</i>
<i>Sporolithon ptychoides</i>	NCU606663 (LAF5846) topotype [<i>rbcL</i> is identical to lectotype of this species]	El Tor, Egypt, Gulf of Suez	Richards <i>et al.</i> 2017	* <i>MF034542</i>	* <i>KY994118</i>	<i>KY980431</i>
<i>Sporolithon 'ptychoides'</i>	ARS02349	Hawaii	Sherwood <i>et al.</i> 2010	-	-	<i>HQ421906</i>
<i>Sporolithon 'ptychoides'</i>	ARS02819	Hawaii	Sherwood <i>et al.</i> 2010	-	-	<i>HQ421797</i>
Sporolithales	ARS02572	Hawaii	Sherwood <i>et al.</i> 2010	-	-	<i>HQ421744</i>
<i>Sporolithon</i>	LAF 6956A holotype	Sackett Bank, NWGMx	Richards <i>et al.</i> 2017	<i>MF034549</i>	<i>KY994126</i>	<i>KY980437</i>
<i>sinusmexicanum</i>		Dry Tortugas Vicinity, SEGMr	Richards <i>et al.</i> 2017	<i>MF034550</i>	<i>KY994127</i>	<i>KY980438</i>
<i>Sporolithon</i>	LAF 6970B	Gulf of Chiriquí, near Mono Feliz, Panama, Pacific Ocean	Richards <i>et al.</i> 2017	<i>MF034548</i>	-	-
<i>sinusmexicanum</i>						
<i>Sporolithon</i> sp.	PHYKOS 4623	Fiji	Bittner <i>et al.</i> 2011	<i>GQ917501</i>	-	<i>GQ917344</i>
<i>Sporolithon</i> sp.	LBC0695	Hawaii	Sherwood <i>et al.</i> 2010	-	-	<i>HQ421810</i>
<i>Sporolithon</i> sp. epilithic	ARS02833	New Zealand	Nelson <i>et al.</i> 2015	<i>FJ361509</i>	<i>KM369123</i>	-
<i>Sporolithon</i> sp.	NZC2175	Brazil	Adey <i>et al.</i> 2015	<i>KP142752</i>	<i>KP142786</i>	-
<i>Sporolithon</i> sp.	GM AF5	Taiwan	Liu <i>et al.</i> 2018	<i>MH377024</i>	-	-
<i>Sporolithon</i> sp.	NTOU001470	Western Australia	Unpublished	<i>KY682926</i>	<i>KY682902</i>	<i>KY682886</i>
<i>Sporolithon</i> sp. 1	1WA	Brazil	Adey <i>et al.</i> 2015	<i>KP142751</i>	<i>KP142785</i>	-
<i>Sporolithon</i> <i>tenue</i>	US 170943	Brazil	Bahia <i>et al.</i> 2015, Richards <i>et al.</i> 2017	<i>MF034545</i>	<i>KY994122</i>	<i>KY980435</i>
<i>Sporolithon</i> <i>yoneshigueae</i>	RB 600359 paratype	Brazil	Bahia <i>et al.</i> 2015, Richards <i>et al.</i> 2017	* <i>MF034546</i>	* <i>KY994123</i>	<i>KY980436</i>
<i>Sporolithon</i> <i>yoneshigueae</i>	RB 600360 paratype	Brazil				

Materials & Methods

Specimen collection. Mesophotic specimens were collected aboard the R/V *Pelican*, the UNOLS (University National Oceanographic Laboratory System) research vessel stationed at LUMCON (Louisiana Universities Marine Consortium), using an hourglass design box dredge (Joyce & Williams 1969) with minimum tows (usually 10 minutes or less) from offshore Louisiana and offshore the Texas-Louisiana border in the Gulf of Mexico in the vicinity of Ewing Bank ($28^{\circ} 05.937' N$; $91^{\circ}; 01.349' W$) and Bright Bank ($27^{\circ} 53.353' N$; $93^{\circ}; 17.964' W$) at depths of 45-90 m. Collection dates were from May 3-11, 2018. Gulf of Mexico specimens are housed at the University of Louisiana at Lafayette Herbarium (LAF). Brazilian specimens were collected using metal dredges at 55 m depth from the Amazon Reef (Moura *et al.* 2016) and by SCUBA diving in the following locations: Fernando de Noronha Archipelago (55 m depth) (Bahia *et al.* 2014), shallow reefs (2-7 m depth) in the Abrolhos bank continental shelf (Jesionek *et al.* 2016), and from a rhodolith bed at 30 m depth in Espírito Santo State (present study). Brazilian specimens are housed at the Rio de Janeiro Botanical Garden Herbarium (RB). Herbarium abbreviations follow Thiers (2019, continuously updated). Table 1 provides a list of specimens and voucher information for taxa included in the analyses.

DNA extraction and sequencing. DNA was extracted from the NWGMx specimens following the protocol of Richards *et al.* (2014) and from Brazilian specimens following the protocol of Jesionek *et al.* (2016). Markers chosen for PCR and sequencing included the plastid-encoded genes *psbA* (encodes photosystem II reaction center protein D1 gene) and *rbcL* (encodes the large subunit of the enzyme ribulose-1,5-bisphosphate carboxylase/oxygenase), and the nuclear-encoded LSU (partial 28S rDNA). PCR and sequencing followed the protocols and primers described in Richards *et al.* (2014, 2016) and Jesionek *et al.* (2016).

Alignment and phylogenetic analysis. A concatenated alignment (2,247 bp) of *psbA* (863 bp) and *rbcL* (1,384 bp) was constructed using MacClade 4.08 (Maddison & Maddison 2000) and Sequence Matrix (Vaidya *et al.* 2011). A single-gene alignment of LSU (549 bp) was constructed and aligned using MUSCLE (Edgar 2004) in MEGA 5.2.2 (Tamura *et al.* 2011) with ambiguous regions cropped to the nearest conserved regions. Maximum Likelihood (ML) analyses with 1,000 bootstrap replicates were conducted according to the protocol of Richards *et al.* (2017). Sequence divergence analyses for *psbA* and *rbcL* were performed in MEGA 5.2.2 (Tamura *et al.* 2011). Alignments were cropped at the 5' and 3' ends prior to divergence analyses to remove missing data.

Microscopy. Scanning electron microscopy was performed with a Hitachi S-3000N Scanning Electron Microscope (SEM) and a JEOL 6300F field emission SEM according to the protocol of Richards *et al.* (2017, 2018b) and with a Zeiss EVO 40 SEM according to the protocol of Bahia *et al.* (2010) at an accelerating voltage of 14-15 kV. Decalcification and light microscopy protocols followed Jesionek *et al.* (2016). Cell dimensions were measured from all available images for eight specimens as described in Maneveldt *et al.* (2017). Conceptacles were not measured due to the small samples size.

Results

Results of the ML analyses of concatenated *psbA* and *rbcL* sequences (Fig. 1) show that the specimens of *Sporolithon amadoi* from Brazil and the NWGMx belong to clade A within *Sporolithon* and form a clade with full support that is sister to the true *S. ptychoides* and *S. molle*. *PsbA* sequences of *S. amadoi* were 6.4% and 6.2% diverged from *S. ptychoides* and *S. molle*, respectively and *rbcL* sequences of *S. amadoi* were 7.6% and 8% diverged from *S. ptychoides*.

and *S. molle*, respectively (Tables 2–3). ML analyses of LSU (Fig. 2) show that *S. amadoi*, specimen LAF 7256, is in a clade separate from the true *S. ptychooides* and also separate from Hawaiian species of *Sporolithon*.

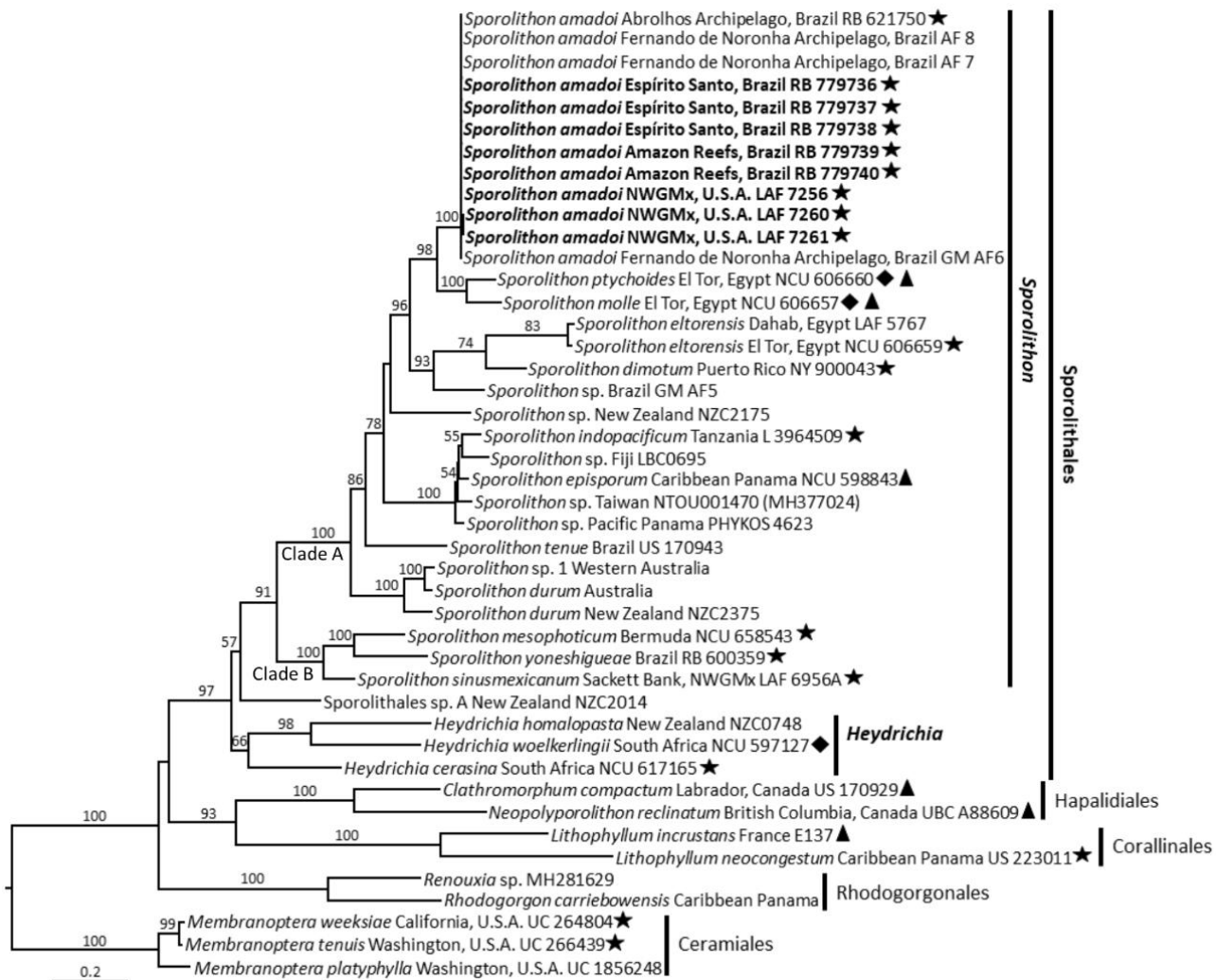


FIGURE 1. Phylogeny of Sporolithales based on ML analyses of concatenated *psbA* and *rbcL* (2,247 bp) sequences, with *Membranoptera* spp. (Ceramiales) as outgroup. Numbers at nodes are bootstrap values (1,000 replicates). Newly generated sequences shown in boldface. Stars represent holotype, isotype, neotype, or paratype specimens; diamonds represent topotype specimens; triangles represent species whose identification is confirmed by comparison of DNA sequences with type material. See Table 1 for GenBank numbers corresponding to specimen voucher numbers and details of type specimen designations.

Sporolithon amadoi J.Richards & Bahia sp. nov. (Figures 3–37)

Holotype (designated here): RB 779736: Recifes Esquecidos, São Mateus, Espírito Santo, Brazil (18°52'32" S; 39°26'13" W), western Atlantic Ocean, 14.iii.2018, depth 30m, collected by SCUBA, *leg.* R.G. Bahia.

Isotypes: RB 779737, RB 779738.

Additional material examined (Paratypes): RB 779739, RB 779740, LAF 7256, LAF 7260, LAF 7261. See Table 1 for specimen details.

Etymology: The specific epithet is in honor of Dr. Gilberto M. Amado-Filho, for his excellent contributions to the ecology and systematics of coralline algae from Brazil.

Description

DNA sequences: Holotype –*psbA* (GB accession = MN434069); Isotypes –*psbA* (GB accessions = MN434070, MN434071). See Table 1 for GB accessions for *psbA*, *rbcL*, and LSU sequences of additional material examined (Paratypes).

Habit and vegetative anatomy: Thallus non-geniculate, thallus thickness reaching more than 20 cell layers (occasionally 12-15 cell layers), primarily forming rhodoliths (Figs. 3, 11, 13, 18, 30) or occasionally growing attached to coral reef substrata, found growing in mesophotic benthic habitats (30-90 m deep) and in shaded environments in shallow (2-7 m deep) reefs. Thallus construction monomerous, with a multi-layered, plumose hypothallium (Figs. 4, 28, 29). Hypothallial cells rectangular in shape, 10.7-42 µm long x 5.6–12 µm wide. In some locations two superimposed layers of thalli were observed, though in other locations growth appeared continuous without layering. Adjacent hypothallial and perithallial cells linked by cell fusions and secondary pit connections (Figs. 5, 19). Perithallial cells 5.2–19.5 µm long x 3–13.6 µm wide (Figs. 5, 6, 12, 19, 20, 21, 31, 32, 33). Pseudodichotomous branching of perithallial cells was occasionally observed (Figs. 31, 32). Intercalary meristematic cells appeared wide and

flattened or approximately isodiametric, 3–8 μm long x 6–14.4 μm wide (Figs. 6, 12, 20, 21, 33).

Epithallium a single layer of cells with thick, heavily calcified cell walls (armored) and a small round or trapezoidal shaped lumen, 1.2–3.6 μm long x 3.1–7.2 μm wide (Fig. 6, 12, 21, 33).

Reproduction: Tetrasporangial sori observed from surface view were raised above the surrounding thallus surface (Figs. 14, 15, 22) and showed tetrasporangial pores, 8.5–16.5 in diameter, surrounded by 9–13 rosette cells (Figs. 7, 8, 23, 24). Section views showed tetrasporangial compartments borne among a basal layer of slightly elongated cells.

Tetrasporangial compartments not sloughed off, and become buried after spore release (Figs 9, 10, 25, 26), that are 65–108 μm long x 41–64 μm wide subtended by a triangular stalk cell 8–16 μm long x 20–32 μm wide (Figs. 10, 16, 27). Paraphyses 3–4 celled. Tetrasporocytes (Fig. 16) develop into cruciately divided tetrasporangia (Fig. 17). A gametophytic specimen (Figs. 30–37) was observed with uniporate conceptacles. However, examination with SEM (Fig. 35) and light microscopy of decalcified sections (Figs. 36, 37) showed empty conceptacles; thus it was not determined if they were male or female conceptacles. Conceptacles become overgrown after gamete or spore release (Fig. 37).

Distribution: Presently known from mesophotic rhodolith beds offshore the NWGMx, and from shallow reefs and mesophotic rhodolith beds in Brazil (see Table 1 for locality details).

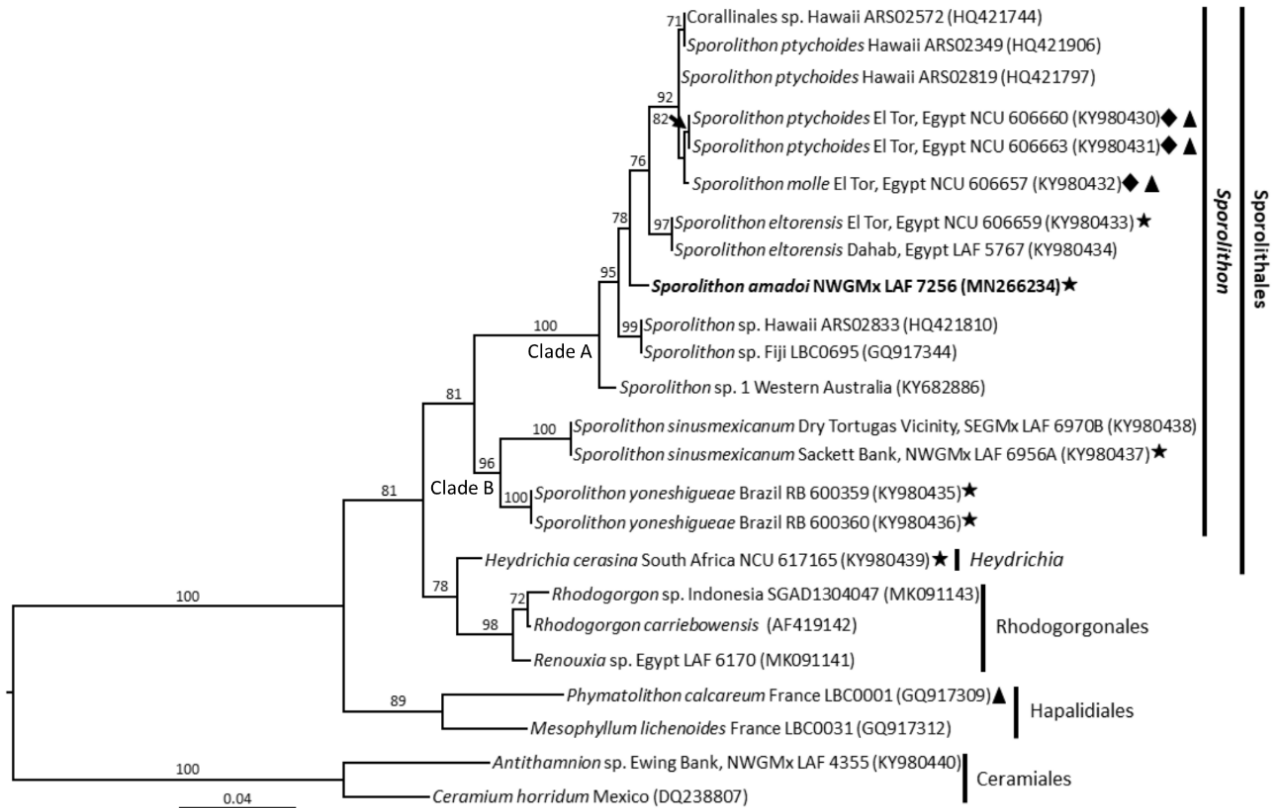


FIGURE 2. Phylogeny of Sporolithales based on Maximum Likelihood analyses of LSU (549 bp) sequences with *Antithamnion* and *Ceramium* (Ceramiales) as outgroup. Numbers at nodes are bootstrap values (1,000 replicates). Newly generated sequence shown in boldface. Stars represent holotype, isotype, neotype, or paratype specimens; diamonds represent topotype specimens; triangles represent species whose identification is confirmed by comparison of DNA sequences with type material. See Table 1 for details of type specimen designations.

Discussion

Sequence divergence values (Tables 2, 3) support the recognition of *S. amadoi* as a distinct species. For example, the *rbcL* sequence of *S. amadoi* is 7.6% divergent from *S. ptychoides* and 8% divergent from *S. molle*, which is greater than the *rbcL* divergence between other closely related species in the Sporolithales (e.g. 3.2% between *S. episporum* (M.Howe) E.Y.Dawson and *S. indopacificum* Maneveldt & P.W.Gabrielson).

The ML analysis shows two fully supported clades of *Sporolithon* spp. (Fig. 1, clades A and B), with *S. amadoi* in clade A along with other species from the tropical western Atlantic, the Red Sea, and the Indo-Pacific Ocean. The LSU tree (Fig. 2) shows that *S. amadoi* is in a

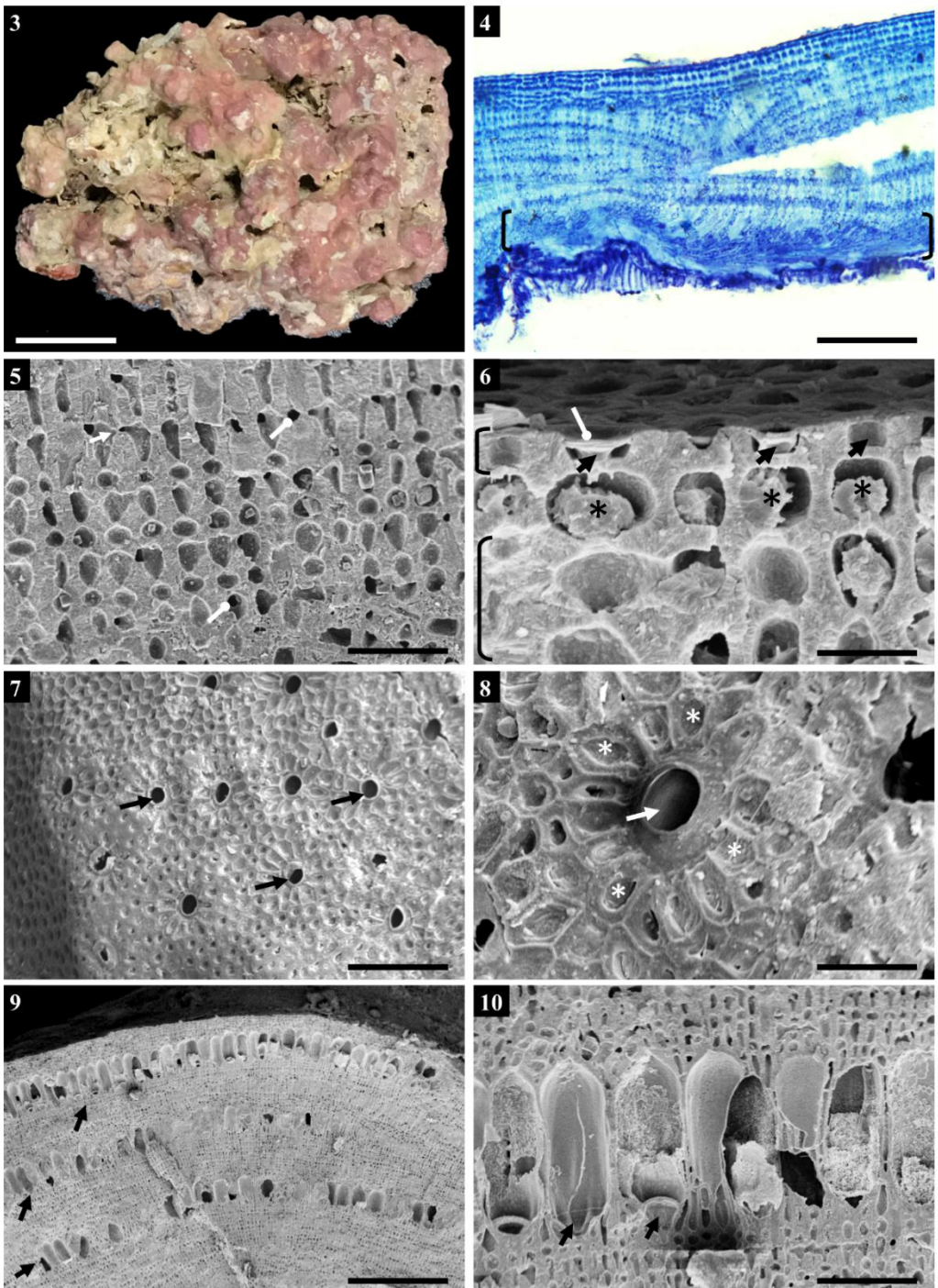
clade separate from Hawaiian species of *Sporolithon*, thus not conspecific with Hawaiian species. Previously Brazilian species of *Sporolithon* could not be compared to the Hawaiian specimens due to a lack of corresponding markers (Richards *et al.* 2017). This is noteworthy because other coralline species, eg. *Mesophyllum erubescens*, are present in both Brazil and Hawaii (Sissini *et al.* 2014). It is interesting that *S. amadoi* is associated with salt domes (diapirs) that are rich in oil deposits in both the northwestern Gulf of Mexico (Felder *et al.* 2014) and the Abrolhos bank continental shelf off the coast of Bahia in northeastern Brazil (Fainstein & Summerhayes 1982, Amado Filho *et al.* 2012, Jesionek *et al.* 2016). However, this species is not restricted to mesophotic habitats and was also found growing in shallow reefs in Brazil.

No exclusive diagnostic morpho-anatomical features or combination of features were found to distinguish *Sporolithon amadoi* from related species, such as *S. ptychoides*, *S. molle*, *S. eltorensis* and *S. dimotum* (Richards *et al.* 2017). However, the new species can be separated from other extant *Sporolithon* species from the Atlantic mainly by the following features: 1) thallus reaching more than 20 cell layers (differentiating from *S. tenue* which has less than 20 cell layers); 2) non-sloughed off tetrasporangial sori that become overgrown and buried after spore release (differentiating from *S. episporum*, *S. sinusmexicanum* and *S. tenue* which all slough off their sori); 3) tetrasporangial pores surrounded by 9-13 rosette cells (differentiating from *S. yoneshigueae* which has 19-24 rosette cells) (Bahia *et al.* 2014, 2015; Richards & Fredericq 2018).

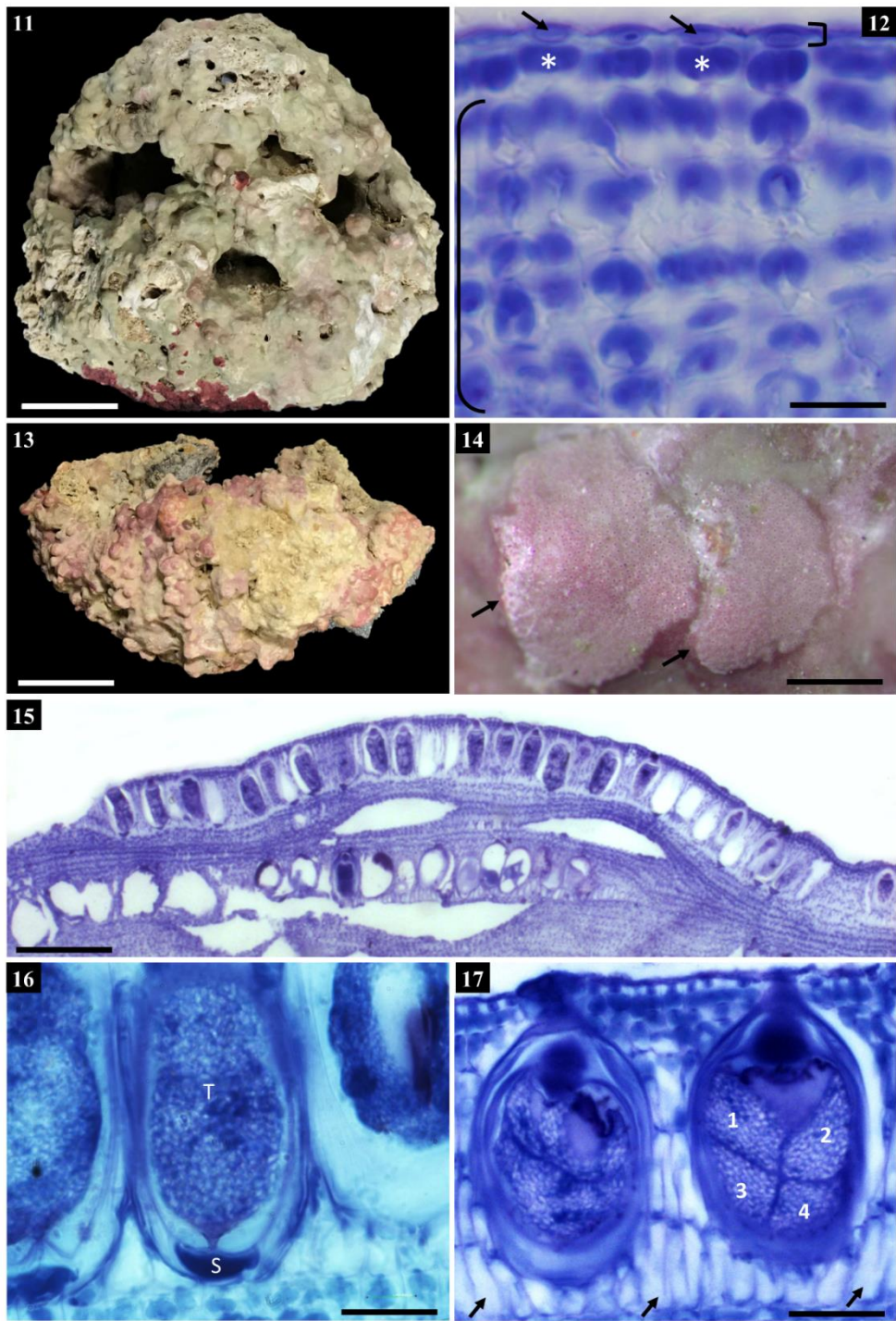
Sporolithon amadoi belongs to the group of rhodoliths that are referred to as biogenic rhodoliths which are formed by the non-geniculate crustose coralline algae themselves, in contrast to autogenic rhodoliths which are a specific type of nucleated rhodoliths that are derived from already existing calcium carbonate rubble (Fredericq *et al.* 2014, 2019; Felder *et al.* 2014;

Richards & Fredericq 2018; Richards *et al.* 2014, 2016, 2017, 2018a, b; Krayesky-Self *et al.* 2017). Fredericq *et al.* (2019) noted that *Sporolithon sinusmexicanum* and other biogenic rhodoliths that include putative cellular inclusions of microalgal life history stages within their perithallial cells, slough off their tetrasporangial sori and surface layers, and that species that do not slough off tetrasporangial sori layers, namely *S. amadoi*, do not show cellular inclusions. In future studies, larger sample sizes of rhodoliths are needed to shed light on whether similar phenomena occur in the gametophytic stages of *S. sinusmexicanum* and *S. amadoi* or in other species of rhodoliths.

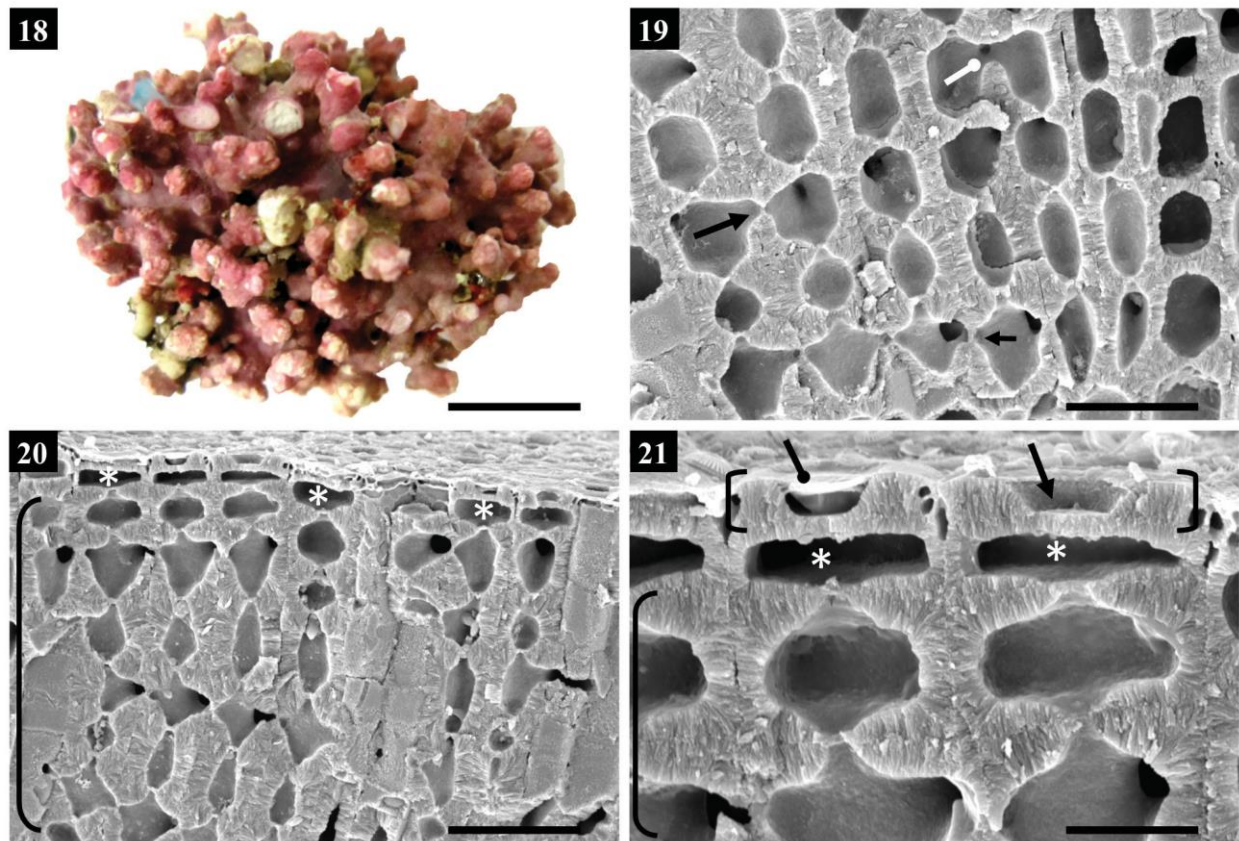
The findings in this study show that *S. amadoi* is a significant component of tropical reefs in the tropical western Atlantic. *Sporolithon amadoi* is the third species of *Sporolithon* described from Brazil, in addition to *S. tenuae* Bahia, Amado-Filho, Maneveldt, & W.H.Adey and *S. yoneshigueae* recently described by Bahia *et al.* (2014, 2015) from NE and SE Brazil, and the second species described from the NWGMx, in addition to *S. sinusmexicanum* J.Richards & Fredericq (Richards *et al.* 2018). Future studies likely will reveal additional new species of *Sporolithon* from the tropical western Atlantic as specimen collection and ongoing DNA sequencing efforts continue.



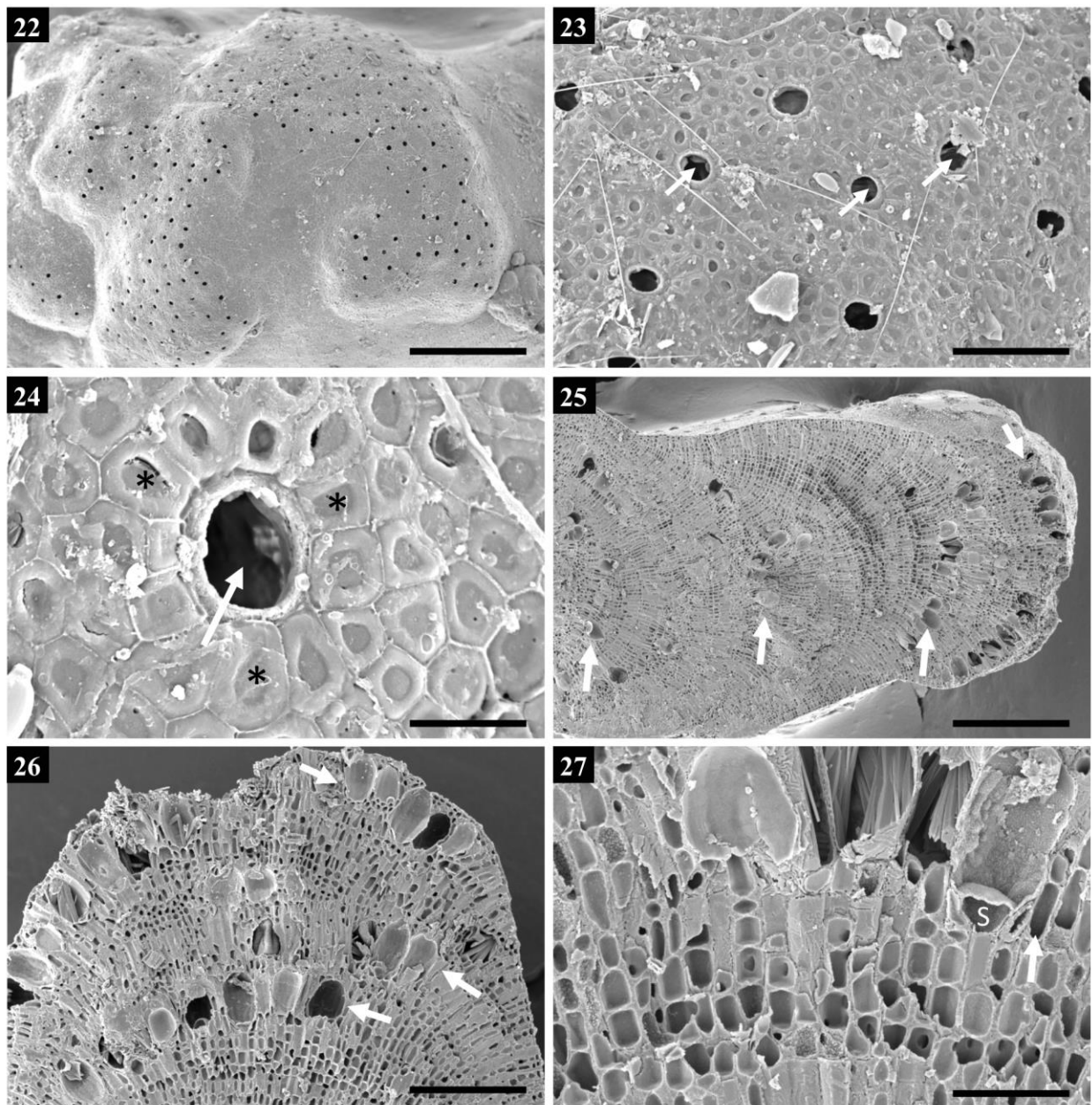
FIGURES 3-10. *Sporolithon amadoi* Holotype, RB 779736. FIG. 3. Habit of holotype. Scale bar = 1.5 cm. FIG. 4. Section of thallus showing monomerous construction and multilayered hypothallium (brackets). Scale bar = 120 μ m. FIG. 5. Perithallium with secondary pit connection (arrow) in x-axis and cell fusions shown as black holes in z axis (circle pointers). Scale bar = 33 μ m. FIG. 6. Vertical fracture showing epithallial cells (arrows), some with intact epithallial cell roofs (circle pointer), intercalary meristematic cells (*) and portion of perithallium (bracket). Scale bar = 9 μ m. FIG. 7. Surface view of tetrasporangial sorus with tetrasporangial pores (arrows) and rosette cells. Scale bar = 48 μ m. FIG. 8. Detail of tetrasporangial pore (arrow) surrounded by rosette cells (*). Scale bar = 18 μ m. FIG. 9. Vertical fracture showing layers of unshed tetrasporangial compartments (arrows). Scale bar = 300 μ m. FIG. 10. Detail of tetrasporangial compartments with stalk cells (arrows). Scale bar = 57 μ m.



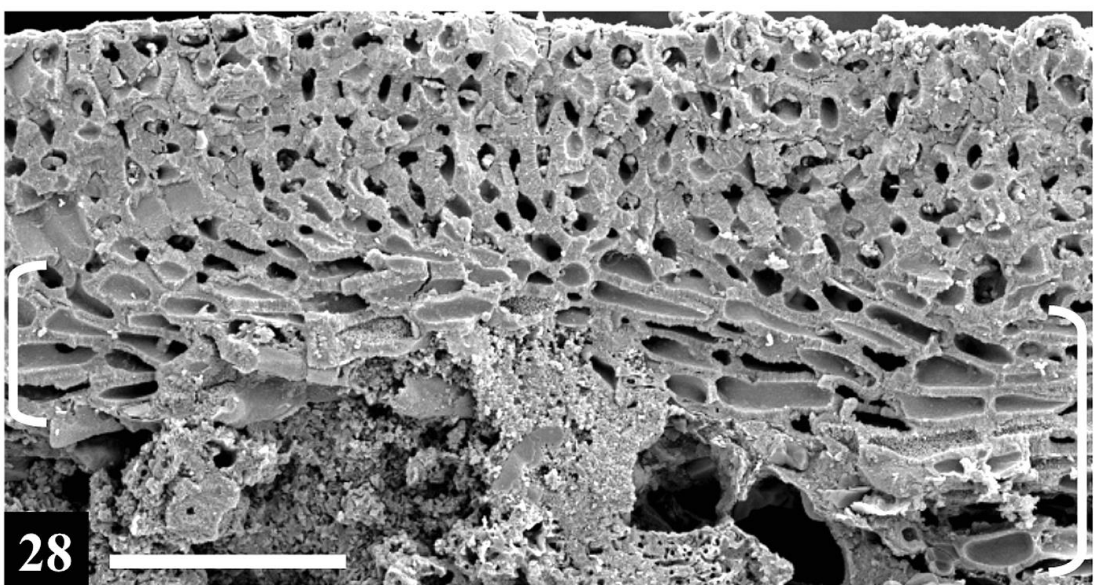
FIGURES 11-17. *Sporolithon amadoi*. FIGS. 11-12, Isotype, RB 779737. FIG. 11. Habit of isotype. Scale bar = 2.1 cm. FIG. 12. Epithallium (arrows, upper bracket), intercalary meristematic cells (*), and perithallium (lower bracket). Scale bar = 10 μ m. FIG. 13. Isotype, RB 779738. Habit of isotype. Scale bar = 2.7 cm. FIG. 14. RB 779740. Surface view of two adjacent tetrasporangial sori (arrows). Scale bar = 0.7 mm. FIG. 15. RB621750. Section of thallus showing layers of tetrasporangial compartments, many with intact tetrasporangia. Scale bar = 200 μ m. FIG. 16. RB621750. Tetrasporocyte (T) with stalk cell (S). Scale bar = 20 μ m. FIG. 17. RB779739. Detail of cruciately divided tetrasporangia (1-4) born among basal layer of slightly elongated cells (arrows). Scale bar = 30 μ m.



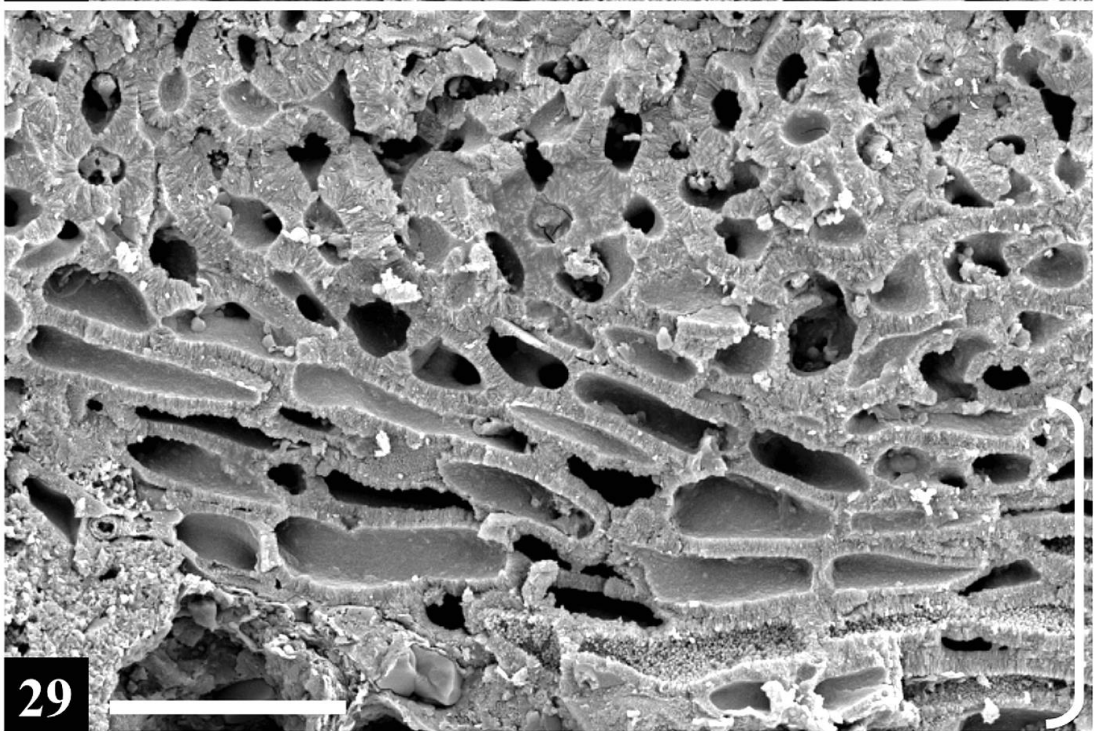
FIGURES 18–21. *Sporolithon amadoi*, LAF 7260. FIG. 18. Thallus habit showing abundant protuberances. Scale bar = 1 cm. FIG. 19. Perithallium with secondary pit connection (arrows) and cell fusion (circle pointer). Scale bar = 23 μm . FIG. 20. Vertical fracture showing perithallium (bracket) intercalary meristem (*) and epithallium. Scale bar = 30 μm . FIG. 21. Vertical fracture showing epithallial cells, one with intact epithallial cell roof (circle pointer) and one with the roof missing (arrow), intercalary meristematic cells (*) and portion of perithallium (bracket). Scale bar = 9 μm .



FIGURES 22–27. *Sporolithon amadoi*, LAF 7260. FIG. 22. Surface view showing adjacent tetrasporangial sori. Scale bar = 400 µm. FIG. 23. Tetrasporangial pores (arrows) and rosette cells. Scale bar = 60 µm. FIG. 24. Detail of tetrasporangial pore (arrow) surrounded by rosette cells (*). Scale bar = 18 µm. FIGS 25–26. Longitudinal fractures of protuberance showing layers of unshed and buried tetrasporangial compartments (arrows). Scale bars = 400, 180 µm. FIG. 27. Magnified view of tetrasporangial compartment with stalk cell (S) born among basal layer of somewhat elongated cells (arrow). Scale bar = 55 µm.

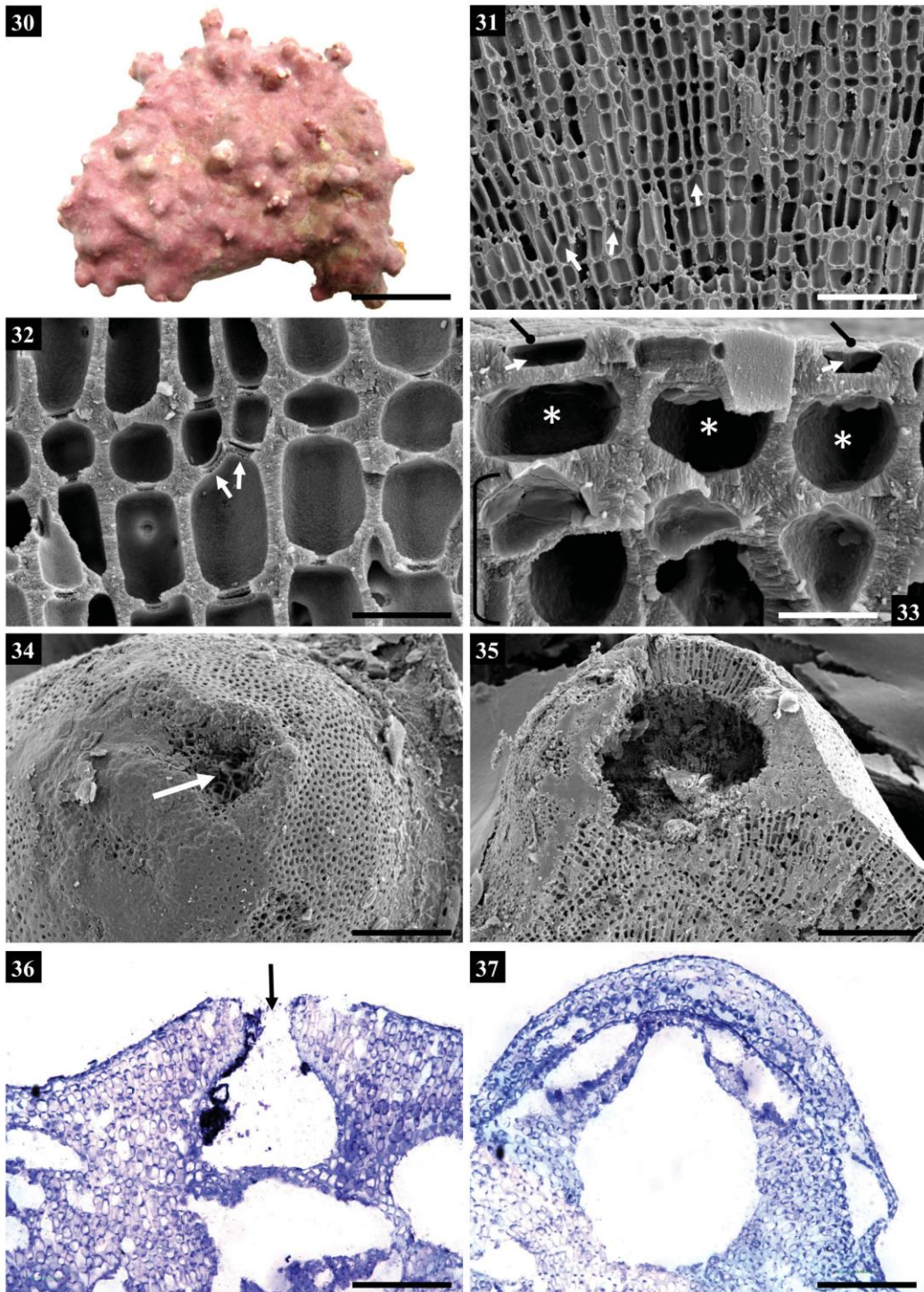


28



29

FIGURES 28–29. *Sporolithon amadoi*, LAF 7261. Vertical fracture showing monomerous construction and multilayered, plumose (noncoaxial) hypothallium (brackets). Scale bars = 80, 40 μm .



FIGURES 30–37. *Sporolithon amadoi*. LAF 7256. FIG. 30. Thallus habit showing protuberances. Scale bar = 1 cm. FIGS. 31–32. Perithallium showing locations of pseudodichotomous branching (arrows). Scale bars = 70, 15 μm . FIG. 33. Vertical fracture showing part of perithallium (bracket), intercalary meristematic cells (*) and epithallial cells (arrows) with intact epithallial cell roofs (circle pointers). Scale bar = 8 μm . FIG. 34. Surface view of uniporate conceptacle showing pore opening (arrow). Scale bar = 110 μm . FIG. 35. Longitudinal section showing conceptacle chamber. Scale bar = 150 μm . FIG. 36. Decalcified longitudinal section showing conceptacle chamber and pore canal (arrow). Scale bar = 125 μm . FIG. 37. Decalcified longitudinal section showing conceptacle chamber overgrown by a vegetative layer. Scale bar = 125 μm .

TABLE 2. Pairwise sequence divergences (%) for *psbA* sequences (850 bp) reported in this study: *Sindo* = *Sporolithon indopacificum*; *Spty* = *S. ptychooides*; *Smol* = *S. molle*; *Selt* = *S. eltoensis*; *Sepi* = *S. episporum*; *Samad* = *S. amadoi*; *Ssp.* = *S. species*; *Sdur* = *S. durum*; *Sten* = *S. tenuie*; *Syon* = *S. yoneshigae*; *Smes* = *S. mesophoticum*; *Ssin* = *S. sinusmexicanum*; *Hwo* = *Heydrichia woelkerlingii*; *Ssp.A.* = *Sporolithales* sp. A; *Hcer* = *H. cerasina*.

1. <i>Sindo</i> L3964509																						
2. <i>Spty</i> NCU 606660	10.4																					
3. <i>Smol</i> NCU 606657	10.4	5.4																				
4. <i>Selt</i> NCU 606659	9.7	8.8	9.4																			
5. <i>Selt</i> LAF 5767	9.7	9.3	9.8	0.9																		
6. <i>Sepi</i> NCU 598843	3.1	9.3	9.5	8.9	9.1																	
7. <i>Samad</i> LAF 7256	8.5	6.4	6.2	6.7	6.9	7.5																
8. <i>Samad</i> LAF 7260	8.5	6.4	6.2	6.5	6.7	7.8	0.2															
9. <i>Samad</i> Holotype	8.5	6.4	6.2	6.7	6.9	7.5	0	0.2														
10. <i>Samad</i> GM AF6	8.5	6.4	6.2	6.7	6.9	7.5	0	0.2	0													
11. <i>Ssp.</i> GM AF5	9.4	8.8	9.1	6	6.2	8.5	6.7	6.5	6.7	6.7												
12. <i>Ssp.</i> NZC2175	8.6	8.4	9.3	7.5	7.5	7.7	6.5	6.5	6.5	6.5	6.1											
13. <i>Ssp.</i> 1WA	9.1	10.4	11.1	8.6	8.4	8.5	8.8	8.6	8.8	8.8	8.7	8										
14. <i>Sdur</i> NZCD375	9.2	10.3	10.3	8.8	8.6	8.5	8.5	8.5	8.5	8.5	8.4	7.4	4.1									
15. <i>Sten</i> US170943	9.4	8	9.3	9.1	9.1	8.7	7.7	7.4	7.7	7.7	7.8	6.8	8.5	7.6								
16. <i>Syon</i> RB 6000359	10.8	10.8	11.4	10.9	10.7	10.6	10.9	10.9	10.9	10.9	11.2	10.4	9.8	9.3	10.1							
17. <i>Smes</i> NCU658543	11.3	11.4	11.4	10.5	10.7	11.4	10.9	10.7	10.9	10.9	11.1	10	10.5	9.8	10.5	5.9						
18. <i>Ssin</i> LAF 6956A	10.4	11.3	11.5	10.8	10.6	10.7	10.5	10.2	10.5	10.5	10.6	9.3	9.2	9.1	8.4	7.9	8					
19. <i>Hwo</i> NCU 597127	11.5	11.5	11.6	10.5	10.6	10.6	11.1	10.9	11.1	11.1	10.2	10.5	10.1	10.4	10	12.5	12.1	10.5				
20. <i>Ssp.</i> A NZC2014	11.8	11.9	12.5	12	11.6	11.1	10.5	10.7	10.5	10.5	10.7	9.5	9.8	9.2	9.9	10.4	10.8	8.8	10			
21. <i>Hcer</i> NCU 617165	9.2	11.2	11.9	10.8	10.7	8.82	9.7	9.7	9.7	9.7	9.9	8.2	9.1	9.8	8.8	11.3	11.4	9.7	9.7	8.2		
Taxa	1.	2.	3.	4.	5.	6.	7.	8.	9.	10.	11.	12.	13.	14.	15.	16.	17.	18.	19.	20.	21.	

TABLE 3. Pairwise sequence divergences (%) for *rbcL* sequences (251 bp) reported in this study: *Sindo* = *Sporolithon indopacificum*; *Spty* = *S. ptychooides*; *Smol* = *S. molle*; *Selt* = *S. eltoensis*; *Sepi* = *S. episporum*; *Samad* = *S. amadoi*; *Ssp.* = *S. species*; *Sdur* = *S. durum*; *Sten* = *S. tenue*; *Syon* = *S. yoneshigueae*; *Smes* = *S. mesophoticum*; *Ssin* = *S. sinusmexicanum*; *Hwo* = *Heydrichia woelkerlingii*; *Ssp.A.* = *Sporolithales* sp. A; *Hcer* = *H. cerasina*.

1. <i>Sindo</i> L3964509																			
2. <i>Spty</i> NCU 606660	10.0																		
3. <i>Smol</i> NCU 606657	7.2	4.4																	
4. <i>Selt</i> NCU 606659	10.8	8.4	8.4																
5. <i>Sepi</i> NCU 598843	3.2	10.0	7.2	10.8															
6. <i>Samad</i> GM AF6	9.6	7.6	8.0	9.2	9.6														
7. <i>Samad</i> LAF 7256	9.6	7.6	8.0	9.2	9.6	0.0													
8. <i>Ssp.</i> GM AF5	9.6	8.8	7.6	4.4	9.2	8.8	8.8												
9. <i>Ssp.</i> NZC2175	7.6	11.6	9.6	12.0	8.4	12.0	12.0	10.4											
10. <i>Ssp.</i> 1WA	10.0	10.4	9.6	10.8	10.4	12.7	12.7	11.2	10.4										
11. <i>Sdur</i> NZCD375	10.8	11.6	11.2	13.1	10.8	14.3	14.3	12.0	11.2	5.2									
12. <i>Sten</i> US 170943	8.0	11.2	10.0	12.4	8.8	12.0	12.0	9.6	9.6	10.0	10.4								
13. <i>Sdim</i> NY 900043	11.2	11.2	10.0	6.8	11.6	8.8	8.8	7.2	10.8	12.7	14.3	12.0							
14. <i>Syon</i> RB 6000359	15.8	15.0	13.8	17.8	14.2	16.6	16.6	16.2	16.6	15.0	15.4	14.6	17.0						
15. <i>Smes</i> NCU 658543	16.7	11.6	13.5	15.9	15.5	13.1	13.1	15.5	16.7	16.3	15.5	16.3	16.3	13.8					
16. <i>Ssin</i> LAF 6956A	13.5	10.0	10.4	13.1	12.0	13.5	13.5	12.0	13.9	13.5	14.3	12.0	13.9	10.9	7.6				
17. <i>Hwo</i> NCU 597127	15.5	16.7	16.7	17.1	15.1	17.5	17.5	15.9	14.7	17.1	16.3	14.3	15.5	19.4	17.5	14.3			
18. <i>Ssp.A</i> NZC2014	12.4	13.9	12.0	16.3	12.4	14.7	14.7	14.7	11.6	13.9	13.9	14.3	15.9	15.0	12.4	8.8	12.4		
19. <i>Hcer</i> NCU 617165	13.9	14.7	13.5	16.3	13.9	15.5	15.5	15.9	14.3	14.3	15.9	12.7	15.9	17.4	16.3	12.4	12.4	11.2	
Taxa	1.	2.	3.	4.	5.	6.	7.	8.	9.	10.	11.	12.	13.	14.	15.	16.	17.	18.	19.

Acknowledgements

This work was funded by NSF grant DEB–1754504 for rhodolith research to SF and by the Brazilian Science Support Agencies, CNPq and FAPERJ, and funds from P&D program ANP/BRASOIL. MJ acknowledges the Coordination for the Improvement of Higher Education Personnel (CAPES) for providing a master's scholarship. RGB acknowledges CNPq for providing a postdoctoral fellowship grant (process PDJ 400654/2014-8) and research fellowship. JLR acknowledges Tom Pesacreta and Mike Purpera at the UL Lafayette Microscopy Center for help and advice using the SEM and William E. Schmidt for assistance with phylogenetic analyses. We also thank the crew of the R/V *Pelican* for help with sampling protocols.

References

- Adey, W.H., Hernandez-Kantun, J.J., Johnson, G. & Gabrielson, P.W. (2015) DNA sequencing, anatomy, and calcification patterns support a monophyletic, subarctic, carbonate reef-forming *Clathromorphum* (Hapalidiaceae, Corallinales, Rhodophyta). *Journal of Phycology* 51: 189–203.
doi: 10.1111/jpy.12266
- Amado-Filho G.M., Moura, R.L., Bastos, A.C., Salgado. L.T., Sumida, P.Y., Guth, A.Z., Francini-Filho, R.B., Pereira-Filho, G.H., Abrantes, D.P., Brasileiro, P.S., Bahia, R.G., Leal, R.N., Kaufman, L., Kleypas, J.A., Farina, M. & Thompson, F.L. (2012) Rhodolith beds are major CaCO₃ bio-factories in the tropical South West Atlantic. PLoS ONE 7(4): e35171.
<https://doi.org/10.1371/journal.pone.0035171>

Bahia, R.G., Abrantes, D.P., Brasileiro, P.S., Pereira-Filho, G.H. & Amado-Filho, G.M. (2010)

Rhodolith bed structure along a depth gradient on the northern coast of Bahia State, Brazil.

Brazilian Journal of Oceanography 58: 323–337.

<http://dx.doi.org/10.1590/s1679-87592010000400007>

Bahia, R.G., Amado-Filho, G.M., Maneveldt, G.W., Adey, W.H., Johnson, G., Jesionek, M.B. &

Longo, L.L. (2015) *Sporolithon yoneshigueae* sp. nov. (Sporolithales, Corallinophycidae, Rhodophyta), a new rhodolith-forming coralline alga from the southwest Atlantic. *Phytotaxa* 224: 140–58.

<http://dx.doi.org/10.11646/phytotaxa.224.2.2>

Bahia, R.G., Amado-Filho, G.M., Maneveldt, G.W., Adey, W.H., Johnson, G., Marins, B.V. &

Longo, L.L. (2014) *Sporolithon tenue* sp. nov. (Sporolithales, Corallinophycidae, Rhodophyta): A new rhodolith-forming species from the tropical southwestern Atlantic. *Phycological Research* 62: 44–54.

Bahia, R.G., Riosmena-Rodriguez, R., Maneveldt, G.W. & Amado Filho, G.M. (2011) Research

note: first report of *Sporolithon ptychoides* (Sporolithales, Corallinophycidae, Rhodophyta) for the Atlantic Ocean. *Phycological Research* 59: 64–69.

<https://doi.org/10.1111/j.1440-1835.2010.00599.x>

Bittner, L., Payri, C.E., Maneveldt, G.W., Couloux, A., Cruaud, C., De Reviers, B. & Le Gall, L.

(2011) Evolutionary history of the Corallinales (Corallinophycidae, Rhodophyta) inferred from nuclear, plastidial and mitochondrial genomes. *Molecular Phylogenetics and Evolution* 61: 697–713.

<https://doi.org/10.1016/j.ympev.2011.07.019>

Broom, J.E., Hart, D.R., Farr, T.J., Nelson, W.A., Neill, K.F., Harvey, A.S. & Woelkerling, W. J. (2008) Utility of *psbA* and nSSU for phylogenetic reconstruction in the Corallinales based on New Zealand taxa. *Molecular Phylogenetics and Evolution* 46: 958–973.

<https://doi.org/10.1016/j.ympev.2007.12.016>

Edgar, R. C. (2004) MUSCLE: multiple sequence alignment with high accuracy and high throughput. *Nucleic Acids Research* 32: 1792–1797.

Fainstein, R. & Summerhayes, C.P. (1982) Structure and origin of marginal banks off Eastern Brazil. *Marine Geology* 46: 199–215.

[https://doi.org/10.1016/0025-3227\(82\)90080-9](https://doi.org/10.1016/0025-3227(82)90080-9)

Felder D.L., Thoma, B.P., Schmidt, W.E., Sauvage, T., Self-Krayesky, S., Chistoserdov, A., Bracken-Grissom, H. & Fredericq, S. (2014). Seaweeds and decapod crustaceans on Gulf deep banks after the Macondo Oil Spill. *Bioscience* 64: 808–819.

doi: 10.1093/biosci/biu119

Fredericq, S., Arakaki, N. Camacho, O., Gabriel, D. Krayesky, D., Self-Krayesky, S., Rees, G., Richards, J., Sauvage, T., Venera-Ponton, D. & Schmidt, W.E. (2014) A dynamic approach to the study of rhodoliths: a case study for the northwestern Gulf of Mexico. *Cryptogamie, Algologie* 35: 77–98.

<http://dx.doi.org/10.7872/crya.v35.iss1.2014.77>

Fredericq S., Krayesky-Self, S., Sauvage, T., Richards, J., Kittle R., Arakaki, N., Hickerson, E. & Schmidt, W. E. (2019) The critical importance of rhodoliths in the life cycle completion of both macro- and microalgae, and as holobionts for the establishment and maintenance of biodiversity. *Frontiers in Marine Science - Marine Ecosystem Ecology* 5: 502.

doi:10.3389/fmars.2018.00502

Gabrielson, P.W., Miller, K.A. & Martone, P.T. (2011) Morphometric and molecular analyses confirm two distinct species of *Calliarthron* (Corallinales, Rhodophyta), a genus endemic to the northeast Pacific. *Phycologia* 50: 298–316.

<https://doi.org/10.2216/10-42.1>

Gabrielson, P.W., Hughey, J.R. & Diaz-Pulido, G. (2018) Genomics reveals abundant speciation in the coral reef building alga *Porolithon onkodes* (Corallinales, Rhodophyta). *Journal of Phycology* 54: 429–34.

<https://doi.org/10.1111/jpy.12761>

Harper, J.T. & Saunders, G.W. (2001) Molecular systematics of the Florideophyceae (Rhodophyta) using nuclear large and small subunit rDNA sequence data. *Journal of Phycology* 37: 1073–1082.

<https://doi.org/10.1046/j.1529-8817.2001.00160.x>

Hernández-Kantún, J.J., Gabrielson, P., Hughey, J.R., Pezzolesi, L., Rindi, F., Robinson, N.M., Peña, V., Riosmena-Rodriguez, R., Le Gall, L. & Adey, W. (2016) Reassessment of branched *Lithophyllum* spp. (Corallinales, Rhodophyta) in the Caribbean Sea with global implications. *Phycologia* 55: 619–639.

<https://doi.org/10.2216/16-7.1>

Hernández-Kantún, J.J., Riosmena-Rodriguez, R., Hall-Spencer, J.M., Peña, V., Maggs, C.A. & Rindi, F. (2015) Phylogenetic analysis of rhodolith formation in the Corallinales (Rhodophyta). *European Journal of Phycology* 50: 46–61.

<https://doi.org/10.1080/09670262.2014.984347>

Hind, K.R., Gabrielson, P.W., Jensen, C.P. & Martone, P.T. (2016) *Crusticorallina* gen. nov., a nongeniculate genus in the subfamily Corallinoideae (Corallinales, Rhodophyta). *Journal of Phycology* 52: 929–941.

<https://doi.org/10.1111/jpy.12449>

Hughey, J.R., Hommersand, M.H., Gabrielson, P.W., Miller, K.A. & Fuller, T. (2017). Analysis of the complete plastomes of three species of *Membranoptera* (Ceramiales, Rhodophyta) from Pacific North America. *Journal of Phycology* 53: 32–43.

Jesionek, M.B., Bahia, R.G., Hernández-Kantún, J.J., Adey, W.H., Yoneshigue-Valentin, Y., Longo, L.L. & Amado-Filho, G.M. (2016) A taxonomic account of non-geniculate coralline algae (Corallinophycidae, Rhodophyta) from shallow reefs of the Abrolhos Bank, Brazil. *Algae* 31: 317–340.

Krayesky-Self, S., Schmidt, W.E., Phung, D., Henry, C., Sauvage, T., Camacho, O., Felgenhauer, B.E & Fredericq, S. (2017) Eukaryotic life inhabits rhodolith-forming coralline algae (Hapalidiales, Rhodophyta), remarkable marine benthic microhabitats. *Scientific Reports* 7: 45850. doi: 10.1038/srep45850.

Lee, J.M., Song, H.J., Park, S.I., Lee, Y.W., Jeong, S.Y., Cho, T.O., Kim, J.H., Choi, H., Choi, C.G., Nelson, W.A., Fredericq, S., Bhattacharya, D. & Yoon, H.S. (2018) Mitochondrial and plastid genomes from coralline red algae provide insights into the incongruent evolutionary histories of organelles. *Genome Biology and Evolution* 10: 2961–2972.

Liu, L. C., Lin, S. M., Caragnano, A. & Payri, C. (2018) Species diversity and molecular phylogeny of non-geniculate coralline algae (Corallinophycidae, Rhodophyta) from Taoyuan algal reefs in northern Taiwan, including *Crustaphytum* gen. nov. and three new species. *Journal of Applied Phycology* 30: 3455–3469.

Maddison, D.R. & Maddison, W.P. (2000) *MacClade4: Analysis of Phylogeny and Character Evolution*. Version 4.0. Sinauer Associates, Sunderland, MA.

Maneveldt, G.W., Gabrielson, P.W. & Kangwe, J. (2017) *Sporolithon indopacificum* sp. nov. (Sporolithales, Rhodophyta) from tropical western Indian and western Pacific oceans: First report, confirmed by DNA sequence data, of a widely distributed species of *Sporolithon*. *Phytotaxa* 326: 115–128.

<http://dx.doi.org/10.11646/phytotaxa.326.2.3>

Mateo-Cid, L.E., González, A.C.M. & Gabrielson, P.W. (2014) *Neogoniolithon* (Corallinales, Rhodophyta) on the Atlantic coast of Mexico, including *N. siankanensis* sp. nov. *Phytotaxa* 190: 64–93.

<http://dx.doi.org/10.11646/phytotaxa.190.1.7>

Moura, R. L., Amado-Filho, G. M., Moraes, F. C., Brasileiro, P. S., Salomon, P. S., Mahiques, M.M., Bastos, A.C., Almeida, M.G., Silva Jr., J.M., Araujo, B.F., Brito, F.P., Rangel, T.P., Oliveira, B.C.V., Bahia, R.G., Paranhos, R.P., Dias, R.J.S., Siegle, E., Figueiredo Jr., A.G., Pereira, R.C., Leal, C.V., Hajdu, E., Asp, N.E., Gregoracci, G.B., Neumann-Leitão, S., Yager, P.L., Francini-Filho, R.B., Fróes, A., Campeão, M. Silva, B.S., Moreira, A.P.B., Oliveira, L. Soares, A.C., Araujo, L., Oliveira, N.L., Teixeira, J.B., Valle, R.A.B., Thompson, C.C., Rezende, C.E. & Thompson, F.L. (2016) An extensive reef system at the Amazon River mouth. *Science Advances* 2: e1501252.

DOI: 10.1126/sciadv.1501252

Nelson, W.A., Sutherland, J.E., Farr, T.J., Hart, D.R., Neill, K.T., Kim, H.J. & Yoon, H.S. (2015) Multi-gene phylogenetic analyses of New Zealand coralline algae: *Corallinapetra*

novaehollandiae gen. et sp. nov. and recognition of the Hapalidiales ord. nov. *Journal of Phycology* 51: 454–68.

<https://doi.org/10.1111/jpy.12288>

Richards, J.L., Sauvage, T., Schmidt, W.E., Fredericq, S., Hughey, J.R. & Gabrielson, P.W. (2017) The coralline genera *Sporolithon* and *Heydrichia* (Sporolithales, Rhodophyta) clarified by sequencing type material of their generitypes and other species. *Journal of Phycology* 53: 1044–59.

<https://doi.org/10.1111/jpy.12562>

Richards, J.L. & Fredericq, S. (2018) *Sporolithon sinusmexicanum* sp. nov. (Sporolithales, Rhodophyta): a new rhodolith-forming species from deepwater rhodolith bed in the Gulf of Mexico. *Phytotaxa* 350: 135–46.

<http://dx.doi.org/10.11646/phytotaxa.350.2.2>

Richards, J.L., Gabrielson, P.W., Hughey, J.R. & Freshwater, D.W. (2018a) A re-evaluation of subtidal *Lithophyllum* species (Corallinales, Rhodophyta) from North Carolina, USA, and the proposal of *L. searlesii* sp. nov. *Phycologia* 57: 318–330.

Richards, J.L., Gabrielson, P.W. & Schneider, C.W. (2018b) *Sporolithon mesophoticum* sp. nov. (Sporolithales, Rhodophyta) from Plantagenet Bank off Bermuda at a depth of 178 m. *Phytotaxa* 385: 67–76.

<http://dx.doi.org/10.11646/phytotaxa.385.2.2>

Sissini, M.N., Oliveira, M.C., Gabrielson, P. W., Robinson, N. M., Okolodkov, Y. B., Riosmena-Rodríguez, R. & Horta, P. A. (2014) *Mesophyllum erubescens* (Corallinales, Rhodophyta)—so many species in one epithet. *Phytotaxa* 190: 299–319.

<http://dx.doi.org/10.11646/phytotaxa.190.1.18>

Tamura, K., Peterson, D., Peterson, N., Stecher, G., Nei, M. & Kumar, S. (2011) MEGA5: molecular evolutionary genetics analysis using maximum likelihood, evolutionary distance, and maximum parsimony methods. *Molecular Biology and Evolution* 28: 2731–2739.

<http://dx.doi.org/10.1093/molbev/msr121>

Thiers, B. (2019) (continuously updated) Index Herbariorum: A global directory of public herbaria and associated staff. New York Botanical Garden's Virtual Herbarium.

<http://sweetgum.nybg.org/ih/>

Vaidya, G., Lohman, D.J. & Meier, R. (2011) SequenceMatrix: concatenation software for the fast assembly of multigene datasets with character set and codon information. *Cladistics* 27: 171–180.

<http://dx.doi.org/10.1111/j.1096-0031.2010.00329.x>

5. CONCLUSÕES GERAIS

- A utilização da ferramenta molecular revelou diversidade críptica para o sudeste brasileiro permitindo a descrição de 3 novos táxons, sendo um gênero e espécie nova (*Tectolithon fluminense*) e duas outras espécies novas para a ciência (*Crustaphytum atlanticum* e *Sporolithon amadoi*).
- Os marcadores *psbA* e *rbcL* foram eficientes na separação de espécies geneticamente próximas, assim como na distinção de gêneros.
- Devido ao volume de informações disponíveis no banco de dados genético do marcador *rbcL* de material histórico, este marcador é fundamental em estudos taxonômicos e filogenéticos de ACNG.
- Duas destas espécies e o gênero novo foram registrados para a costa do Estado do Rio de Janeiro que representa apenas 8,5% da costa brasileira. Este fato demonstra o grande potencial desta região do Atlântico Sul para novos registros.
- *Tectolithon fluminense* ocorreu em 6 dos 11 municípios, demonstrando ser uma alga aparentemente comum para a costa do estado do Rio de Janeiro. Além disso, existe registro desta espécie para a região sul do Brasil (Ilha do Arvoredo, Santa Catarina) e sua ocorrência em demais áreas da costa brasileira poderá ser revelada em trabalhos futuros.
- *Sporolithon amadoi* é uma espécie críptica que possui características morfoanatômicas que correspondem ao holótipo de *Sporolithon ptychoides*, mas diverge geneticamente do tipo desta espécie. Muitas características se sobrepõem neste gênero, principalmente em indivíduos próximos geneticamente.
- O fato de serem registradas 3 novas espécies e um gênero novo para o sudeste brasileiro, evidencia como a taxonomia alfa é importante para as ACNG, fornecendo base de dados para estudos futuros de filogenia e filogeografia do grupo.

- Os resultados apresentados nesta tese, refletem uma parte da diversidade críptica da região sudeste, até então desconhecida por estudos prévios que utilizaram apenas dados morfoanatômicos. Dados gerados, ainda estão sendo analisados com possíveis novos registros. Estudos adicionais, incluindo áreas não amostradas, têm grande potencial de revelar novas espécies e novas ocorrências de ACNG para esta região.
- A comparação genética com material tipo, demonstra ser a única maneira inequívoca de se nomear espécies de ACNG, visto a cada vez mais evidenciada ausência de caracteres diagnósticos para separação de espécies de ACNG.